# Electrocatalytic detection of herbicide, amitrole on the platform modified with polyaniline cobalt phthalocyaninato doped with cobalt oxide nanoparticles

**By**

**PETER T. MAFUWE**

**REG (R112541Q)**

Submitted in partial fulfillment of the requirements for the degree of

**Bachelor of Science Honours in Chemical Technology**

Department of Chemical Technology

in the

Faculty of Science and Technology at the

**Midlands State University**

**Supervisor: Dr. Mambo Moyo**

November 2016

## DEDICATION

This work is dedicated to God Almighty who proved to me that nothing is impossible with him and also to my loving and caring mother Carol Madzima who stood by me against all odds, during the course of this degree.

## ACKNOWLEDGEMENTS

My profound gratitude goes to my supervisor Dr M. Moyo for his continuous encouragement, advice, guidance and inspiration throughout this research. I would like to give thanks to my late supervisor Dr Mugadza for his wonderful support and introducing me into the field of electrochemistry. Many thanks also are extended to the MSU laboratory staff and my family for their unwavering support. I would also want to thank Ms. Gonzo, Mr.Mambanda, Tichaona Chirowa, Fadzi Chirowa, Christopher Chirowa, Steven Chirowa, Evelyn Mariwowo,Linda Mastika,Thabiso Magudu, Famous Chirongwe, Privy Mafuwe, Indrah Chuma,Farai Dokotera, Gracious Chitabati, Sarah P Muhezihwa, Theresa Makura, Mrs. Jongwe,Talent Mubaiwa and Talent Sithole for their contributions in making this research possible. Above all, I would want to extend my gratitude to God Almighty for showing me that no mountain is too high to climb as long as I am with him.

## ABSTRACT

An electrochemical sensor based on polyaniline cobalt phtahlocyanito doped with cobalt oxide nanoparticles was developed for the electrocatalytic oxidation of amitrole.FTIR, Electrochemical impedance spectroscopy (EIS) and Bode plots were used in the characterization of the synthesized modifiers CoTCPc, PANI, $Co_2O_3$NPs and to ascertain the chemical linkage between CoTCPc and PANI while cyclic voltammetry, linear sweep, chronoamperometry and differential pulse voltammetry were used to assess the electrocatalytic efficiency of the linked product towards oxidation of amitrole. The surface area of the modified electrode was 0.40 $cm^2$ and the surface coverage was $7.60\times 10^{-13}$ $molcm^2$.The catalytic rate constant was of $6.26\times10^5 M^{-1}s^{-1}$and the apparent electron transfer rate constant was $8.84 \times 10^{-3}$cm $s^{-1}$.The adsorptionequilibrium constant was $3.8\times 10^3$ $M^{-1}$and Gibbs free energy was -20.42kJ. The limit of detection was $6.612 \times 10^{-8}$M and the limit of quantification was $2\times 10^{-7}$ M. Interference studies were done and the electrode displayed the ability to detect both amitrole and nitrates. The electrode displayed good reproducibility with lower oxidation potential at 0.8 V and high sensitivity towards amitrole.


## DECLARATION

I,Peter T. Mafuwe, hereby declare that I am the sole author of this dissertation. I authorize Midlands State University to lend this dissertation to other institutions or individuals for the purpose of scholarly research.

Signature ……

Date …….

## APPROVAL

This dissertation entitled “Electrochemical detection of herbicide, amitrole on the platformmodified with polyaniline cobalt phthalocyaninato doped with cobalt oxide nanoparticles electrode” by Peter T Mafuwe meets the regulations governing the award of the degree of Chemical Technology of Midlands State University, and is approved for its contribution to knowledge and literal presentation.

Supervisor……..

Date……

## Table of Contents

## LIST OF ABBREVIATIONS

**EIS** - Electrochemical impedance spectroscopy

**CA**- Chronoamperometry

**CoTCPc**- Cobalt (II) tetracarboxyl phthalocyanine

**CV-** cyclic voltammetry

**$Co_2O_3$NPs-** cobalt oxide nanoparticles

**CoTCPc-PANI–** Cobalt tetracarboxyl phthalocyanine polyaniline

**CoTCPc-PANI/$Co_2O_3$NPs –** Cobalt tetracarboxyl polyaniline doped with cobalt oxide nanoparticles

**DPV-** Differential pulse voltammetry

**DMSO-** dimethylsulphoxide

**FTIR-** Fourier Transfer Infrared

**GCE-** Glassy carbon electrode

**LSV-** Linear sweep voltammetry

**LOD-** Limit of detection

**LOQ-** Limit of quantification

**MPCs-** Metallatedphthalocyanines

**PANI-** polyaniline

## LIST OF FIGURES

## LIST OF SCHEMES

## LIST OF TABLES

# CHAPTER 1

## Introduction

### 1.0 Introduction

The present chapter gives an overview of the research, aims, objectives, problem statement and justification on the components such as polyaniline (PANI), cobalt phthlocyanines (CoPcs), cobalt oxide nanoparticles ($Co_2O_3$NPs) used for electrode modification in the detection of amitrole.

### 1.1 Background

The rapid increase in population growth in the developing world has resulted in increase of agricultural produce through farming in order to meet the food requirements by people[1]. In an effort to maintain the high food production, human activities during farming have resulted in the use of pesticides and herbicides in order to kill and destroy weeds and pests so as to enhance agricultural produce. One of the most commonly used herbicide is amitrole (3-amino-1, 2, 4 triazole, Fig 1.1). It is a non-selective herbicide that is used in combination with other active ingredients to control a wide range of weeds in agricultural areas. The herbicide is widely used as an industrial herbicide to control weeds grown near roads and railways [2].

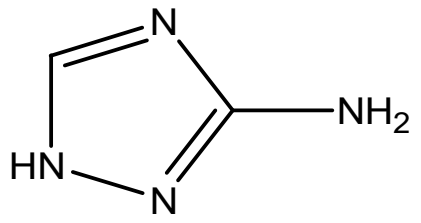


3-amino-1,2,4 triazole

**Fig 1.1:** Chemical structure of amitrole

Amitrole was banned in 1971 for its use in food crops by the EPA, since it was proved to be a carcinogenic agent for animals and interferes with lymphoblast transformation as well as inhibiting cell growth [1]. The organic pollutants are responsible for a lot of environmental damage especially when they accumulate in the environment, both in land fields and water [3] . It is a potential pollutant to natural water resources due to its solubility, polarity and low volatility in water. Therefore, levels of amitrole should be monitored so that they do not exceed the regulatory level of 0.1 $\mu g\ L^{-1}$ in drinking water, set by the European Economic Commission (EEC) [2].

High performance liquid chromatography (HPLC) was used extensively in amitrole detection. However, due to the high polarity of the compound, its determination by reversed –phase technique with usual aqueous phases is not possible, since the resolution between the amitrole and solvent peaks is poor [4]. Determination of amitrole by gas chromatography is also difficult, owing to its high polarity and low volatility. Amitrole is ionized at low pH hence ion exchange can be used for its extraction from water. However, the presence of inorganic cations causes a rapid solution of amitrole in drinking water, even after the standard chemical pre-treatment to remove these cations before extraction [5]. The presence of amitrole in plants can be detected using fluorescence techniques [6].Paper chromatography and thin layer chromatographies have also been used for a quantitative estimation of amitrole. The major draw of all these methods is that preliminary extraction and concentration from the aqueous medium is necessary before trace amounts of amitrole can be quantitatively determined.

However on the other hand, electrochemical techniques have been proved to be more reliable and cost effective for the determination of amitrole. Electrochemical methods, offer good advantages in terms of simplicity, direct use in point of care assay and portability [7]. However,

electrochemical detection of amitrole at conventional bare electrodes suffers from draw backs such as high over potential and electrode fouling. These limitations can be overcome by employing chemically modified electrodes such as nafion/lead –ruthenium oxide pyrochlore[8], pre-anodized nontronite coated screen printed electrodes [9], electrochemically activated multiwalled carbon nanotubes MWCNT) paste electrodes [6], cobalt phthlocyanines and nickel nanoparticles [8].

## 1.2 Aim of the study

To assess the efficiency of the modified glassy carbon electrode on the electrochemical detection of amitrole.

## 1.3 Objectives

- To synthesize cobalt (II) tetra carboxylic phthlocyanines (CoTCPc), polyanaline (PAN), cobalt oxide nanoparticles ($Co_2O_3$) and polyanaline phthalocyaninato Cobalt (II) doped with cobalt oxide nanoparticles PAN-CoTCPc/$Co_2O_3$.
- To characterize the electrode modifiers using FTIR, cyclic voltammetry and electrochemical impedance spectroscopy.
- To determine the surface coverage of the modified electrode CoTCPc-PANI/$Co_2O_3$NPs-GCE by performing scan rate studies in 1 mM Ferricyanide solution.
- To carryoutpH studies in phosphate buffer solution for the optimization of pH for the analysis amitrole by using CoTCPc-PANI/$Co_2O_3$NPs-GCE electrode.
- To perform comparative studies on modified electrodes a) Bare GCE, b) CoTCPc-GCE, c) PANI-GCE, d) CoTCPc-PANI-GCE and e) CoTCPc-PANI/$Co_2O_3$NPs-GCE on the analysis of 1mM amitrole in pH 4 phosphate buffer solution.
- To determine the effective surface coverage of CoTCPc-PANI/$Co_2O_3$NPs-GCE electrode by performing scan rate studies in pH 4 phosphate buffer solution containing 1 mM amitrole
- To determine the electrode transfer kinetics, Tafel slopes, Langmuir adsorption isotherm and catalytic rate constants on CoTCPc-PANI/$Co_2O_3$NPs-GCE electrode in pH 4 buffer solution containing different concentrations of amitrole.
- To determine the limit of detection of amitrole in pH 4 phosphate buffer solution by using DPV and chronoamperometry.

- To study the effect of interferences in the presence of amitrole on the modified glassy carbon electrode.

- To perform repeatability, reproducibility and stability studies of the developed electrode towards oxidation of amitrole in pH 4 phosphate buffer solution.

- To apply the developed electrode on the detection of amitrole in agricultural waste water by using differential pulse voltammetry (DPV)

## 1.4 Problem statement

The increase in health concern risk associated with the exposure to mutagenic, teratogenic and carcinogenic herbicide in the environment has resulted in the interest of the development of suitable method of analysis that is cheaper and easier to use in identifying and quantifying amitrole [10].The current conventional methods that are used to monitor amitrole are high performance liquid chromatography, ion chromatography [2], gas chromatography [4], paper chromatography [11] and thin layer chromatography[12]. However these methods have limitations in that they are very expensive, time consuming, laboratory borne, they need a lot of skill in the operation and sometimes suffer from low detection limit. Furthermore, a large amount of sample volume and solvent are needed in separation and extraction procedure [13]. Apparently there is a need to overcome all these challenges. Consequently a cheaper, faster, easier to use, low power consuming, miniaturizable, user friendly and on site analytical device suitable to compliment or substitute for these classical methods is developed in form of polyaniline cobalt phthalocyanine /doped with cobalt oxide nanocomposite based electrochemical sensor for the detection and quantitative determination of amitrole.

## 1.5 Justification

Traditional environmental monitoring approaches are based upon discrete sampling methods followed by laboratory analysis. Therefore the is a need to design convenient tools for the electroanalysis of amitrole in the environment matrices .Electrochemical techniques particularly cyclic voltammetry (CV), chronoamperometry and square wave voltammetry (SWV) are employed as alternative methods for the detection and electrochemical characterization of amitrole [2,8,14]. Research into the development of electrochemical sensors continues to be rapidly growing in electrochemistry.Improvements in the stability, selectivity and scope of such sensors are highly desirable in order to meet challenges posed by clinical and environmental samples. Characteristics of electrochemical sensing systems include high sensitivity and selectivity a wide linear range, minimal space, power requirements and low cost instrumentation [15]. Therefore in the present study MPcs, cobalt oxide nanoparticles and polyaniline are used as they have good electron transfer properties, chemically linking them together could produce very good electron transfer mediators for electrocatalysis. Also, MPcs carrying electro active metal like Co have excellent redox properties and if chemically coupled to polyaniline, very efficient electrochemical sensors could be produced. Cobalt tetra carboxyl phthalocyanine were used in this study as they have good electrocatalytic properties due to their high electron density, easy to synthesize and also the presence of the peripheral groups on ring that can be fine-tuned in order to increase its catalytic properties [16]. Polyaniline were also used in this study because of good environmental stability, ease of synthesis, low cost, high electrical properties (due to their delocalized π-π conjugated systems),mechanical flexibility and also the presence of the amine group on the polymer backbone chain [17] allows the chemical linking with the peripheral group on MPc forming an amide bond hence providing an electron transfer bridge. Cobalt oxide

nanoparticles were also applied in this study as they have high effective surface area, mass transport, catalysis and control over the local micro environment [18].The modifiers were combined together in order to reduce the over potential of the bare glassy carbon electrode and also to increase sensitivity towards the detection of amitrole.

# CHAPTER 2

# LITERATURE

## 2.0 Summary

The section focuses on phthlocyanines discovery, synthesis and characterization and their combination with polyaniline and cobalt oxide nanoparticles and their use in electrochemistry

## 2.1 Phthalocyanines

### 2.1.1 Discovery

Phthalocyanines (Pcs) are macrocyclic aromatic compounds consisting of four isoindole subunits linked together by aza nitrogen atoms[19]. They are stable green or blue pigments which exhibit intriguing physical and chemical properties[20]. The discovery of phthlocyanines dates back to 1907 when they were made accidentally during o-cyanobenzamide synthesis [21]. In 1929, Scottish Dyes obtained a patent for preparation of Pcs from phthalic anhydride, a metal salt and ammonia, then in 1934,Linstead co-workers deduced the structure of this macromolecule and gave it the name phthalocyanines[22]. The name phthalocyanine was coined by Linsted to describe both its origin from phthalic anhydride (phthalo) and its strikingly beautiful colour which was similar to cyanine dyes[23].

### 2.1.2 Structure of phthlocyanines

Phthalocyanines (Pcs) are formed by porphyrin-like metal central ring bonded to four aromatic rings, they are also known as 29H,31H-tetrabenzo-5,10,15,20 tetrazaporphine or tetra-benzotetraazaporphyrins[21]. Pcs consists four protracted benzo subunits and four nitro atoms meso directed on the macrocycle. The Pc structure can accommodate in the centre of the ligand

two protons or about 70 metals and semimetals as cations in different states forming metallophthalocyanines complex [24].

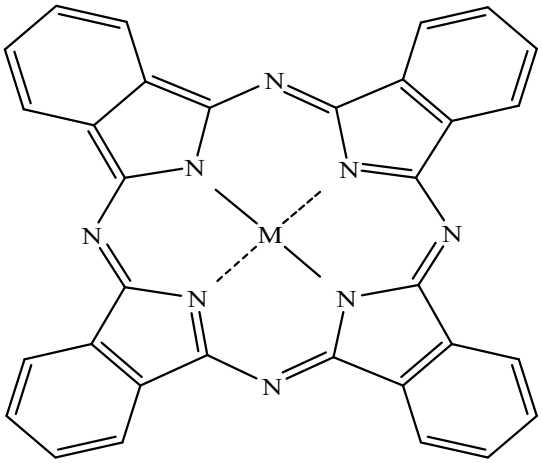


**Fig 2.1:** Structure of metallo-phthalocyanine

### 2.1.3 Applications of phthalocyanines

MPcs have attracted widespread interest in their technological applications due to their high chemical adaptability and good stability[25]. Various MPcs have been used by authors in different functional devices and applications such as organic field effect transistor(OFET), sensors, light emitting devices, information storage and photovoltaic for solar energy conversion as well as biological applications such as photodynamic therapy and drug delivery[26]. MPc-based materials have widely been studied for their excellent catalytic properties due to their high degree of electrochemical reversibility and fast redox changes [27].

### 2.1.4 General synthesis of phthalocyanines

Various 1.2–disubstituted benzene precursor have been employed successfully for phthalocyanine synthesis i.ephthalonitriles, isoindolines, phthalic acid, phthalimides, phthalic acid and anhydride derivatives, 1.2- dibromobenzenes and 2 cyanobenzamide[28]. Depending on

the temperature, base, nature of the substituents, solvent, choice of precursor, metal salt and the metal to be inserted into the macrocycle with wide range of conditions have been utilised[29].

I. Reaction of phthalonitrile with metal or metal salt in a high boiling liquid like nitrobenzene or quinoline. In this reaction phthalonitrile and metal chloride with mole ratio 4:1 is heated to 180-190 $^0$C for 2 h in quinoline or mixture of quinoline and trichlorobenzene. Cobalt, nickel, chromium, iron, lead and titatinum phthalocyanine have been synthesised by this method. Direct method of synthesis of metal – free phthalocyanine ($H_2Pc$) involves heating of phthalonitrile with a base ($NH_3$) in a solvent (1-pentanol).

II. Reaction of phthalic acid or phthalic anhydride with urea and metal salts in the presence of a catalyst or phthalimide with a metal salt in the presence of catalyst. A stiochiometric mixture of phthalic anhydride, a metal salt, urea and catalyst is heated at 170-200 $^0$C for 4 h in medium such as nitrobenzene, chlorobenzene .

III. Reaction of phthalocyanine or liable metal phthalocyanine with a metal forming a more stable Pc.

IV. Reaction of o-cyanobenzamide with a metal.

V. Polymeric phthalocyanine are synthesised by starting with a tetrafunctional benzene 1.2.4.5- tetracyano benzene or pyrometallic.

VI. The phthalonitrile route is expensive but gives high purity products thus this method is mostly used for technological application where high purity and high quality is required.

### 2.1.5 General synthesis of Metallophthalocyanines

Many methods of preparation of MPcs have been developed which include: (1) The reaction of phthalonitrle with a metal salt using a strong base,(2) the reaction of phthalic anhydride,

phthalic acid or phthaliamide with urea, metal salts and a catalyst and (3) the reaction of 1.3 diiminoisoindolines with a metal salt in a hydrophilic solvent [30].

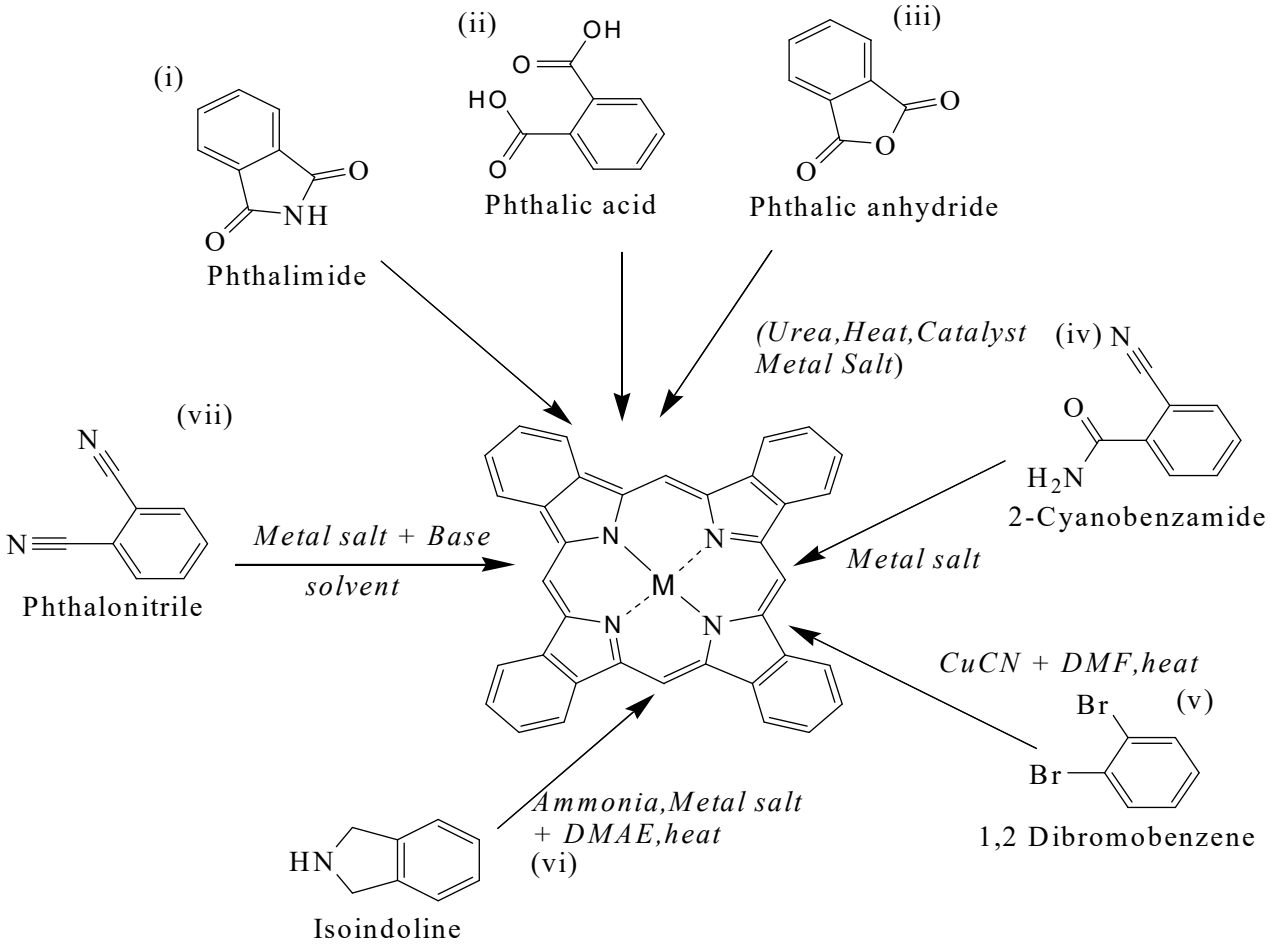


**Scheme 2.1:** The general synthesis of MPcs [31].

### 2.1.6 Metallophthalocyanines (MPc) in electrocatalysis

Several studies have shown that MPcs are excellent candidates as electrochemical reaction catalyst for oxidations of thiols, sulphide ions, hydrazine, hydrogen peroxide, nitrite, and nitric oxide, while capable of reducing oxygen and carbon dioxide [19,32]. The main contributor for its electrocatalytic properties lies on the binding behavior of the metal center with the ligand sphere.

Many applications of MPcs as redox active materials in the aqueous solutions are based on the oxidation of either the metal center or the phthalocyanine ring [26].

Metallophthalocyanines have the ability to gain or lose many electrons and still retain their molecular structure and stability due to their dual donor -acceptor function [26,33]. This property accounts for their ability to exhibit electrocatalytic activity towards various technologically important redox reactions ranging from use in organic synthesis, removal of waste from water, to detection of low concentrations of compounds. The electrocatalytic activity is believed to be mediated by the metal and/or the ring because electrocatalytic activities are generally observed at potentials close to those of the metal and/or the ring [34]. The catalytic activity of the MPc complex largely depends on the particular central metal and the total oxidation state of the complex as well as the presence of substituents on the MPc backbone [35].

The established mechanism of electrocatalysis by MPcs is believed to be a two-step process initiated by the electrochemical oxidation of the central metal or the ring, followed by the transfer of electrons from the species being oxidized to the metal or the ring, regenerating the initial catalyst. Equations (2.1) and (2.2) show the mechanism for metal-based electrocatalytic oxidation of an analyte:

$$M^{II}\,Pc^{-2} \rightarrow M^{III}Pc + e^{-} \qquad (2.1)$$

$$M^{II}Pc^{-2} + A \rightarrow M^{II}Pc^{-2} + A_{OX} \qquad (2.2)$$

where A is the analyte of interest and $A_{ox}$ is the oxidation product of A [36].Many studies have been done to detect analytes using CoTCPc. In a previous study amitrole was detected using CoTCPc and SWCNTs linked with ethylene amine [37].

## 2.2 Polyaniline

Among the family of intrinsically conducting polymers (ICP) polyaniline (PANI) has been found to be attractive and extensively studied owing to good environmental stability, ease of synthesis, low cost,high electrical conductivity and mechanical flexibility attained by the polymer[38] .It has unique multiple oxidation states as well as acid /base doped /dedoping response which has actually make it excellent for acid/bas chemical vaporsensor. All these properties have prompted its potential application in various devices such as super capacitors[39],sensor [40],electrochromic[41],actuators [42].

### 2.2.1 Discovery

The discovery of polyaniline can be dated back to its intermittent report in the early $20^{th}$ century. Investigation continued until 1862 when the ultimate report included the electrochemical method for the determination of small quantities of aniline [43].The hypothesis then survived through some experiments by A.G MacDiamid and his co-workers by demonstrating that the conductive state of polyaniline occurred from the protonic doping of emeraldine form of polyaniline [44].This conductive polymer polyaniline continued to extensively gained attention, offering chances to deal with basic matters of importance to technology including e.g. metal –insulator.

### 2.2.2 Application of polyaniline

The polyaniline has electronic, magnetic, and optical properties similar to metals, in addition to the flexibility and processibility of conventional polymers [45]. PANI has potential applications in various technologies like electromagnetic shielding, conductive coating, corrosion protection, artificial muscles, bio sensing, molecular sensors, secondary battery electrodes, super capacitors, catalyst substrate, photo catalyst and conducting molecular wires. Considering these good properties potential application of PANI and ability to support positive as well as negative

carriers due to the presence of conjugated π-electrons along the backbone [46],it can be used in synthesis of heterostructures nano composites (NCs).Polyaniline –semiconductor nanocomposite are known to possess quite different chemical, physical, optical and electrical properties from those characteristic of the parent polyaniline due to the interaction of delocalized carries between semiconductors quantum dots and PANI [17].These nanocomposite materials play a promising role in the fabrication of electronic device that combine superior electronic, magnetic and optical properties.

### 2.2.3 Structure and oxidation state of polyaniline

The structure of polyaniline in its mixed oxidation state is shown in Fig 2.2, n equals the degree of polymerization (DP) .The polyaniline structure showed two main units diiminoquinone – diaminobenzene as shown Fig 2.2 during protonation these two trapped unit in the emeraldine base are delocalized and the resulting emeraldine salt is formed.Thus emeraldine base is best considered as the most useful form of polyaniline [47],apart from been highly stable at room temperature the doped form which is emeraldine salt (ES)is highly electrically conducting [48].The two other forms of polyaniline Leucomeraldine and Permigraniline are poor conductors even in their doped state.This transformation of polyaniline to different forms with different colors, apart from the oxidation state showed part of its uniqueness in its properties compared to other polymers.The emeraldine salt (green colour ) obtained as the product of the polymerisation of aniline in acidic medium (electrolyte ) can easily be further oxidised to pernigraniline (dark blue colour )which can further be treated with alkali to form violet pernigraniline[49].However emeraldine salt can also be reduced to Leucomeraldine. All the various stage of reduction and oxidation conformation and colours has led to the difference in the conductivity of polyaniline which has provided its application in some devices such as super capacitors

electrochromic[50].Fig 2.3 showed the different structure of polyaniline in its doped form from fully reduced Leucomeraldine via protoemeraldine to fully oxidisedpernigraniline.

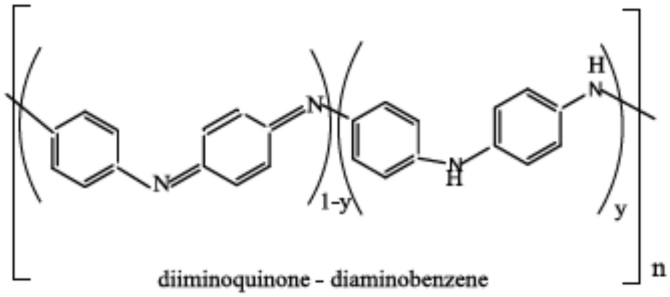


**Figure 2.2: Structure of polyaniline** [51]**.**

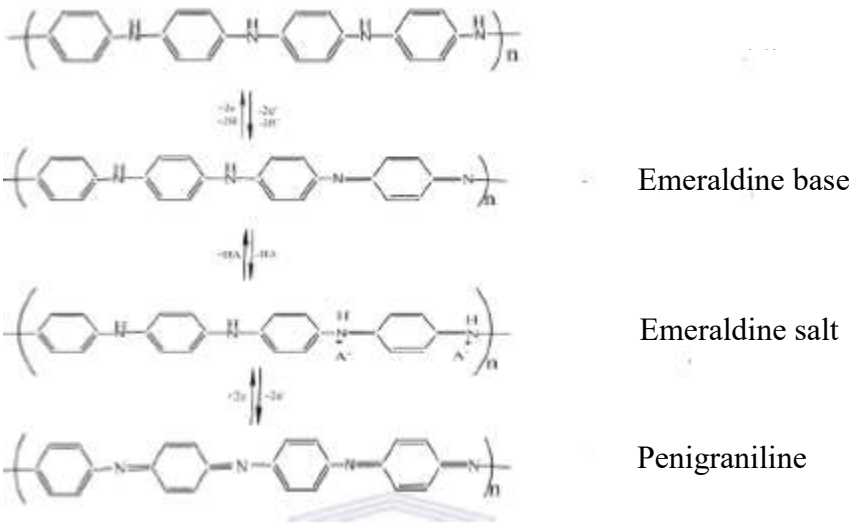


**Figure 2.3 Different structures of polyaniline in its doped form** [51]**.**

### 2.2.4 Conductivity in polyaniline

Conductivity in polyaniline makes it one of its uniqueness compared to other electro conducting polymers in that the formation of the radical cations in the mechanism as well as the conjugation double bond system involve nitrogen atoms whereasin other electro conducting polymers,the formation of their radical cations ions involve the carbon atoms [52].As a result the electrical

conductivity of polyaniline reliance is on both the level of oxidation and reduction.Thus emeraldine form of polyaniline provides the opportunity to be protonated by doping to form a conducting form of emeraldine salt as illustrated in Figure 2.4 [17].

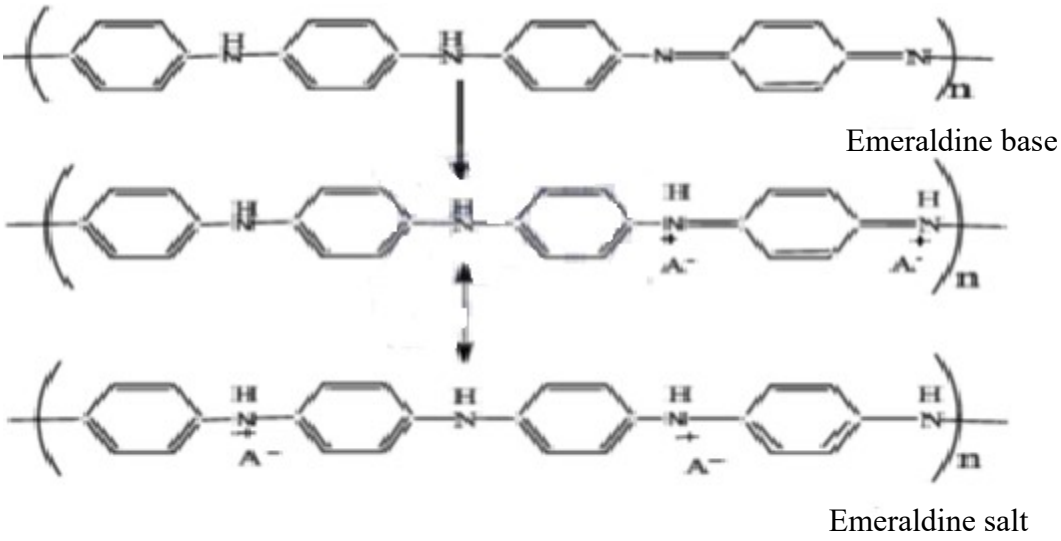


**Figure 2.4 Schematic illustration of doped form of polyaniline (emeraldine salt) for protonation** [51]**.**

### 2.2.6 Synthesis of Polyaniline

The method of synthesis commonly adopted to prepare polyaniline is electrochemical chemical oxidative polymerization method. The reaction mechanism of the two techniques is based on oxidative coupling of monomer to produce polymer [49].

### 2.2.7 Chemical oxidative polymerization

The method is broadly used to synthesize large amount of conducting polymers and does not involve the use of electrode.The oxidation of monomers to cations radical and coupling of these

cation radicals to form dications in a repetitive process and in the presence of an oxidizing agent to produce polymer is referred to as chemical oxidative polymerisation.In a chemical synthesis the monomer is exposed to an oxidising reagent in a basic medium e.g. ammonium persulfate (APS) or anhydrous $FeCl_3$,the reaction is then initiated resulting in the formation of the polymer in its doped and conducting state.Figure 2.5 showed a typical illustration of chemical oxidation reaction e.g. polyaniline.A neutral polymer can as well be achieve if the material is made to pass through  a strong reducing agent such as sodium borohydridehydrazine or ammonia [53].

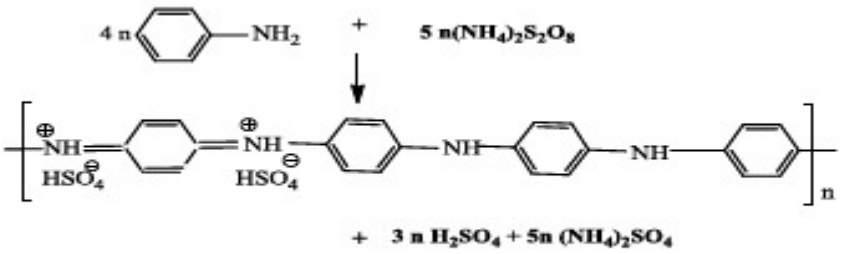


**Fig 2.5 Schematic illustration of chemical synthesis of polymer (e.g. polyaniline)** [51]**.**

### 2.2.8 Electrochemical polymerization

In electrochemical polymerization,the use of electrodes is alternatively involved.The process is usually carried out in a single or dual –compartment cell by adopting a standard cell three electrode configurations in a supporting electrolyte normally dissolved in an appropriate solvent [54].The condition of method can be through potentiostatic (under voltage condition),potentiodynamic or galvanostatic (under current condition) using a suitable power supply.Electrochemical method of synthesis is a simple method to take up and apart from the advantage of obtaining a conductive polymer which is doped at the same time, the process allows

a broadly choice of cation ion and anions as “dopant ion “for use [55].The synthesis method by electro polymerization also depends on oxidation reaction, although reduction is also possible. The general mechanism involved in the electrochemical synthesis of polyaniline from aniline monomer is illustrated in Figure 2.6, showing the radical cation from aniline monomer which is considered to be the rate determining step of the reaction coupling to generate dimerization ,removal of two $H^+$ ion to generate a neutral dimer ,and further chain propagation through oxidation of the neutral dimer into dimer radical that can react with a monomer or dimer ,giving rise to elongation of the polyaniline backbone.The chain propagation finally leads to formation of a polymer (e.g polyaniline film on the electrode [55].

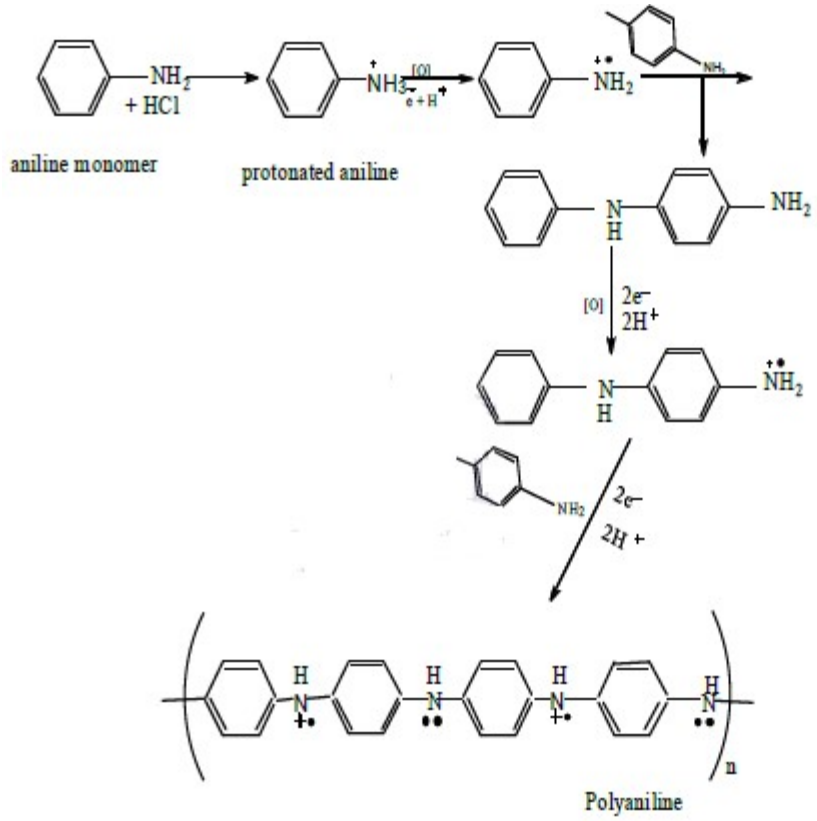


**Fig 2.6 Possible reaction mechanism to generate polyaniline from polymerisation of aniline** [39]**.**

### 2.3 Metallic oxide Nanoparticles

The use of metal Nano-particles for electro-analysis has increased. This is due to their unique optical, electronic, magnetic and catalytic properties [56]. In electro analysis, nanoparticles are used as functional materials. There are four main advantages in using NP modified electrodes with regard to electro analysis which are high effective surface area, mass transport, catalysis and control over the local micro environment [57].

#### 2.3.1 Cobalt oxide nanoparticles as electrode modifiers

Transition metal oxide nanoparticles have variable oxidation state which gives them many applications. Cobalt oxide $Co_3O_4$ is an important transition metal oxide because of its application in various fields of research and industry including pigments, gas sensor, magnetic materials, catalyst, anode materials for rechargeable Li-batteries, electro chromic devices, electrochemical systems and high-temperature solar selective absorbers[58]. The difference in oxygen defect, oxygen holes and oxygen adsorbed in different state of cobalt in $Co_2O_3$, a mixed valance material that is formally CoII CoIIIO4 ) are thought to be the reason for high activity and selectivity of this metal oxide catalysts [59].

#### 2.3.2 Synthesis of Cobalt oxide nanoparticles

$Co_3O_4$ nanoparticles have been prepared by various physical and chemical techniques such as combustion method, microwave irradiation, hydrothermal/solvothermal method [60], sol-gel process [61], chemical spray pyrolysis and polyol method [62]. The thermal decomposition method has been widely used due to its simplicity. This technique offers advantages of low temperature processing, short reaction time and production of inorganic nanomaterial's with narrow size distribution [58].

## 2.4 Physical characterization techniques

### 2.4.1 Fourier-Transform Infrared Spectroscopy

Fourier Transform Infrared Spectroscopy (FTIR) is a commonly used technique for the identification of the chemical functional groups in a compound [63]. The IR radiation passes through a sample and some of the radiation is absorbed by the sample while the rest is transmitted then a signal is sent to the detector creating a molecular fingerprint of the sample i.e. IR spectrum [64,65]. Each functional group within a molecule will have various bond energies resulting in infrared absorption at different wavelengths. When a molecule vibrates, the atoms move towards and away from each other at a certain frequency [66]. In this work, FTIR was used to confirm the functional groups present in CoTCPc, polyaniline, cobalt oxide and PANI-CoTCPc.

### 2.4.2 Infra-red spectra for metallophthalocyanines

The infrared spectra of MPc complexes are complex. The main bands in the aromatic MPc ring that are crucial and visible are the C-H stretching vibration at around 3030 $cm^{-1}$, the C-C benzene ring stretching vibrations at around 1600 $cm^{-1}$ and 1475 $cm^{-1}$ and the C-H out-of plane vibrations at 750–790 $cm^{-1}$[65]. Metal sensitive bands appear at about 1490 $cm^{-1}$ and 1410 $cm^{-1}$.

## 2.5 Electrochemistry instrumentation

Electrochemistry studies the relationship between electrical and chemical occurrences. It is one effective technique to study electron transfer properties. When electron transfer is between a solid substrate and a solution species it is termed heterogeneous process [67]. Inversely if electron transfer reaction occurs between two species both of which are in solution the reaction is homogeneous. Therefore, electrochemistry can specifically be defined as the science of structures and processes at and through the interface between an electronic (electrode) and an ionic conductor (electrolyte) or between two ionic conductors [68]. Due to its diversity electrochemistry has found application in various working fields such as: analytical chemistry, environmental, electrochemistry, micro electrochemistry, solution electrochemistry and surface electrochemistry [69].

### 2.5.1 The Potentiostat

The working principle of a Potentiostat actually depends on its connection to the electrochemical cell.Thus according to the typical illustration which is the common one, it controls the potential of the counter electrode CE against the working electrode WE so that the potential difference between the reference electrodes (RE) is distinct and agrees with the values specified by the user. Therefore in potentiostatic /galvanostatic mode the current flow between the working electrode and the current is controlled.The potential difference between the reference electrode and working and the current flowing between the current and working electrode are constantly monitored [70].

### 2.5.2 Electrochemical cell and electrodes

A typical electrochemical cell may consist of the following a sample dissolve in a solvent, or an ionic electrolyte and obviously, three or sometimes two electrodes.They can come in different shapes, sizes and materials (e.g. glass, Teflon ,polyethylene etc.).The choice of cell also depends on the amount of sample the technique and the analytical data to be achieved .A glass cell with close fitting that have ports electrodes and purging line is commonly used.The arrangement of the electrode should also be considered.More often, the reference electrode is placed as close as possible to the working electrode and sometimes there may be need to place the reference in a separate compartment to avoid contamination[70].

### 2.5.3 Electrodes

Generally an electrode provides the interface across which a charge can be transferred or where the effect of the charge can be felt e.g. the working electrode (WE) which is where the reaction of interest takes place.So the electrode is an utmost important part of the system. The shape, size and analyte and style of modification on the surface all depends on the application process[71].

### 2.5.4 The reference electrode (RE)

The reference electrode is an electrode with a steady and recognizable electrode potential .It is used as point of reference to control and measure the potential of other electrodes.The saturated calomel electrodes (SCE),silver /silver chloride Ag/AgCl) electrode are the most commonly used reference electrode for aqueous solutions[72].

### 2.5.5 Counter electrode (CE)

The counter electrode (also known as auxiliary electrode) is usually made of an inert material of platinum Pt or metallic foil, gold (Au),graphite or sometimes glassy carbon may be used Counter electrode does not usually take part in the electrochemical reaction but the total surface act as

source of electron so that current can flow between the working electrode and counter electrode which make it not to be isolated from the reaction.The surface area must however be higher than that of the working electrode so that it will be not a limiting factor in the kinetics of the process under investigation [73].

### 2.5.6 Working electrode (WE)

The working electrode is where there reaction or transfer of interest is taking place.At an appropriate potential oxidation or reduction of a substance on the surface of the working electrode will bring about a mass transport of a new material along with current been produced. The commonly used materials for working electrodes are glassy carbon (GC),Platinum (Pt),gold (Au).Others include small mercury drop and film electrodes.The size and shape also varies and depends on application.The quality of an ideal working electrode includes a wide potential range low resistance as well as a surface that is reproducible [74].

### 2.5.7 Choice of supporting electrolyte

The choice of the supporting electrolyte depends on the chemical reactions taking place on the electrode surface and taking into account the solubility of the reactants. Water and organic solvents are the most used electrolytes in electrochemical analysis. Purging with nitrogen is necessary in order to remove signals due to oxygen during analysis [75].

### 2.5.8 Mass Transport Processes

The fundamental movement of charged or neutral species in an electrochemical cell to the electrode surface is facilitated by three processes which are diffusion, migration and convection [76].

Diffusion is a mass transport due to spontaneous movement of analyte species from regions of high concentrations to lower ones [67,77]. Electrochemical reactions are heterogeneous and hence they are frequently controlled by diffusion. If the potential at an electrode oxidizes or reduces the analyte, its concentration at the electrode surface will be lowered and therefore more analyte moves to the electrode from the bulk of the solution which makes it the main current-limiting factor in Voltammetric process [73]. Although migration carries the current in the bulk solution during electrolysis diffusion should also be considered because as the reagent is consumed or the product is formed at the electrode, concentration gradient between the vicinity of the electrodes and the electro active species arise. Under some circumstances the flux of electro active species to the electrode is due almost completely to diffusion [78].

Migration is the movement of charged particles due to the influence of an electric field. It is undesirable and is eliminated by addition of a large excess of easily ionisable salt (supporting electrolyte) [79,80]. Convection involves the movement of charged particle due to a mechanical energy associated with stirring or flow of the solution or rotating of the electrode. It is eliminated by maintaining the cell under quiet and stable condition [78].

### 2.5.9 Cyclic Voltammetry

Cyclic voltammetry is a powerful electro analytical technique that provides information about the characteristic electrochemical processes an analyte undergoes in solution [81]. During cyclic voltammetry the potential of an electrode is scanned linearly from an initial potential to a final

potential and then back to the initial potential. The potential at which the peak current occurs is known as the peak potential ($E_p$) where the redox species has depleted at the electrode surface and the current ($I_{pa}$-anodic peak current) or ($I_{pc}$-cathodic peak current), gives an indication of the rate at which electrons are being transferred between the redox species and electrode.

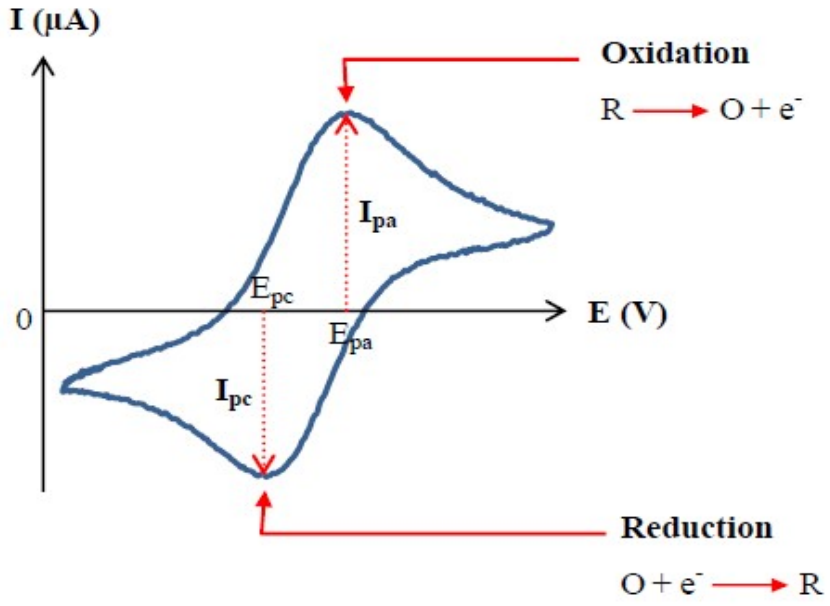


**Fig 2.7: A typical cyclic voltammogram for a reversible single electro transfer [82]**.

The peak current $I_p$ in this voltammogram is given by Randles-Sevcik equation

$$I_p = (2.69 \times 10^5) n^{3/2} A c D^{1/2} \qquad \textbf{(2.3)}$$

$I_p$ is the peak current (in amperes)$n$ is the number of electrons passed per molecule of analyte oxidized or reduced A is the electrode area (in $cm^2$), D is the diffusion coefficient of analyte (in $cm^2\ s^{-1}$), ν is the potential sweep rate (in $V\ s^{-1}$) and C is the concentration of analyte in bulk solution (in mol $cm^{-3}$) [83].

### 2.5.10 Differential Pulse Voltammetry

Since the sensitivity of CV is low the aim of pulsed voltammetricmethods is to lower detection limits. The relationship between current and concentration gives quantitative information about the system studied and this can be clearly seen if diffusion controls the current magnitude [84].In differential pulse voltammetry (DPV) fixed voltage pulses are superimposed on a linear potential ramp and are applied to the working electrode at a period of selected time just before the potential pulse drops. The current is measured twice which first at a point just before the pulse is being imposed and then again just before the pulse begins to drop. In DPV when a potential pulse is applied to an electrode the capacitive current flows proportionally to it but decays exponentially with time. The magnitude of the faradaic currentdecreases as an exponential function versus $(t)^{1/2}$ [85].

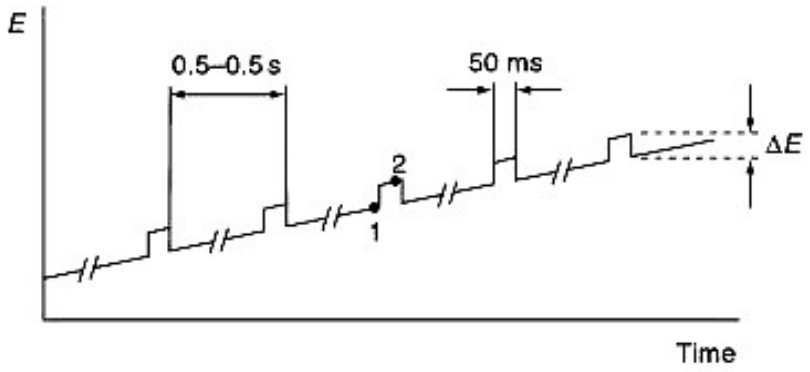


**Fig 2.8: Excitation signal for differential pulse voltammetry [78].**

Figure 2.8 shows a typical diagram on how potential pulses, approximately for 50 milli -seconds, are applied on a linear ramp. The first current measured$i$ ($t_1$) will be subtracted from the second one$i(t_2)$ and the difference [$\Delta t$ = $i(t_2)$- $i(t_1)$] will be plotted against the applied potential. The

resulting voltammogram will show current peaks which are in direct proportion with the concentration of the electro active species of interest. In DPV the charging current contribution is so small, about more than an order of magnitude than that of normal-pulse voltammetry that it is negligible. The Faradaic current decays accordingly to the square root of time producing an excellent signal to noise ratio. Due to these significantly enhanced characteristics DPV enables the detection at nano molar level (1 $\mu gL^{-1}$) thus proving hugely useful in electrochemical sensing applications such as heavy metal detection [86] and various organic compounds such as ascorbic acid, [87]aflatoxin B 1 [88], uric acid [84] and nitro phenol [89].

### 2.5.11 Chronoamperometry

The basis of all controlled potential techniques is the measurement of the current response to the applied potential of which chronoamperometry is one of them [85]. It involves stepping the potential of the working electrode from a value where there is no faradaic reaction to a potential where the electro active species reacts until its concentration is effectively zero. The current decreases with time due to the decreasing amount of the electro active species at the electrode vicinity .The current decay is described by the Cottrell equation 2.4

$$i(t) = \frac{nFA \quad ^{1/2}}{\pi^{1/2} t^{1/2}} = kt^{1/2} \qquad (2.4)$$

Where i(t) = current

N= number of electrons

F =Faraday's constant

C =bulk concentration of electroactive species

D=diffusion coefficient

T= lapsed time (s)

K= catalytic rate constant $M^{-1}s^{-1}$

This technique is often used for measuring the diffusion coefficient and the surface area of the working electrode [90].It can also be used as a preconcetration tool especially for metal ions which can be concentrated by reduction onto the electrode surface [91].

### 2.5.12 Electrochemical Impedance

Impedance methods are based on perturbation of the electrochemical cell with an alternating signal of small magnitude and monitoring of the response [91]. One way of modeling electrochemical processes at the electrode-solution interface involves comparison of the electrochemical process to an equivalent electrical circuit containing combinations of resistances and capacitances for example the Randles model inset shown in Figure 2.9[16].

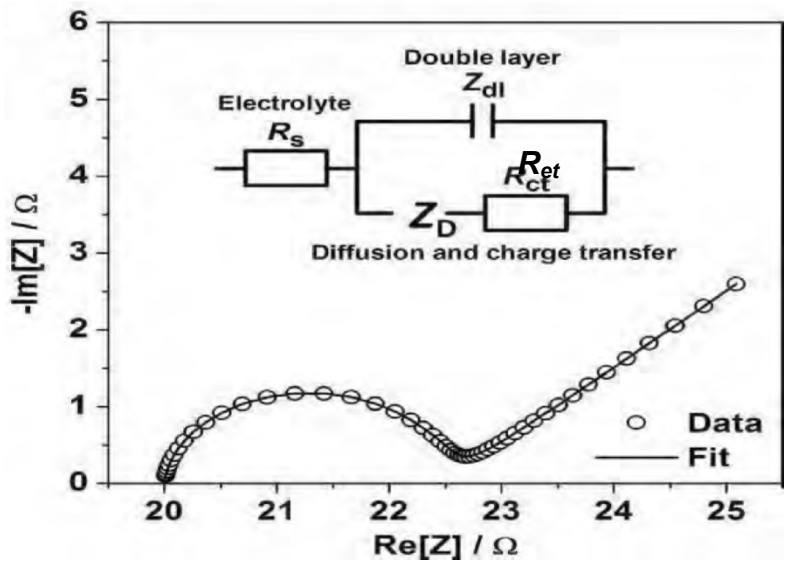


**Fig 2.9: Typical Nyquist plot [92].**

The semicircle portion observed at higher frequencies, corresponds to the electron transfer-limited process whereas the linear part is characteristic of the lower frequency range and represents the diffusion-limited electron transfer process [90]. In the case of very fast electron-transfer processes, the impedance spectrum could include only the linear part whereas a very slow electron-transfer step results in a big semi-circle region that is not accompanied by a straight line [91]. The semicircle diameter equals $R_{et}$. The intercept of the semi-circle with the Re[Z]-axis at high frequencies is equal to $R_s$, the solution resistance [79].

The rate of electron transfer at the electrode surface is expected to increase when a catalyst is attached to the bare surface, i.e the electron-transfer resistance ($R_{et}$) at the electrode surface should decrease when a catalyst is used as the modifier [75]. The semi-circle diameter ( $R_{et}$) in the Nyquist plot is expected to be smaller when an electrode is modified with a catalyst than when it is bare. Therefore a comparison of the semi-circles obtained from the bare and modified electrodes determines whether the modifier is a catalyst or not. Depending on the efficiency of the catalyst $R_{et}$ can be so low i.e is insignificant when compared to $Z_W$ the Warburg impedance due to diffusion of the ions of the redox probe through the solution [91].

### 2.5.13 Bode Plots

The nature of the Bode plots confirms the structural differences between the bare electrode and modified electrodes.Bode plots (phase angle versus log f)Fig 2.10a),shows a well- defined symmetrical peak for the bare electrode at particular angle and corresponding frequency representing the relaxation process at the electrode solution interface [22].This relaxation process shifts to different phase angles and frequencies on modification of the electrode. These shifts

indicate that the reactions are now occurring at a modified surface rather than the bare electrode [24].The slopes in Fig 2.10b should be close to -1 for ideal capacitors.

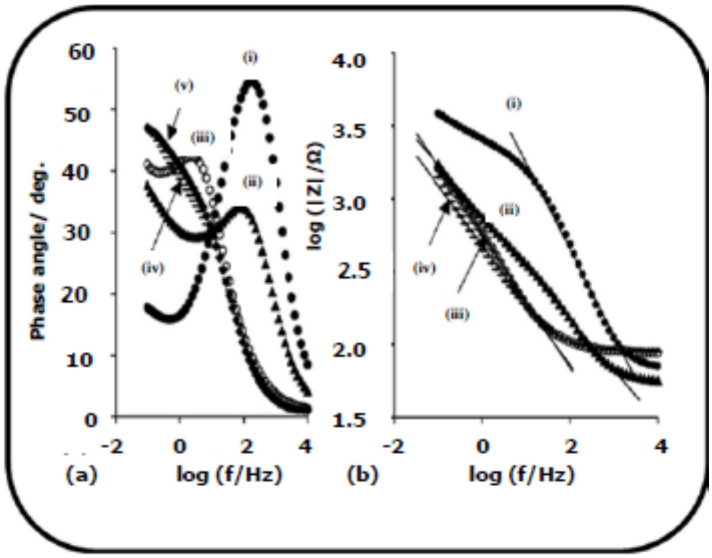


**Fig. 2.10: Typical Bode plots of (a) phase angle vs. logarithm of frequency and (b) logarithm of complex impedance vs. logarithm of frequency for the following electrodes (i) bare, (ii) CoTAPc, (iii) SWCNT-CoTAPc(linked), (iv) SWCNT/CoTAPc(mix) and (v) SWCNT in 0.1M KCl containing 1 mM [Fe(CN)6]3−/4− solution** [93]**.**

**2.6 Electrocatalysis**

Electrocatalysis can be defined as a process whereby, an electro catalyst participate as a catalyst in electrochemical reaction. The electro catalyst can be a specific form of catalyst that function at the surface of the electrode or may be the surface of the electrode itself [73].Thus catalyst materials modify and increase the rate of chemical reaction without being consumed in the process.The process can be heterogeneous which involves chemical reaction occurring at the surface of the electrode and electron transfer usually take place leading to a new product formation (in catalytic electro synthesis)or homogeneous reaction which is a sequence of reactions that involve a catalyst in the same phase as the reactants. However a homogeneous catalyst is most commonly co-dissolved in a solvent with the reactants (coordinating complex or

enzymes ) [94].The ability to catalyse some reaction is one of the most outstanding properties of conducting polymers. The kinetics of electrode processes of some solution specie is able to be improved by a thin layer of conducting polymerdeposited onto the surface of a substrate electrode. These electrocatalytic processes at a conducting polymer electrode is presently yielding application in various fields of electrochemistry [95].

Three processes are considered to be happening during the electrocatalytic conversion of solution species at conducting polymer modified electrode.Firstly heterogeneous electrons transfer between the electrode and a conducting polymer layer and electron transfer within the polymer film [96].This process is normally accompanied by the movement of charge compensating anions and solvent molecules within the conducting polymer film and possibly changes the conformational structure of the polymer [95].However many factors determine the rate of this process and which include electric conductivity of polymer layer electron self-exchange rate between the chains /or clusters of polymer and anion movement within polymer films also seems to be greatly significant. Secondly, the diffusion of solution species to the reaction zone where the electrocatalytic conversion occurs.Unlike simple electrode reaction this process can be more complicated in case, the diffusion of species within the film in addition to the possible electrostatic interaction of this specie with the polymer film should be taken into account[50].

In the third process a chemical (heterogeneous) reaction takes place between solution species and conducting polymer.Consequently the kinetic behaviour and Voltammetric responses are difficult to interpret and some simplify model has been considered for this to a greater extent. This includes experimental technique (e.g. spectroelectrochemistry ) that has been able to yield valuable information on the subject [81].In which case various catalytic surfaces have been

successfully employed for facilitating the detection of environmentally relevant analyte with otherwise slow electron transfer kinetics [32].

In this work electro catalysis method engaged the transfer of electrons between the analyte and electrode surface. In this regard the catalyst on the modified electrode becomes oxidised in the electrolyte and then interacts with the analyte which are mostly in their reduced state. There is electron process taking place which leads to the oxidation of the analyte and simultaneous reduction of the catalyst .The schematic illustration is shown in Figure 2.11

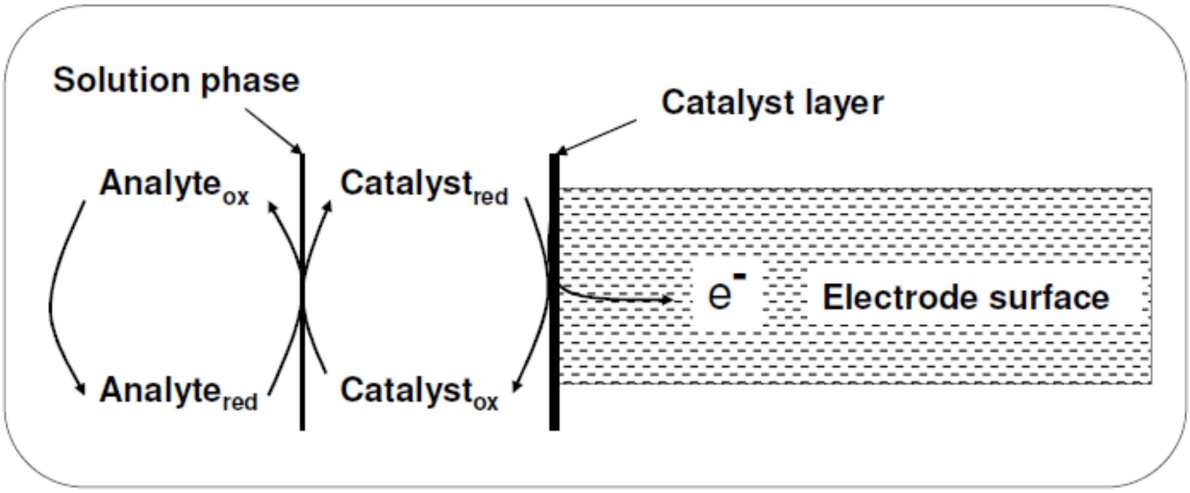


**Fig 2.11 Schematic diagram of electrocatalytic process on the surface of a modified electrode** [51]**.**

### 2.7 Chemical modified Electrodes (CMEs)

Chemically modified electrode (CMEs) involves an approach to electrode system design that finds application in electrochemical investigation which includes the relationship of heterogeneous electron transfer and chemical reactivity of electrode surface as well as ionic transport phenomena in polymers[15]. The distinguishing feature of a chemically modified

electrode is that it can allow a thin film of selected conducting material to be bound on its surface for the purpose of improving the chemical electrochemical optical, electrical transfer of electron and other desirable properties of the film in a rational chemically designed manner [97].Therefore the significant drive for modifying electrode surface is electrocatalysis of the electrode reaction of an analytical desired substrate.It is often observed that redox reaction of analyte on a naked/unmodified electrode surface using voltammetry technique such cyclic voltammetry or square wave voltammetry are slow so that oxidation or reduction occurs at a potential that is greatly higher than positive or negative respectively than the expected thermodynamic potential [98].Such situation can be sorted by accelerating the desired reaction with an immobilized mediator catalyst.The mediator is attached on the surface of the electrode to function as facilitator for charge transfer between the analyte and electrode (as illustrated in Figure 2.12).The oxidized form of the mediator catalyst is rapidly reduced and then its reduced form reacts with the analyte specie in solution it can thus be indicated that the electron transfer occurred between the mediator and the electrode and not between electrode and the analyte directly.From the illustrated equation below a mediator can be represented by M and the analyte A[99]

$$Mox + ne^{-} \rightarrow Mred \qquad (2.5)$$

$$Mred + Aox \rightarrow Mox + Ared \qquad (2.6)$$

Therefore three features can be ascribed to a mediated electro catalysis firstly the catalyzed reaction occurs near the formal potential of the mediator catalyst couple (oxidized and reduced form)unless a catalyst-analyte abduct is formed in which case reaction occurs at the potential for abduct. Secondly the formal potential of the mediator catalyst and that of the analyte must be

alike as this decreases the reduced plus the analyte reaction energy thus the choice is also associated with a maintained and agreeably fast reaction rate.And finally for a successful catalyzed reaction of analyte to occur the reaction must be less negative or positive potential for reduction or oxidation respectively than required for the naked electrode reaction of analyte [100].Therefore under this condition a surface concentration of an electrochemical material can be determined by applying the following equation below with respect to surface confined specie in this reverse ,$I_P$ (μA) is directly proportional to the scan rate, v ($mVs^{-1}$)

$$\Gamma = \frac{Q}{nFA} \qquad (2.7)$$

$$I_P = \frac{nn^2 F^2 A\Gamma v}{4RT} \qquad (2.8)$$

Chemically modified electrodes can be obtained by various methods which include attaching molecules on the electrode surface through adsorption, covalent binding andself-assembled monolayer etc. [98]by immobilizing multimolecular layers films on electrode (mainly polymer) and by designing heterogeneousand spatially defined layered microstructures onto electrode surface or within the bulk of the electrode materials [73]. Modification of electrodes can be done in different ways such as irreversible adsorption, covalent attachment of a monolayer and coating the electrode with a film of polymer or other material [55].The type of modification used is based mainly on the possible application. For this workthe glassy carbon electrode was used as an electro analytical sensor thus modification was directed towards selectivity and lower detection limits for some environmental pollutant. Polyaniline cobalt phthalocyaninato doped with cobalt oxide nano particles was used for the modification of the glassy carbon electrode by drop-dry method.

Electrode modification can be achieved by using different techniques such as drop-drying, spin coating, electrochemical polymerization and electrodeposition. These processes are described below;

- The drop-dry method involves placing a drop of the modifier on the electrode surface and letting it dry [101]. The major advantage of this approach is that the coverage is immediately known from the original solution concentration and droplet volume.
- Dip-drying is when the electrode is immersed into a solution containing the modifier for a specific period of time sufficient for spontaneous film formation to occur by adsorption [102].
- Electrodeposition also referred to as redox deposition, involves film formation where the modifier is oxidized or reduced to its less soluble state [103]. This can be done by applying a fixed potential over a fixed period (chronoamperometry) while stirring ) or by using cyclic voltammetry [104].
- Electrochemical polymerization – a solution containing a monomer is oxidized or reduced to an activated form that polymerizes to form a polymer film directly on the electrode surface. Unless the polymer film itself is redox active, electrode passivation occurs and further film growth is prevented [54].
- Composite –the chemical modifier is simply mixed with an electrode matrix material, as in the case of an electron transfer mediator combine with the carbon particles plus binder) of a carbon pate electrode [105].

The desired effect of electrode modification in most cases is an increased catalytic effect towards a certain analyte. Electro catalysis at a modified electrode is usually an electron transfer reaction between the electrode and some solution substrate which when mediated by an immobilized

redox couple (the modifier) proceeds at lower over potential than would otherwise occur at the bare electrode [98].

### 2.8 Summary of the aims of the research

The application of nanotechnology is now subject of concern in terms of developing electrochemistry. Polyaniline and nanoparticles are known to enhance electrocatalysis by improving surface area of the electrode and producing excellent catalytic character compared to bare glassy carbon electrodes. Chemical or physical coupling of these nanomaterial's with phthlocyanines can produce very efficient electrochemical sensors. Based on this known attractive characteristics, the research is being pursued.

# CHAPTER 3

# EXPERIMENTAL

## 3.0 Introduction

In the present chapter, chemicals, equipment, synthetic routes and characterization techniques used in this study are reported. The synthesis of $Co_2O_3$NPs, CoTCPc, PANI, PANI-CoTCPc and PANI-CoTCPc doped with cobalt oxide nanoparticles were done and evaluated for their electro catalytic towards amitrole. Electrochemical characterization of amitrole was evaluated using cyclic voltammetry, impedance spectroscopy (EIS), bode plots, chronoamperometry, linear sweep and differential pulse voltammetry (DPV). Factors such pH and scan rate were investigated to evaluate the applicability of the best electrode in the detection of amitrole.

## 3.1 Chemicals and reagents

Chemicals which were used in this study were of analytical grade and were used without further purification. Ammonium molybdate $(NH_4)_2MoO_4$), amitrole, trimellitic acid anhydride ($C_9H_4O_5$), Potassium ferrocyanide ( $K_3[Fe(CN)_6]$), aniline ($C_6H_5NH_2$), ammonium persulphate, ammonium chloride ($NH_4Cl$), urea ($CO(NH_2)_2$ ), sodium hydroxide(NaOH), cobalt (II) chloride ($CoCl_2.6H_2O$), thionyl Chloride ($SoCl_2$), hydrogen peroxide ($H_2O_2$), nitrobenzene ($C_6H_5NO_2$), dimethyformamide (DMF), ethanol ($C_2H_5OH$), potassium chloride (KCl),Hydrochloric acid (HCl), di-potassium hydrogen orthophosphate ($K_2HPO_4$) and potassium di-hydrogen orthophosphate ($KH_2PO_4$).

## 3.2 Equipment

FTIR spectra were obtained using Thermo scientific Model equipped with OMNIC software. Sonicator model KQ-250B was used for agitation of samples. Electrochemical analysis was performed using Auto labpotentiostat PGSTAT 302N equipped with NOVA version 1.10 software and encompassed with a three electrochemical cell comprising of a glassy carbon electrode (GCE), platinum wire counter and Ag|AgCl reference electrode.

## 3. 3 Synthesis procedures

### *3.3.1 Cobalt Tetracarboxyl-phthalocyanine (CoTCPc)*

The synthesis of CoTCPc was done according to a reported procedure [30]. Trimellitic acid anhydride (4.8 g), urea (15 g), ammonium chloride (0.27 g), ammonium molybdate (0.27 g) and cobalt (II) chloride (4.10 g) were mixed and finely ground. The mixture was then added to 40 mL of nitrobenzene and heated under reflux at 185 $^0$C for 4 h. A dark coloured solid was formed in solution, filtered off and washed several times with methanol. Then the solid was Soxhlet extracted for 12 h to further remove any nitrobenzene left and then dried overnight at 70 $^0$C to form the amide complex. Finally, the amide complex was boiled with 275 mL of 1 M HCl and excess NaCl. The solution was neutralized by 1 M NaOH and then separation of the solid was done by vacuum filtration. To the resultant sodium salt solution 1 M HCl was added to precipitate the tetracarboxyl-complex. The solution was then filtered and the resultant blue/green complex was dried at 70 $^0$C in an oven and finally stored in a desiccator prior to further procedures[37,106,107].The scheme is shown in Figure 3.1.

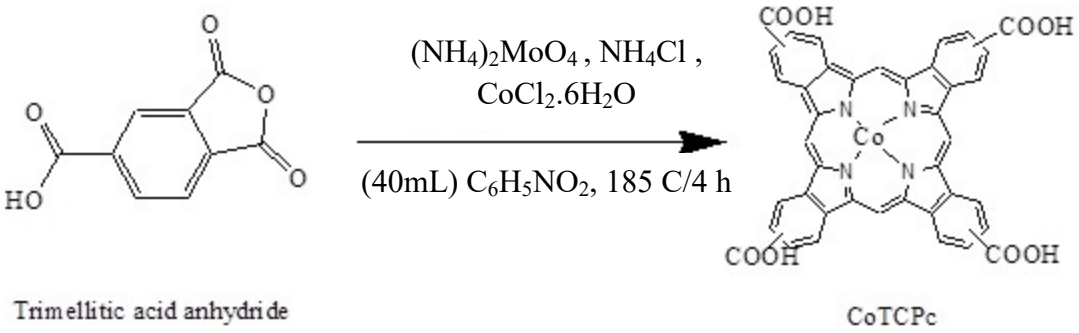


**Scheme 3.1: Synthesis of cobalt tetracarboxyl- phthalocyanine (CoTCPc) [34]**.

*3. 3.2 Polyaniline*

Aniline was first distilled under vacuum to remove impurities. The purified aniline (0.2 M) was dissolved in 10 mL of 1 M HCl aqueous solution. While maintaining vigorous stirring at room temperature ammonium peroxydisulfate (APS 0.05 M) was dissolved in 10 mL of 1 M HCl to form an oxidant solution[108]. The oxidant solution was then quickly poured into the aniline solution at room temperature followed by immediately magnetic stirring for 2h. Polymerization can be observed when green color of PANI emeraldine salt became visible. The stirring was stopped after 2h and left undisturbed to react for 24h. After which the precipitated polymer was collected by filtration and repetitively  washed with water ethanol and hexane until the filtrate became colorless Polyaniline sample was collected having been dried under vacuum at 60°C [109].

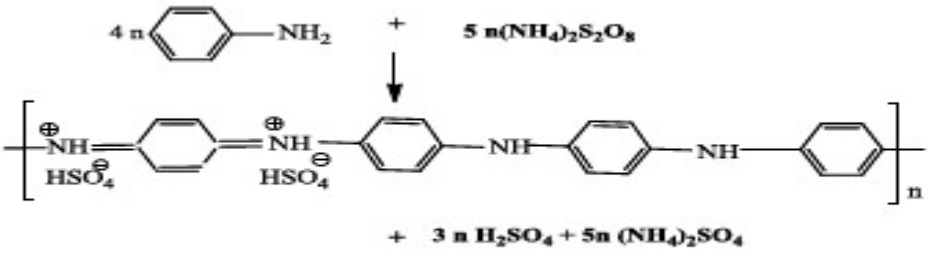


**Scheme 3.2 Schematic representation for the synthesis of polyaniline** [51]**.**

*3.3.3 $Co_2O_3$ Nanoparticles*

The synthesis of cobalt nanoparticles is shown in scheme 3.3 following a reported procedure [62]. Cobalt nitrate (0.6 M) was dissolved in 100 mL deionized water. Then 100 mL aqueous KOH (3.2 M) was added drop wise to the precursor solution. A pink precipitate appeared immediately which was easily oxidized by air and low heat or weak oxidizing agents to Co $(OH)_3$ forming a dark brown precipitate which was separated and washed with deionized water and dried in an oven at 110°C for 20 h. The dried cobalt hydroxide was ground and preserved in a desiccator [110]. Cobaltic-cobaltous oxide $Co_3O_4$ was prepared by heating the dark brown cobaltic hydroxide at 300°C. The chemical reactions for the process are illustrated in equations 3.1 to 3.4.

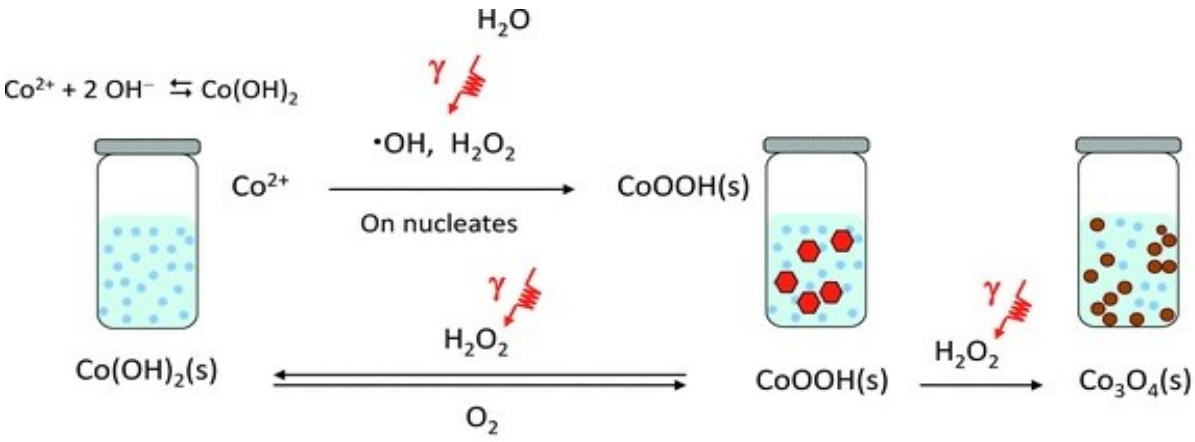


**Scheme 3.3 Schematic representation for the synthesis of cobalt oxide nanoparticles** [60]**.**

$$Co(NO_3)_2.6H_2O + KOH \longrightarrow Co(OH)NO_3 + KNO_3 \quad \text{eq. 3.1}$$

$$Co(OH)NO_3 + KOH \longrightarrow Co(OH)_2 + KNO_3 \quad \text{eq. 3.2}$$

$$4Co(OH)_2 + O_2 + H_2O \longrightarrow 4Co(OH)_3 \quad \text{eq. 3.3}$$

$$3Co(OH)_{3(s)} + \frac{1}{2}O_{2(g)} \xrightarrow{\text{Heat } 300^{\circ}C} Co_3O_4\,(s) + 6H_2O\,(l) \quad \text{eq. 3.4}$$

The synthesized cobaltic cobaltous oxide was stored a desiccator prior to further studies [23].

*3.3.4 PANI-CoTCPc complex*

A mass of 2 g of CoTCPc was stirred in a volume of 15 mL of $SOCl_2$ at 70 $^0$C for 24 h then excess $SOCl_2$ was removed by placing the mixture in a rotary evaporator for 30 min. The resultant CoTCPc-COCl was then combined with 5 mg of polyaniline (PANI) in 25 mL of DMSO with stirring and heated at 70$^0$C for 96 h. After cooling the mixture was then centrifuged and the resultant solid PANI-CoTCPc was washed several times with distilled water and ethanol. Then resultant solid was then dried and stored in a desiccator to carry out further studies [8,37]. A summary of the scheme is shown 3.4.

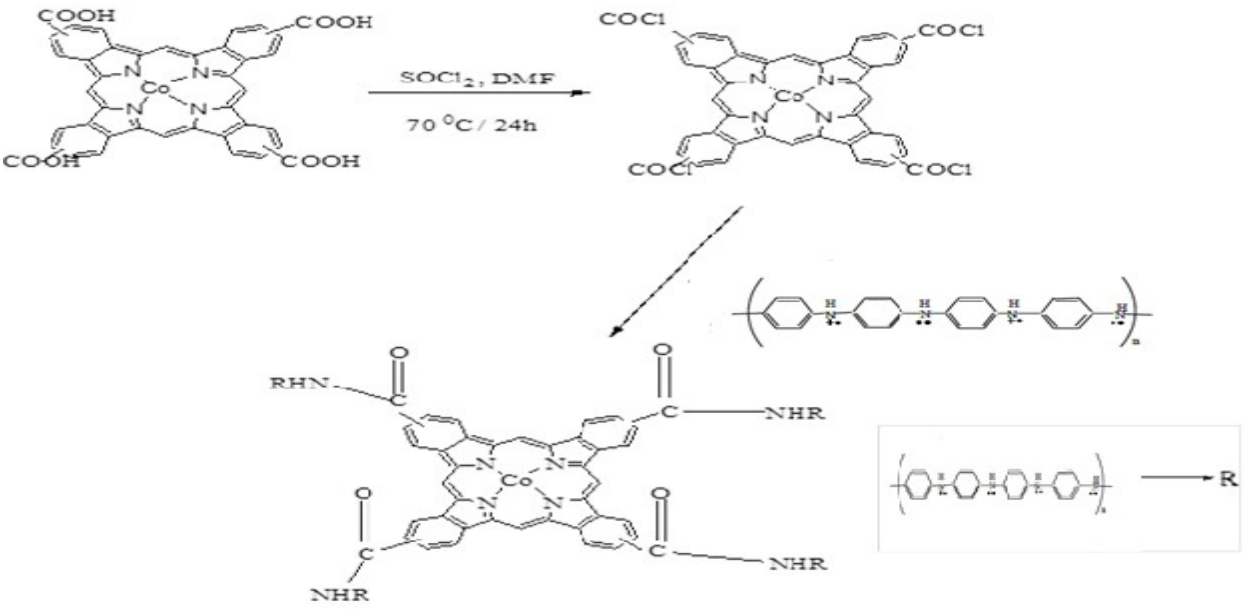

**Scheme 3.4**: Synthesis cobalt (II) phthalocyanato polyaniline (CoPc-PANI)

*3.3.5 PANI-CoTCPc doped with $Co_2O_3$ nanoparticles*

A mass of 10 mg of $Co_2O_3$ nanoparticles was added to 0.1 g of PANI-CoTCPc in 10 mL of DMF at r.t.p for 12 h. The resultant solution was ultrasonicated for 30 min and then centrifuged for 30 min. Then the solid was separated by decanting and the residue was dried and stored in a desiccator [8,93].

## 3.4 Physical characterization of CoTCPc complexes and composites

*3.4.1 Fourier Transfer Infrared Spectroscopy (FTIR)*

All the synthesized compounds $Co_2O_3$NPs, CoTCPc, PANI, PANI-CoTCPc and PANI-CoTCPc doped with cobalt oxide nanoparticles were characterized by FTIR . The 0.0100g of samples were mixed in a mortar and pesteland combined with 1g KBr to form a pellet and this was characterized within the range 400 - 4000 $cm^{-1}$ .

## 3.5. Electrode modification

The BCGE was polished with alumina paste on Buehler Felt pads and then was ultrasonically cleaned in ethanol for about 5 min. The electrode was further cleaned in water for about 5 min then finally rinsed with distilled water and then dried. A mass of 0.1 g of the prepared conjugates was dissolved in a volume of 50 mL of DMSO and these solutions were ultra-sonicated for 30 min. The cleaned BCGE was modified using the drop and dry method using CoTCPc, PANI, $Co_2O_3$, PANI-CoTCPc and PANI-CoTCPc/$Co_2O_3$NPs. The electrode was dipped in solution of the modifiers in DMSO and then dried using nitrogen gas.

### 3.5 Electrochemical characterization

#### 3.5.1 Electrochemical behaviour of modifiers in 1mM $[Fe(CN)_6]^{3-/4-}$ solution

Cyclic voltammetry was used for the investigation of electron transfer kinetics for the bare GCE, CoTCPc-GCE, PANI-GCE, CoTCPc-PANI-GCE and CoTCPc-PANI/$Co_2O_3$-GCE. The study was carried out in 1 mM $[Fe(CN)_6]^{3-/4}$ solution at a scan rate of 100 mV/s from -0.4 to 0.6 V.

#### 3.5.2 Electrochemical impedance spectroscopy and bode plots

Electrochemical impedance spectroscopy and bode plots were carried out in 1 mM $[Fe(CN)_6]^{3-/4-}$ solution for bare GCE, CoTCPc-GCE, PANI-GCE, CoTCPc-PANI-GCE and CoTCPc-PANI/$Co_2O_3$-GCE in order to confirm the electron transfer resistance of the electrodes in correspondence to results obtained in cyclic voltammetry. Bode plots and electrochemicalimpedance spectroscopy occurs at the same time during analysis but in different windows.

Table 3.1 Parameters for electrochemical impedance and bode plots

| | |
|---|---|
| Potential (V) | 0.400 |
| Set cell | on |

#### 3.5.3 Scan rate studies in in 1mM $[Fe(CN)_6]^{3-/4}$ solution

Scan rate studies were performed in1mM $[Fe(CN)_6]^{3-/4-}$ solution by using CoTCPc-PANI/$Co_2O_3$NPs electrode in order to determine the surface coverage of the modified electrode. The studies were carried by using cyclic voltammetry there parameters used are shown in table 3.2

Table 3.2: Parameters for cyclic voltammetry for scan rate studies in 1mM $[Fe(CN)_6]^{3-/4-}$ solution

| | |
|---|---|
| Start potential (V) | -0.400 |
| Upper vertex potential (V) | 0.600 |
| Lower vertex potential (V) | -0.400 |
| Stop potential (V) | -0.400 |
| Step potential (V) | 0.00244 |
| Scan rate (V/s) | 0.100 to 0.450 |

### 3.6. Optimisation of parameters

#### 3.6.1 Effect of pH

The effect of pH was studied in the range from pH 3 to 8. Adjusting of the buffer solution was carried out with dilute concentration of 0.1 M NaOH and 0.1 M HCl. The studies were carried out by preparing different pH phosphate buffer solution containing 1 mM of amitrole. The studies were carried out in cyclic voltammetry by using CoTCPc-PANI/$Co_2O_3$-GCE electrode. Parameters used for pH studies are shown below

Table 3.3 Parameters for cyclic voltammetry for pH studies in 1 mM amitrole

| | |
|---|---|
| Start potential (V) | 0.0 |
| Upper vertex potential (V) | 1.2 |
| Lower vertex potential (V) | 0.0 |
| Stop potential (V) | 0.0 |
| Scan rate (V/s) | 0.100 |

### 3.6.2 Comparative studies in pH4 phosphate buffer solution

Comparative studies were performed in pH 4 phosphate buffer solution containing 1mmM amitrole.The studies were carried out by using modified electrodes, Bare GCE, CoTCPc-GCE, PANI-GCE, CoTCPc-PANI-GCE and CoTCPc-PANI/$Co_2O_3$-GCE in order to confirm the reduction in potentials and increase in anodic peak currents on the oxidation of amitrole.Cyclic voltammetry was used for this study.Parameters used for comparative studies were similar to those used for pH studies (Table 3.3).

### 3.6.3 Scan rate studies in pH 4 phosphate buffer solution

Scan rate studies were carried out in-order to determine the effective surface coverage of the modified electrode CoTCPc-PANI/$Co_2O_3$-GCE.There studies were done inpH 4 phosphate

buffer solution by using CoTCPc-PANI/$Co_2O_3$-GCE modified electrode. Cyclic voltammetry was used for this study.Parameters used for the analysis are similar to those shown in table 3.3 but using different scan rates from 50 to 400 mV/s.

### 3.7 Kinetic studies

Kinetic studies were carried out in 1mM amitrole solution in pH 4 phosphate buffer.The studies were performed in cyclic voltammetry by using CoTCPc-PANI/$Co_2O_3$-GCE modified electrode. Parameters used for the analysis are similar to those shown in Table 3.3 but using different scan rates from 50 to 400 mV/s. This study was performed in order to determine whether the detection of amitrole was diffusion controlled or not.This was observed on plotting graphs of anodic peak current against square root of scan rate.

### 3.8 Order of reaction

The order of reaction was performed using cyclic voltammetry, it was carried out by varying the concentration of amitrole 5 mM, 10mM, 15mM, 20 mM and 25 mM and observing its behavior on CoPc-PANI/ $Co_2O_3$ NPs-GCE at 0.1 V/s scan rate and potential of 0.2 V to 1.0 V.The order of reaction were obtained by plotting the graph of log current against log [amitrole].

### 3.9 Langmuir adsorption isotherm studies

Langmuir adsorption isotherm was carried out using linear sweep voltammetry.The study was performed by using working standard solutions of amitrole 10 µM, 20µM, 30µM, 40 µM and 50 µMprepared from serial dilution of 1 mM amitrole in phosphate buffer solution pH 4 .The working standard solution were prepared in 50mL volumetric flask and diluted to the mark with pH 4 phosphate buffer solution.The response behavior was observed on CoPc-PANI/ $Co_2O_3$ NPs-GCE. Parameters used for linear sweep voltammetry

Table 3.4 Parameters for linear sweep voltammetry for langmuir adsorption isotherm studies

| | |
|---|---|
| Start potential (V) | 0.200 |
| Stop potential (V) | 1.200 |
| Step potential (V) | 0.00244 |
| Scan rate (V/s) | 0.100 |
| Interval time (s) | 0.02440 |

Langmuir adsorption constant were obtained from plotting the graph of $[amitrole]/_{I_{cat}}$ $against$ $[amitrole]$ the gradient of the line is equivalent to the inverse of ß adsorption constant.

### 3.10 Catalytic rate constant

Catalytic rate constant was performed using chronoamperometry. The studies were performed by preparing working standard solutions of 20 µM, 40 µM, 60 µM and 80 µM form 1mM stock solution of amitrole in pH 4 phosphate buffer solutions.The working standard solution were prepared in 50 mL volumetric flask and diluted to the mark with pH 4 phosphate buffer solution. The prepared working standard solutions were filled in the electrochemical cell respectively and the behavior was observed on CoPc-PANI/ $Co_2O_3$ NPs-GCE.Catalytic rate constant was obtained by plotting graph of slope against √ [amitrole].The gradient of the slope is equivalent to πk which gives the catalytic rate constant. Parameters used in chronoamperometry

Table 3.5 Parameters for chronoamperometry for catalytic rate constant studies

| | |
|---|---|
| Set potential (V) | 0.000 |
| Set potential (V) | 0.800 |
| Set potential (V) | 0.800 |
| Duration (s) | 5 |
| Interval time (s) | 0.01 |

### 3.11 Differential pulse voltammetry

Limit of detection was carried out using differential pulse voltammetry. The study was carried out by preparing working standard solution of 0.2µM, 0.4µM, 0.6µM,0.8µM, 1.0µM, 1.2µM, 1.4µMand 1.6µM from 1mM stock solution of amitrole in pH 4 phosphatebuffer.The working standards were prepared in 50mL volumetric from flask and diluted to mark with pH 4 phosphate buffer solutions. The prepared 50mL solution of working standards were placed in the

electrochemical cell respectively and the behavior was observed on CoPc-PANI/ $Co_2O_3$ NPs-GCE electrode.

Table 3.6 Parameters for DPV

| | |
|---|---|
| Initial potential (V) | 0.400 |
| End potential (V) | 1.200 |
| Step potential (V) | 0.00500 |
| Modulation amplitude (V) | 0.0500 |
| Interval time | 0.50000 |
| Scan rate V/s | 0.0100 |

### 3.14 Stability studies

Stability studies was performed on CoPc-PANI/ $Co_2O_3$ NPs-GCE in 1mM amitrole solution in phosphate buffer pH 4 by performing 20 cycles by using cyclic voltammetry technique at 0.1V/s scan rate at 0.2 to 1.0V.

### 3.16 Reproducibility studies

The developed sensor was analyzed in a solution containing 1mM of amitrole solution by employing the DPV technique. Before and after each analysis the electrode was washed using distilled water in order to remove adhered particles at a scan rate of 0.01 V/s. potential of 0.2 to 1.2 V and amplitude of 0.05 V.

### 3.17 Effect of interference

Interference studies were investigatedusing DPV technique.1mM of amitrole was detected in the presence of nitrates that are assumed to interfere with detection of amitrole.Equimolar solutions of analytes were prepared in the same matrix with amitrole in phosphate buffer solution pH 4. The mixture was analyzed from 0 to 1.2V potential and amplitude of 0.05V.

### 3.18 Real sample analysis

Real sample analysis was performed using DPV technique on agricultural waste water obtained from MSU agricultural department. The sample was filtered in order to remove suspended solids. An aliquot of amitrole was added to a 100 mL volumetric flask. Standard addition method was used by adding 10mL of the prepared working solution containing 2µM, 5 µM, 5 µM and 7.5 µM of amitrole into three different 100 mL volumetric flask. From the prepared standard solutions a volume 10mL was added to the sample and were diluted to mark by 0.1 M phosphate buffer at pH 4.

# CHAPTER FOUR

# RESULTS AND DISCUSSION

## 4.0 Introduction

The chapter highlights the findings obtained from the experiments. Results from IR are discussed. Where Cyclic voltammetry, Electrochemical impedance spectroscopy, linear sweep voltammetry, Differential pulse voltammetry and chronoamperometry were used in electrochemical studies.

## 4.1 Characterization using FTIR

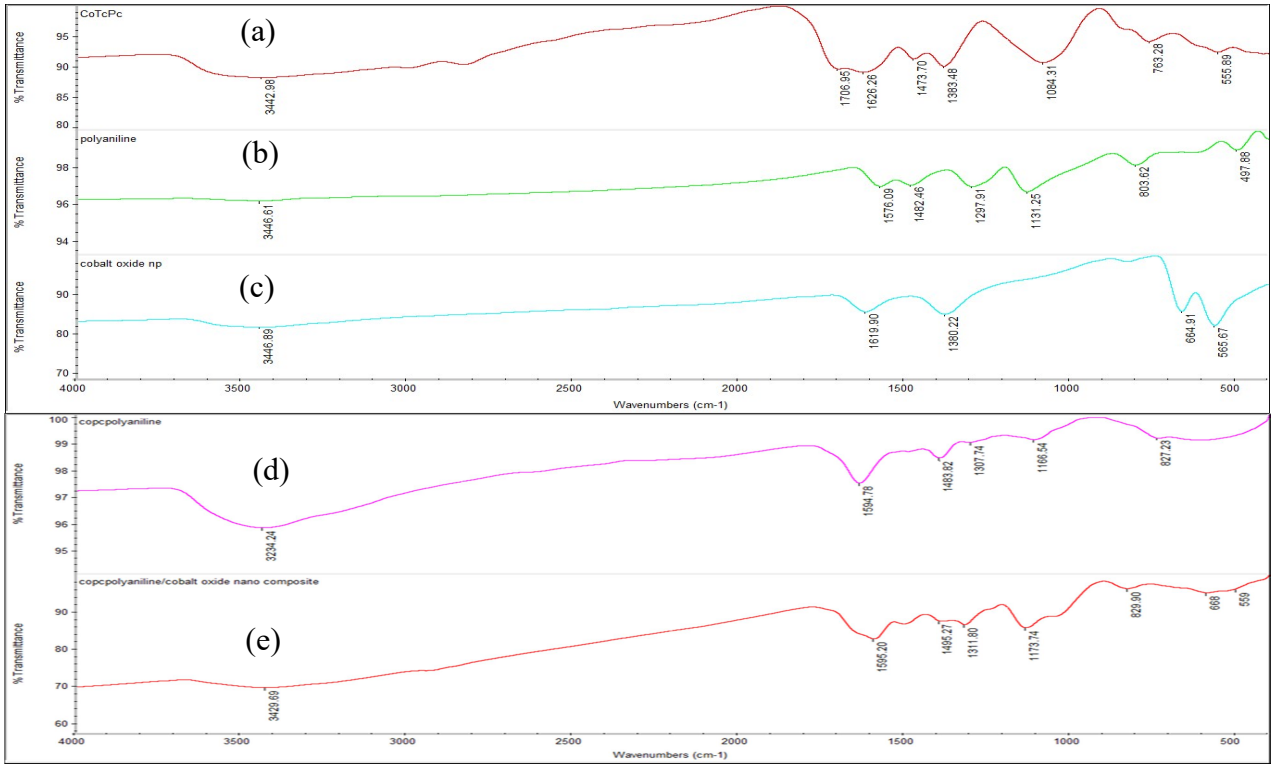


**Fig 4.1FTIR spectra for a) CoTCPc b) PANI c) $Co_2O_3$NP d) CoTCPc-PANI and e) CoTCPc-PANI/$Co_2O_3$NPs**

**Fig 4.1** shows the infrared spectrum of the cobalt tetracarboxyl phthalocyanine, polyanaline cobaltoxide nanoparticles, polyaniline cobalt (II) tetracarboxyl phtahlocyanito andpolyaniline cobalt (II)tetracarboxyl phtahlocyanito doped with cobalt oxide nanoparticles were obtained in the range of 4000 $cm^{-1}$ to 500 $cm^{-1}$. Figure 4.1a shows the infrared spectra obtained for the CoTCPc, which showed peaks at 3443.00 $cm^{-1}$ which is assigned for O-H stretching and peak at 1704.01$cm^{-1}$ is assigned to the C=O, both these bonds are attributed to the carboxylic acid stretching bands [111].The peaks at 1626 $cm^{-1}$ 1496 $cm^{-1}$ and 1084 $cm^{-1}$, which coincided with the following bands O – H, C = C, C – C, and C – O respectively.

Fig 4.1b shows the FTIR spectrum of PANI, shows the characteristic at 1581.33 and 14808.81$cm^{-1}$ are assigned to the C=C stretching of quinoid ring and benzenoid rings respectively. The characteristics peaks at 1294.74 and 1135.23 $cm^{-1}$ are attributed to the C-N stretching vibration of the secondary aromatic amine group and aromatic C-H in plane bending vibration respectively [47].The peak at 799.96$cm^{-1}$ represent C-H the small peak at 617.28 $cm^{-1}$ represented para-distributed aromatic rings indicating polymer formation [112].

Figure 4.1c shows the spectrum of Cobalt oxide nanoparticles the spectrum has two strong bands due to (Co-O) with modes at 661.46 $cm^{-1}$ and 563 $cm^{-1}$These two sharp peaks indicates the presence of crystalline $Co_3O_4$[62].According to literatureit supports tthat the band at 661 $cm^{-1}$ is attributed to ($Co^{2+}$-O) vibration in a tetrahedral hole and the band at 563 $cm^{-1}$ attributed to ($Co^{3+}$-O) vibration in an octahedral hole.Peak at 3424.96 $cm^{-1}$ is assigned to $H_2O$ absorbed by the KBr [61].There are other peaks at the position 1383.73 $cm^{-1}$ and 1600.66 $cm^{-1}$These peaks could be assigned respectively, to C-N and C-H bond which are indication of the presence of impurities of PVP which was used during synthesis for stabilisation of the nanoparticle [110].

Fig 4.1 d) shows the FTIR spectrum CoPC in the presence of polyaniline the intensity of the quinoid ring and the benzoid ring shifts to 1594$cm^{-1}$ and 1498$cm^{-1}$, respectively.Further the C-N stretching vibrations appeared at 1294.74 $cm^{-1}$ in PANI which was shifted to 1307$cm^{-1}$ in CoPC/PANI. The C-H stretching in polyaniline shifted from 799.96 to 827.23$cm^{-1}$[113]. Shift of bands were a result of formation of the phthalocyanine-amide complex. Fig 4.1 e) shows the spectrum of CoTCPc-PANI/$Co_2O_3$NP the spectrum is similar to that of CoTCPc-PANI but with other bands appearing at 668.25 $cm^{-1}$ and 559.43 $cm^{-1}$ indicating the presence of cobalt oxide nanoparticles[61]in the CoTCPc-PANI composite .Also the slight shifts of bonds in the CoTCPc-PANI/$Co_2O_3$NP indicates that's cobalt oxide nanoparticles had been incorporated in the CoTCPc-PANI composite.

## 4.2 Electrochemical Characterization

Cyclic voltammetry was used to characterize the modified electrode in a redox probe (Fig 4.2).

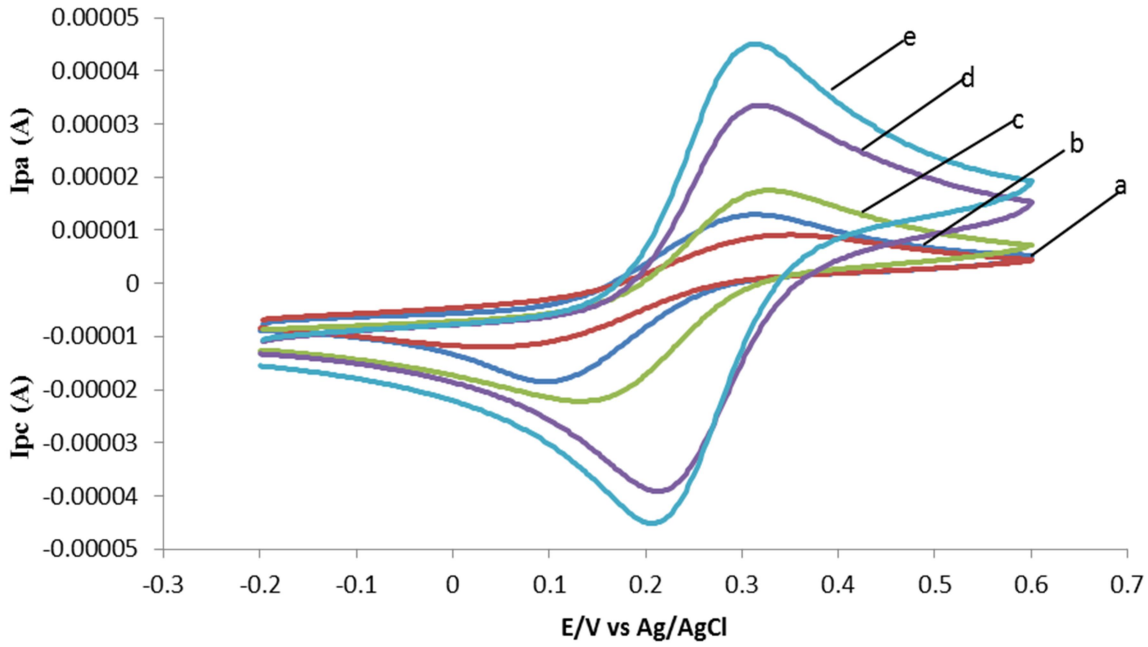


**Fig 4.2: Voltammograms of bare (a), CoTCPc-GCE (b), PANI-GCE (c), CoTCPc-PANI-GCE (d), CoTCPc –PANI-$Co_2O_3$-GCE (e) in 1 mM $[Fe(CN)_6]^{3-/4-}$ prepared 1 M of KCl . Scan rate = 100 mV/s**

The cathode to anode peak potential separation (ΔEp) for the modifiers used in this study is shown in the Table 4.1. The order in terms of electron transfer efficiency is therefore CoTCPc-PANI-$Co_2O_3$-GCE (80 mV) > CoTCPc-PANI-GCE (100 mV) > PANI-GCE (150 mV) > Bare-GCE (200 mV) > CoTCPc-GCE (260 mV). This confirms the good electron transfer kinetics of CoTCPc-PANI-$Co_2O_3$NPs-GCE compared to the rest of the modified electrodes, including the bare GCE.The electron transfer kinetics of the modifiers on the surface of glass carbon were also

confirmed by the increase in anodic peak current (Table 4.1) the order of electron transfer is therefore CoTCPc-GCE ($I_{Pa}$: 88 $\times 10^{-5}$A) > Bare-GCE ($I_{Pa}$: 126 $\times 10^{-5}$A)> PANI-GCE ($I_{Pa}$: 170 $\times 10^{-5}$A) > CoTCPc-PANI-GCE ($I_{Pa}$: 332 $\times 10^{-5}$A) > CoTCPc-PANI-$Co_2O_3$-GCE ($I_{Pa}$: 440 $\times 10^{-5}$A).

Table 4.1 Summary parameters obtained from cyclic voltammetry experiments in $[Fe(CN)_6]^{3-/4-}$ solution.

| Electrodes | $I_{pa}$ (x$10^{-5}$ A) | $I_{pc}$(x$10^{-5}$A) | $\Delta E_{(pa-pc)}(mV)$ |
|---|---|---|---|
| Bare GCE | 126 | -184 | 200 |
| CoTCPc-GCE | 88 | -113 | 260 |
| PANI-GCE | 170 | -195 | 150 |
| CoTCPc-PANI-GCE | 322 | -390 | 100 |
| CoTCPc-PANI/$Co_2O_3$NPs-GCE | 440 | -448 | 80 |

The lower peak potential separation (80 mV) and high anodic peak current ($440\times10^{-5}$ A) for CoTCPc-PANI-$Co_2O_3$-GCE compared to the rest of the modifiers electrode is possibly due to the linkages between the CoTCPc and PANI as well as their good alignment on the electrode surface which makes, electron exchange between the redox probe and electrode modifier much faster confirming its improved electron transfer compared with the rest of the modified electrodes[14].

Also the increase in peak current for CoTCPc-PANI-$Co_2O_3$NPs is due to cobalt oxide nanoparticles increasing the surface area of the modifier for catalysis hence increasing electron

transfer process. The large peak potential separation of 260 mV and low anodic peak current of $88\times10^{-5}$ A for CoTCPc-GCE implies that on its own, it has poor electron transfer properties[111], however when coupled with polyaniline, its catalytic properties are activated as evidenced by the reduction in peak potential separation of 100 mV and high anodic peak current of 322 $\times10^{-5}$ A. This is explained in terms of the electron donating nature of PANI which reduce the redox potentials for the center as well as the good electron transfer properties of the cobalt oxide nanoparticles [45].The amide linkage formed between CoTCPc and PANI facilitates the easy flow of electrons to and from the linked CoTCPc molecule. Improved electron transfer kinetics is also a result of the nanostructured sizes of the conjugates which enables them to provide a large surface area for the transfer of electrons. Having confirmed the superiority of CoTCPc-PANI-$Co_2O_3$NPs electrode over the other electrodes it was used in the further characterization.

### 4.3 Electrochemical impedance spectroscopy

Electrochemical impedances spectroscopy (EIS) measurements in $[Fe(CN)_6]^{3-/4-}$ solution were investigated to assess the electron transfer properties of the modified glassy carbon electrode

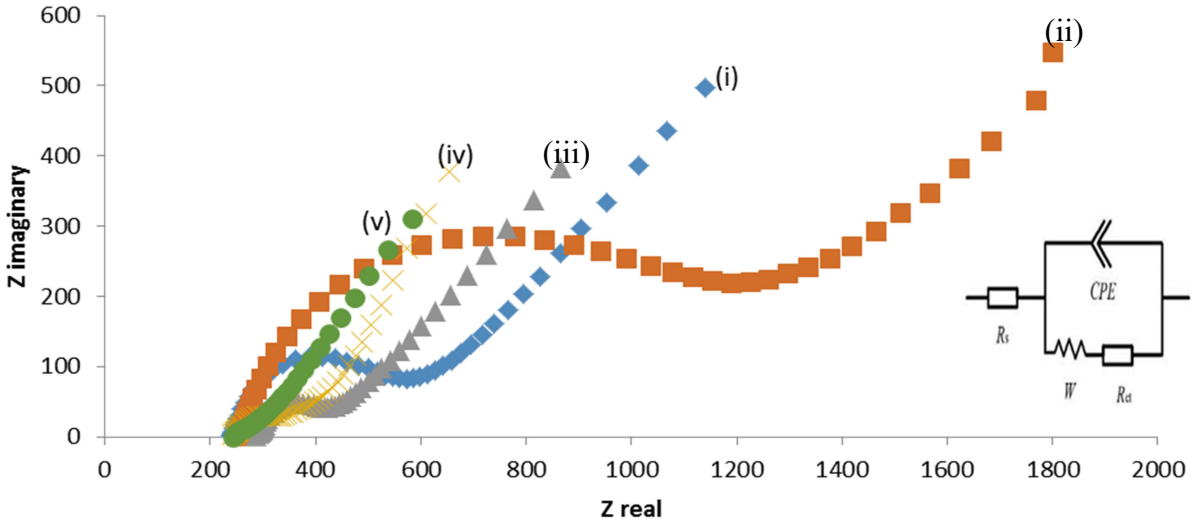


**Fig 4.3 Nyquist plots obtained for i) bare GCE ii) CoTCPc-GCE iii) PANI-GCE iv) CoTCPc-PANI-GCE and v) CoTCPc-PANI/$Co_2O_3$NPs-GCE in 1mM $[Fe(CN)_6]^{3-/4-}$ solution in 1M of KCl.** ***Inset*** **is the Randles circuit model used in fitting the data.**

Fig 4.3 shows a Nyquist plots for bare-GCE, CoTCPc-GCE, PANI-GCE, CoTCPc-PANI and CoTCPc-PANI/$Co_2O_3$NPs-GCE. The Nyquist plot data was fitted using Randles equivalent region (electron-transfer properties) and low frequency region (electrolyte diffusion controlled properties). The region of interest to this work is the high frequency region which is the kinetically controlled region and will give us the kinetics of the modified bare glassy carbon electrode. Kinetically controlled region in the Nyquist plot is of high importance since it shows the semi-circle which is related to the charge –transfer resistance ($R_{CT}$). The smaller the $R_{CT}$, the more conducting the electrode or the materials used to modify the electrode [114]. The $R_{CT}$ value for a bare electrode surface was 113.9 kΩ $cm^{-2}$ and this value was 179.9 kΩ$cm^{-2}$on CoTCPc-GCE, 86.5 kΩ$cm^{-2}$ on PANI-GCE, 65.4 kΩ$cm^{-2}$ CoTCPc-PANI-GCE and 58.2 kΩ$cm^{-2}$ on

CoTCPc-PANI/$Co_2O_3$NPs-GCE. The Rct value was the smallest at CoTCPc-PANI/$Co_2O_3$NPs-GCE compared to all other electrodes. The decrease in $R_{ct}$ values at CoTCPc-PANI/$Co_2O_3$NPs-GCE is attributed to PANI and $Co_2O_3$Nps being a good conductors of electrons [23,112] and the combination of the three electro catalytically active materials (PANI, $Co_2O_3$Nps and CoTCPc) having synergistic effects in terms of enhancing electron transfer to and from the electrode surface. The high $R_{ct}$ value of CoTCPc indicates that on its own CoTCPc has a small electron transfer property as compared to the bare. Its electron transfer properties can be enhanced by forming linkages with amine groups hence forming an electron transfer bridge [111].

**Table 4.2**The summary of parameters obtained from electrochemical impedance spectroscopy experiments in $[Fe(CN)_6]^{3-/4-}$ solution.

| Electrode | $R_{ct}(k\Omega\ cm^{-2})$ |
|---|---|
| BARE GCE | 113.9 |
| CoTCPc-GCE | 179.9 |
| PANI-GCE | 86.5 |
| CoTCPc-PANI-GCE | 65.4 |
| CoTCPc-PANI/$Co_2O_3$NPs-GCE | 58.2 |

### 4.4 Surface area determination

The surface area of CoTCPc-PANI-$Co_2O_3$NPs GCE was determined in 1 mM $K_3[Fe(CN)_6]$ by applying the Randles –Sevcik Equation[81].

$I_p = (2.69 \times 10^5)n^{3/2}D^{1/2}CA_{eff}v^{1/2}$(4.0)

where $i_p$ the peak current, n is equal to the number of electrons transferred at the surface of the electrode

$Fe(CN)_6^{3-} + e^- \longrightarrow Fe(CN)_6^{4-}$(4.1)

Thus, n is equal to 1, D is the diffusion coefficient of the analyte in solution 7.6 x $10^{-6}$ $cm^2s^{-1}$ and C is the solution concentration in (mol $cm^{-3}$),$A_{eff}$ is the effective surface area and v is the scan rate ($Vs^{-1}$). Based on this, $i_p$ is proportional to $v^{1/2}$ and produces a linear plot with slope m given by the Equation

$m = (2.69 \times 10^5)n^{3/2} A_{eff} D^{1/2}C$ (4.2)

Figure 4.4 shows the obtained voltammograms at different scan rates from (a) 50 mV/s, (b) 100 mV/s, (c) 150 mV/s, (d) 200 mV/s, (e) 250 mV/s, (f) 300 mV/s and (g) 350 mV/s. The plots of peak current, $I_P$ for both anodic and versus square root of scan rate ($v^{1/2}$) (Figure 4.4 insert) were linear ($R^2 = 0.9984$ and 0.9902) signifying a diffusion –controlled redox process [115].

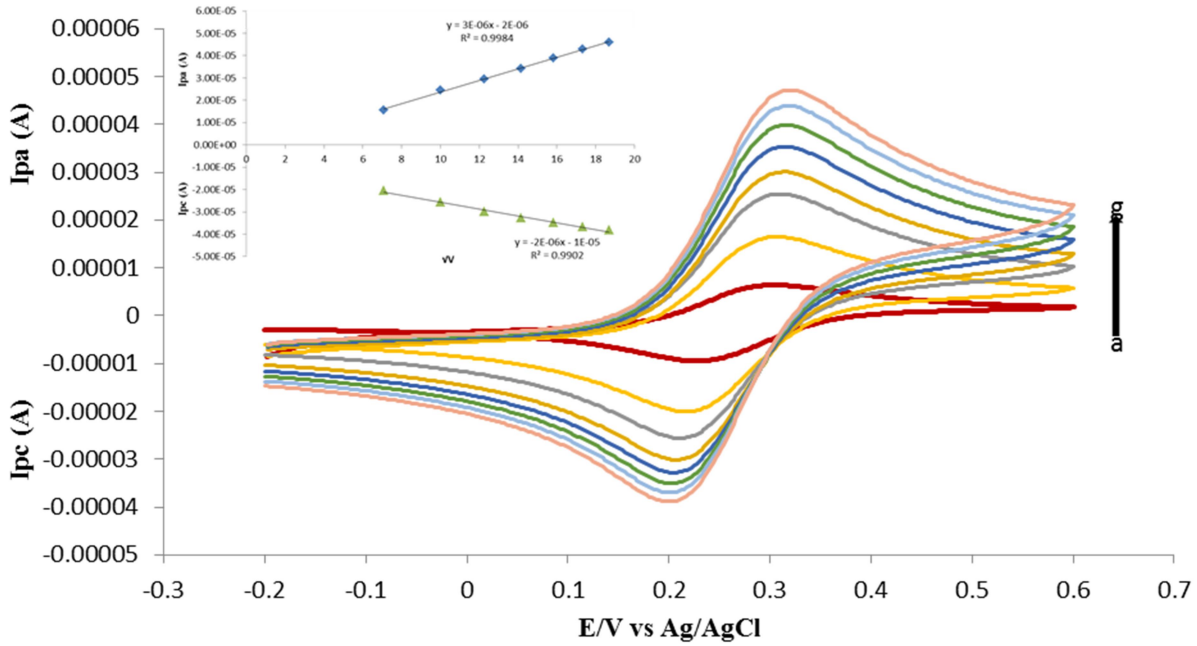


**Fig 4.4 Effect of scan rate on peak potentials and currents (a) 50 mV/s, (b) 100 mV/s, (c) 150 mV/s, (d) 200 mV/s, (e) 250 mV/s, (f) 300 mV/s, (g) 350 mV/s, on CoTCPc-PANI-$Co_2O_3$ NPs-GCE. *Inset:* Plot of Ipa, Ipcversus √v.**

The CoTCPc –PANI-$Co_2O_3$NPs had an effective surface are of 0.40 $cm^2$ comparing with known surface area of bare electrode of 0.0712 $cm^2$ [8].This indicates that the modified electrode displayed a large surface area for electro catalysis.

### 4.6Optimization of parameters

#### 4.6.1 Effect of pH

pH is one of the factors affecting oxidation of amitrole[12].

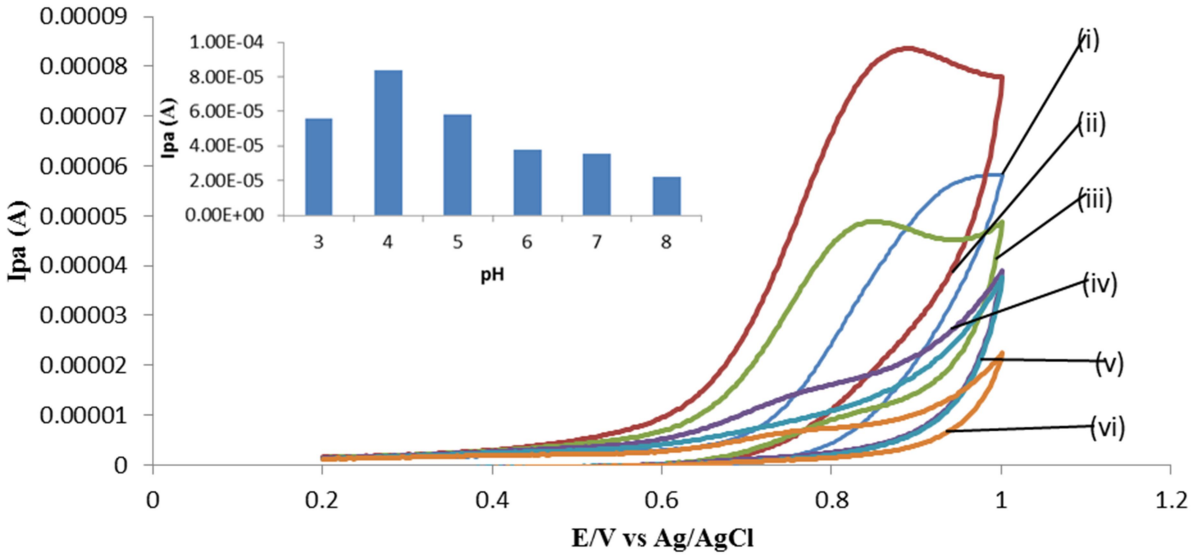


**Fig 4.5 Cyclic Voltammograms for CoTCPc-PANI/$Co_2O_3$NPs-GCE in (i) pH 3, (ii) pH 4, (iii) pH 5, (iv) pH 6, (v) pH 7 and (vi) pH 8 phosphate buffer solution containing 1mM amitrole. Inset: plot of $I_{pa}$ vs pH .Scan rate = 100 mV/s.**

The studied pH range was from pH 3 to 8. The peak current maximum response was obtained at pH 4. The plot of pH against current showed that as the pH changed from pH 4 to lower acidic values, the peak current decreased. Under basic pH, the peak current was very low and almost insignificant proving that oxidation of amitrole occurred under acidic conditions at the Co (III) $Pc^{-1}$/Co (III) $Pc^{-2}$ surface [6].

### 4.7 Comparative cyclic voltammetry in pH 4 buffer

Cyclic voltammograms of the modified electrodes a) bare GCE b) CoTCPc-GCE c) PANI-GCE d) CoTCPc-PANI-GCE e) CoTCPc-PANI/$Co_2O_3$NPs-GCE were obtained by scanning the electrodes in pH 4 phosphate buffer solution at a scan rate 100mV/s as shown in Fig 4.6

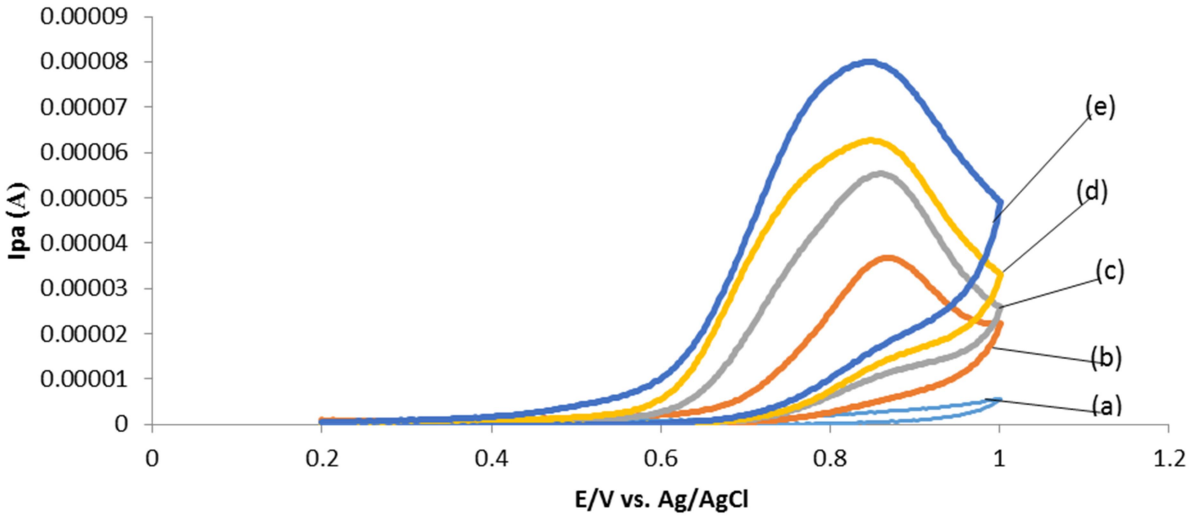


**Fig 4.6 Cyclic Voltammograms for a) bare GCE b) CoTCPc-GCE c) PANI-GCE d) CoTCPc-PANI-GCE e) CoTCPc-PANI/$Co_2O_3$NPs-GCE, in phosphate buffer pH 4. Scan rate = 100mV/s.**

The peaks observed represent the initial ring oxidation process of the phthalocyanine, Co(III)$Pc^{-1}$/Co(III)$Pc^{-2}$ [2,8]. The CoTCPc-PANI/$Co_2O_3$NPsGCE showed improved catalysis at lower potential (0.82V) and higher anodic peak current (79.4 x$10^{-5}$ A) compared to other BGCE modifiers.

**Table 4.3** shows the magnitudevalues of $I_{pa}$ and $I_{pc}$in phosphate buffer pH 4.

| Electrodes | $I_{Pa}$(1 x10$^{-5}$ A)$E_{pa}$(V) | |
|---|---|---|
| Bare GCE | | 5.20.98 |
| CoTCPc-GCE35.9 0.85 | | |
| PANI-GCE 540.84 | | |
| CoTCPc-PANI-GCE62.5 | 0.83 | |
| CoTCPc-PANI-$Co_2O_3$NPs-GCE 79.3 | | 0.82 |

**4.8Surface coverage**

Fig 4.7 shows the increase in the anodic peak current as the scan rate is increased from 100 mV/s to 500 mV/s for CoTCPc-PANI/$Co_2O_3$NPs. Fig 4.7 insert shows a plot of anodic peak current versus sweep rate for the CoTCPc-PANI/$Co_2O_3$NPs-GCE in pH 4. The linear relationship of the plot is characteristic of surface-immobilized redox species. The surface coverage of CoTCPc-PANI/$Co_2O_3$NPs on GCE was estimated from the plot of anodic peak current versus scan rate, according to Eq.4.3[116].

$$I_P = \frac{n^2F^2\nu A_{eff}\Gamma}{4RT} \quad (4.3)$$

Where Ip is the peak current, n is the number of transferred electrons, F is the Faraday constant which is equal to 9.6487 C/mol, v is the scan rate, Γ is the surface coverage in molcm$^{-2}$, $A_{eff}$ is the surface area of the modified electrode, R is the gas constant (8.314 KJ/mol) and T is the temperature in kelvin. The value of surface coverage was found to be7.6 x $10^{-13}$ mol cm$^{-2}$

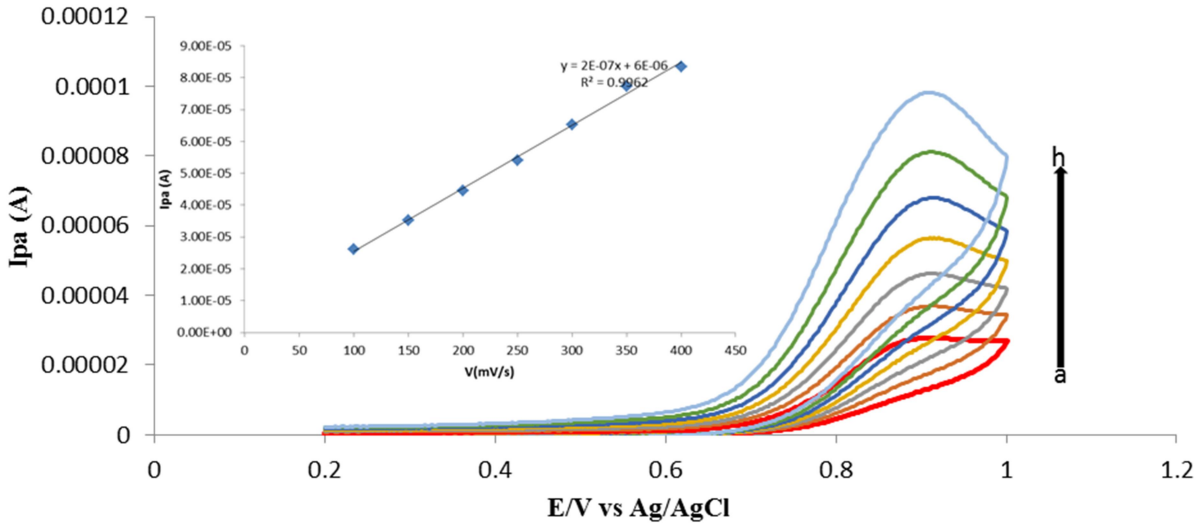


**Fig 4.7 Cyclic Voltammograms for CoTCPc-PANI/$Co_2O_3$NPs-GCE in pH buffer with increasing scan rate 100 mV/s a) 150 mV/s b) 200 mV/s c) 250 mV/s d) 300 mV/s e) 350 mV/s f) 400 mV/s g) 450 mV/s h).Insert: Plot of $I_{pa}$ vs. *v***

### 4.9Comparative study in 1 mM Amitrole in pH buffer 4

Comparative studies in 1mM amitrole was carried out for all electrodes Bare-GCE, CoTCPc-GCE, PANI-GCE, CoTCPc-PANI-GCE and CoTCPc-PANI/$Co_2O_3$NPs-GCE in order to observe the reduction in potential and increase in anodic peak current on the electrocatalysis of amitrole. The bare GCE, CoTCPc-GCE, PANI-GCE, CoTCPc-PANI-GCE and CoTCPc-PANI/$Co_2O_3$NPs-GCE were used in the oxidation of amitrole for comparative purposes, Fig 4.9

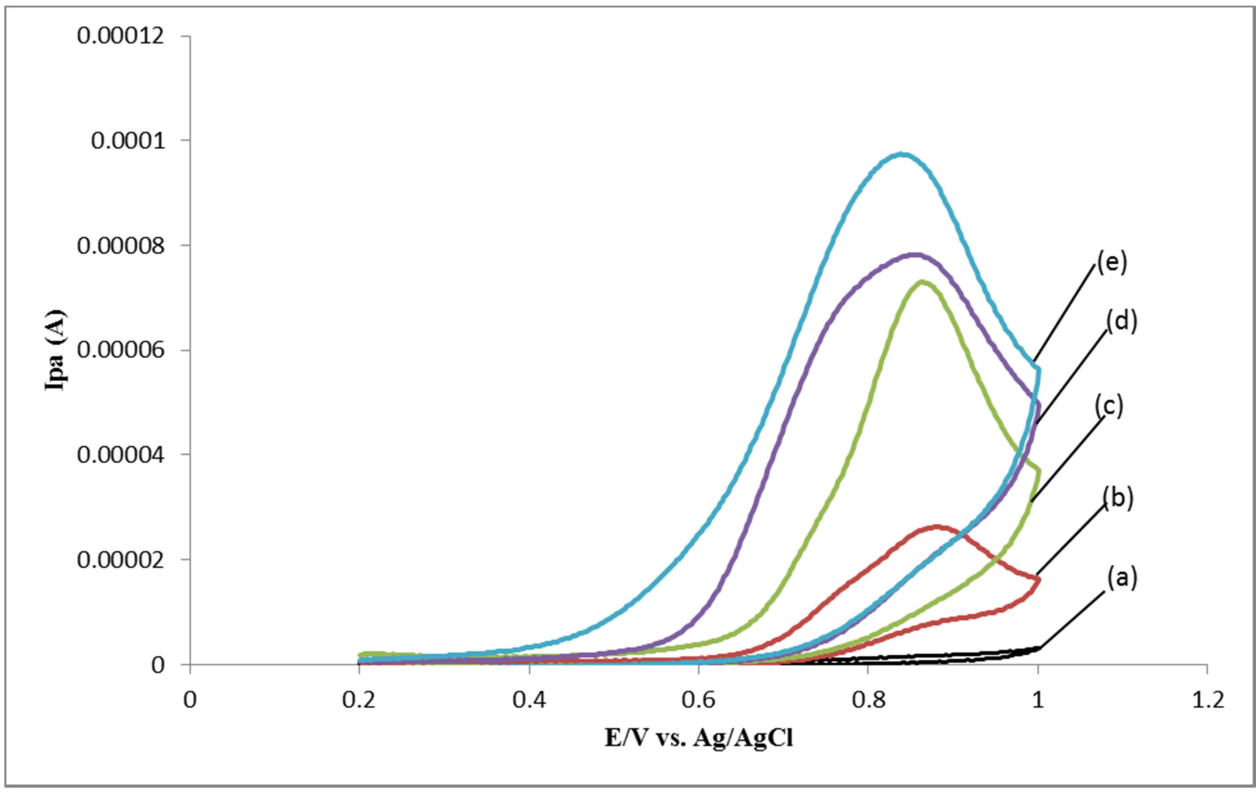


**Fig 4.8 Cyclic voltammograms of a) BGCE, CoTCPc-GCE, PANI-GCE, CoTCPc-PANI-GCE, CoTCPc-PANI/$Co_2O_3$NPs-GCE in 1mM Amitrole pH 4 PBS.**

An increase in anodic peak current was observed (Table 4.3) compared to the voltammograms in pH 4 buffer thus confirming that the electrodes detected amitrole. Since the complex, CoTCPc-PANI/$Co_2O_3$NPs is a combination of CoTCPc, PANI and $Co_2O_3$NPs it was reasonable to assess

their individual oxidation potentials to enable conclusive deductions to be made about their catalytic efficiencies relative to CoTCPc-PANI/$Co_2O_3$NPs electrode. The observed peaks in the region 0.8 – 1.0 V are due to the oxidation of amitrole as observed in other studies [8,111]. The oxidation potentials for amitrole at bare GCE, CoTCPc-GCE, PANI-GCE, CoTCPc-PANI-GCE and CoTCPc-PANI/$Co_2O_3$NPs-GCE are 0.98 V, 0.85V, 0.84 V, 0.83 V and 0.81 V respectively.

The CoTCPc –PANI/$Co_2O_3$NPs shows higher oxidation currents ($I_{pa}$ = 95.7x$10^{-5}$ A) at reduced oxidation over potentials ($E_{pa}$= 81V) compared to the rest of the electrodes confirming its better catalytic properties.The sharp rise in current inception of the oxidation of amitrole is a clear indication of the good electrocatalytic properties of CoTCPc –PANI/$Co_2O_3$NPs electrode. Due to the nature of chemical linking conjugates form three dimensional surface arrays on the electrode surface. These arrays have very large surface area and are highly porous, therefore easily accessed by the analyte, resulting in the easy oxidation of amitrole on CoTCPc – PANI/$Co_2O_3$NPs. Having confirmed the superiority of CoTCPc –PANI/$Co_2O_3$NPs over other electrodes it was used in the further characterization of amitrole.

**Table 4.4** Comparative studies of Ipa in buffer and amitrole solution

| Electrodes | $I_{pa}$ (1 $x0^{-5}$ A)$I_{pa}$($x10^{-5}$ A) | |
|---|---|---|
| Buffer | Amitrole | |
| Bare-GCE | 1.4 | 5.6 |
| CoTCPc-GCE | 25.4 | 35.7 |
| PANI-GCE | 54.3 | 70.5 |
| CoTCPc-PANI-GCE | 62.1 | 77.2 |
| CoTCPc-PANI/$Co_2O_3$NPs-GCE | 79.1 | 96.6 |

## 4.10 Electrochemical Impedance spectroscopy

A three electrode electrochemical impendence spectroscopy (EIS) was used to probe the redox and structural features of the different working electrodes (WE). Fig 4.9 shows the Nyquist plots obtained in 1 mM amitrole. The bare GCE, CoTCPc –GCE, PANI-GCE, CoTCPc –PANI-GCE displayed identical semi-circular Nyquist plots with straight line portion at lower frequencies.

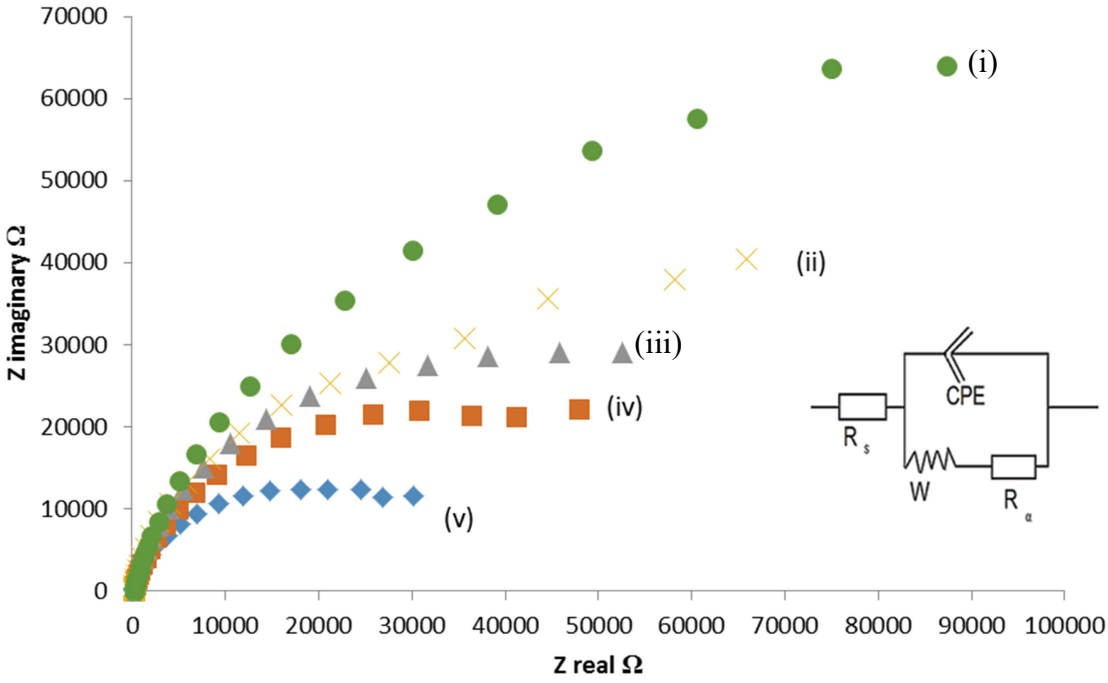


**Fig 4.9 Nyquist (phase angle versus log f) plots obtained for (i) bare GCE, (ii) CoTCPc, (iii) PANI, (iv) CoTCPc-PANI and (v) CoTCPc-PANI/$Co_2O_3$NPs in 1 mM amitrole (pH 4 PBS). Inset: Suggested Randle equivalent circuit model for the impedance spectra**.

Semicircle represents a combination of charge transfer resistance and the double layer capacitance of the electrode modifiers and are in agreement with kinetically controlled movement of electrons [91]. The origin of the semicircle in Nyquist plots has been attributed to microscopic roughness which brings heterogeneity in solution resistance and the double layer capacitance [117]. A very large semi-circle at higher frequencies was observed for the bare GC electrode in the presence of amitrole (highest charge transfer resistance), followed by CoTCPc-GCE, PANI-GCE, CoTCPc-PANI-GCE and CoTCPc-PANI/$Co_2O_3$NPs-GCE in that order. At the frequency region of the impedance under study the charge-transfer resistance ($R_{ct}$) decreased

due to the facilitation of the electron transfer by the electrode modifiers [16]. The plots of CoTCPc-PANI/$Co_2O_3$NPs-GCE have the lowest charge-transfer resistance (smallest diameters) with value of 87.6 kΩ and hence the highest oxidation currents observed on oxidation of amitrole at reduced over potentials .These charge transfer resistance data proves that amitrole is oxidized at lower potentials which is agreement with cyclic voltammetry, (Fig 4.7). The apparent electron transfer rate constants, $k_{app}$,were obtained using Eq.4.4[14].

$$kapp = RT/FRctC \qquad (4.4)$$

Where C is the concentration (amitrole, 1.0 x $10^{-3}$ mol $cm^{-3}$),with R and F having their usual meanings the increase in $k_{app}$ value from CoTCPc (4.04 x $10^{-3}$)to CoTCPc-PANI-GCE (5.56 x $10^{-3}$ cm $s^{-1}$) could be attributed to the conducting and electrocatalytic properties of polyaniline the electrode when modified with CoTCPc-PANI/$Co_2O_3$NPs gave the $k_{app}$ value of 8.84 x $10^{-3}$cm $s^{-1}$ . The increase in $k_{app}$value at CoTCPc-PANI/$Co_2O_3$ could be attributed to the $Co_2O_3$NPs being a good conductor of electrons. As reflected in its $k_{app}$and $R_{CT}$values, CoTCPc-PANI/$Co_2O_3$NPs-GCE exhibited fastest electron transfer processes towards amitrole compared to other electrodes investigated in this work, ( Table 4.3).The combination of the three materials clearly shows an increase in the apparent electron transfer rate constant . Generally the presence of an electro-catalyst facilitates electron transfer at the electrode /analyte interface as shown by increase in the values of $k_{app}$(Table 4.4).

**Table 4.5**: Estimated EIS parameters obtained for different electrode

| Electrode | $R_{CT}$ (kΩ) | $k_{app}$cm $s^{-1}$ |
|---|---|---|
| Bare GCE | 87.3 | $3.05x10^{-3}$ |
| CoTCPc-GCE | 65. 9 | $4.04 \times x10^{-3}$ |
| PANI-GCE | 52.6 | $5.06\ x10^{-3}$ |
| CoTCPc-PANI-GCE | 47.9 | $5.56\ 1x0^{-3}$ |
| CoTCPc-PANI/$Co_2O_3$NPs | 30.1 | $8.84\ x10^{-3}$ |

The Bode plots (plot of phase –shift) versus the log frequency) for each electrode was investigated as shown in Fig 4.10.

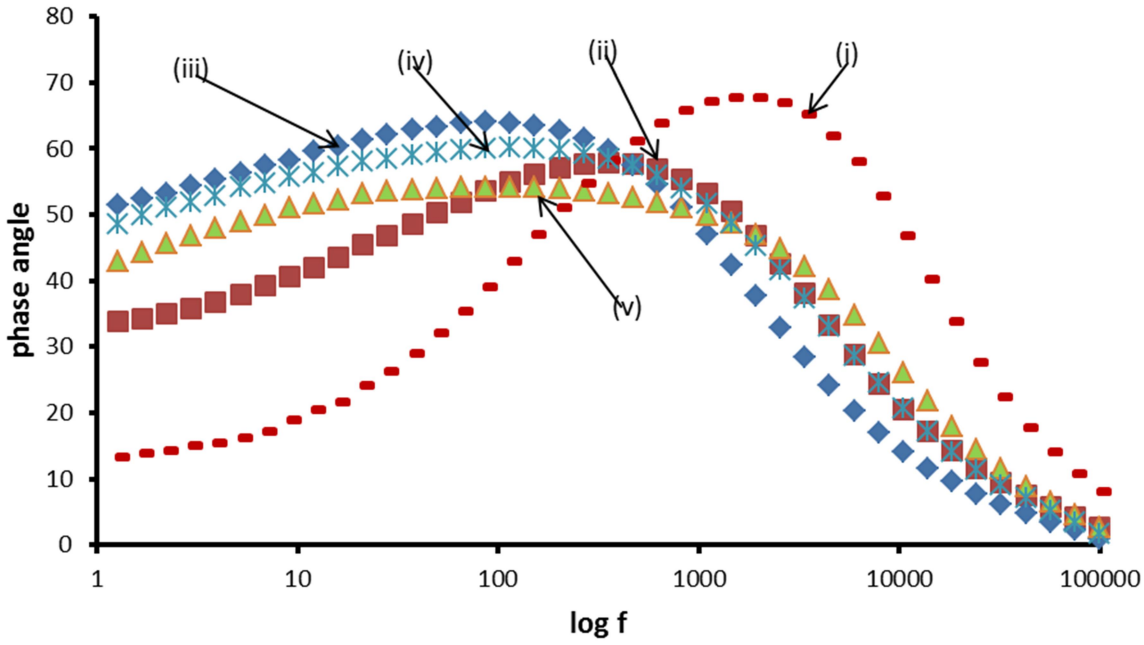


**Figure 4.10 Bode (phase angle versus log f) plots obtained for (i) bare GCE, (ii) CoTCPc-GCE, (iii) PANI-GCE, (iv) CoTCPc-PANI-GCE, (v) CoTCPc-PANI/$Co_2O_3$NPs in 1 mM amitrole (pH4).**

Bode plots were used to obtain frequency related information, which cannot be obtained from their Nyquist plots. The nature of the Bode plots confirmed the structural differences of the GCE modified electrodes and the bare GCE [118]. The bare GCE showed unsymmetrical peak with a maximum phase angle value of 67.9° (Fig4.10) corresponding to the relaxation process of the GCE/amitrole interface. After modification of GC electrodes with CoTCPc, PANI, CoTCPc-PANI and CoTCPc-PANI/$Co_2O_3$NPs, all the peaks shifted towards lower frequencies for the relaxation processes of the modifier –GCE/amitrole interfaces, with the PANI spectrum showing a broad band which stretches from lower frequencies to higher frequencies. The relaxation process of the CoTCPc-PANI/$Co_2O_3$NPs-GCE/amitrole was at a phase angle of 58.8. Changes in phase angle and frequencies confirmed that the oxidation of amitrole was taking place at

modified platform rather than on the bare GCE surface. Both the Nyquist and the Bode plots confirmed the poor electron transfer kinetics for the CoTCPc-GCE for amitrole. Such a trend was also observed from the cyclic voltammetry of amitrole on different electrode where CoTCPc –PANI/Co2O3NPs showed reduced potentials and improved currents. At the frequency region of the impedance under study the charge transfer Rct, decreased for the electrode modifiers due to facilitation of the electron transfer which is an indication that films form high electron conduction pathways between the electrode and electrolyte /analyte [2].

The phase angles values for all electrode surfaces studied in this work are less than the ideal 90○ for a true capacitor. The bare GCE had a phase angle at 67.9○ corresponding to the GCE | amitrole interface.4.11 Kinetic studies of amitrole

The effect of varying scan rate of 1 mM amitrole at CoTCPc-PANI/$Co_2O_3$NPs was studied and increase in peak current and shifts in peak potentials towards more positive values were observed for the conjugate as the scan rate increases from 100 to 450 mV/s.This is an indication of irreversibility of the redox reaction. The plot of current against square root of scan rate showed a linear relationship, with a correlation value of 0.995 showing that the electrocatalytic oxidation of amitrole is diffusion controlled Fig 4.11

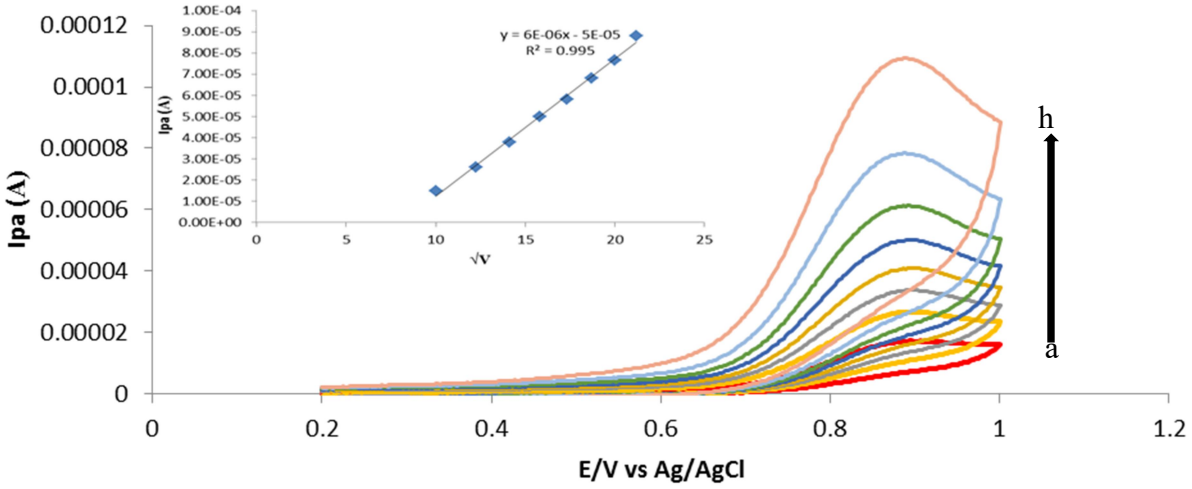


**Fig 4.11: Effect of scan rate on peak potentials and currents a) 100 mV/s, b) 150 mV/s, c) 200 mV/s, d) 250 mV/s, e) 300 mV/s, f) 350 mV/s, g) 400 mV/s and h) 450mV/s on CoTCPc-PANI/$Co_2O_3$NPs for amitrole oxidation. [Amitrole] = 1mM. *Inset*: plot of $I_{pa}$ vs√v.**

### 4.12Tafel slopes

Fig 4.12 shows a linear plot of peak potential, E versus log *v*. An increase in scan rate from 100 to 450 mV/s resulted in the amitrole oxidation peak shifting towards positive potentialsindicating the chemical irreversibility of the electrocatalytic oxidation process. The relationship between peak potential and scan rate for an irreversible diffusion process is given by Eq [22].

$$E_p = \frac{2.3R}{2(1-\propto)n_{\propto}F} logv + K \qquad (4.5)$$

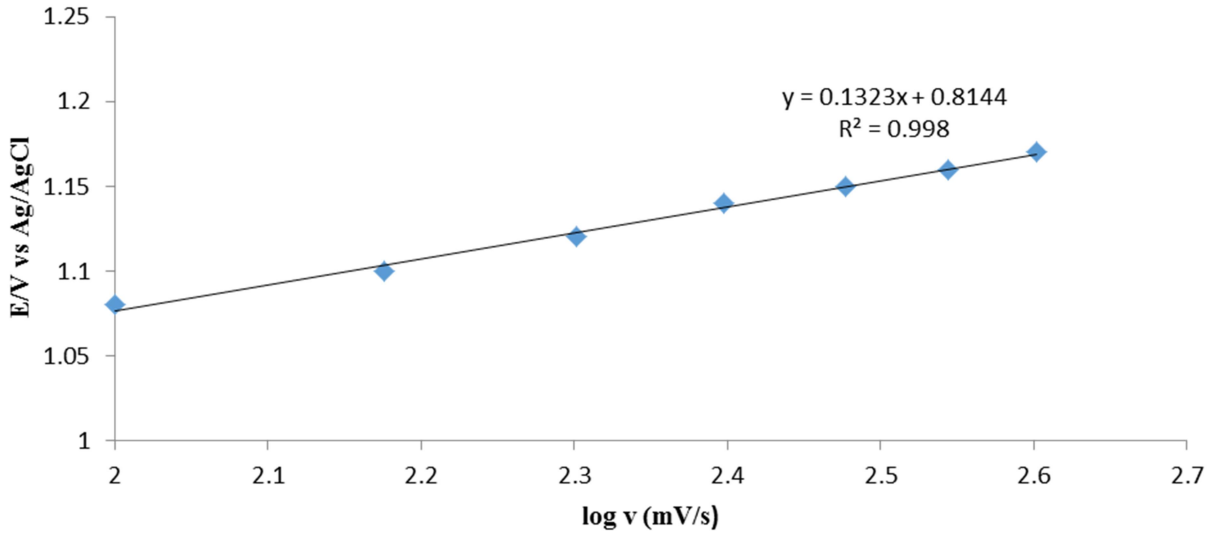


**Fig 4.12: Plot of potential versus log scan rate in 1mM amitrole**

Plots of Ep versus log *v* gave a linear relationship as represented by the Eq. Tafel slope of 265 mV decade $^{-1}$ (2 × slope of plot was obtained for amitrole). Tafel slopes of this magnitude have no kinetic meaning but could indicate a passivated phenomenon occurring on the electrode surface. Tafel slopes much greater than the normal 30-120 mV decade$^{-1}$ for a one electron rate determining step have been observed [116] and have been either to chemical reaction coupled to electrochemical steps or to substrate catalyst interactions in a reaction intermediate. Similar Tafel

slopes have been observed in systems involving species with very high surface to volume ratio like MPc and carbon nanotubes [111].

### 4.13Mechanism of amitrole oxidation with CoTCPc-PANI/$Co_2O_3$NPs-GCE

The number of electrons involved in amitrole oxidation at the CoTCPc-PANI/$Co_2O_3$NPs-GCE surface was obtained from a plot of oxidation against pH of amitrole solution

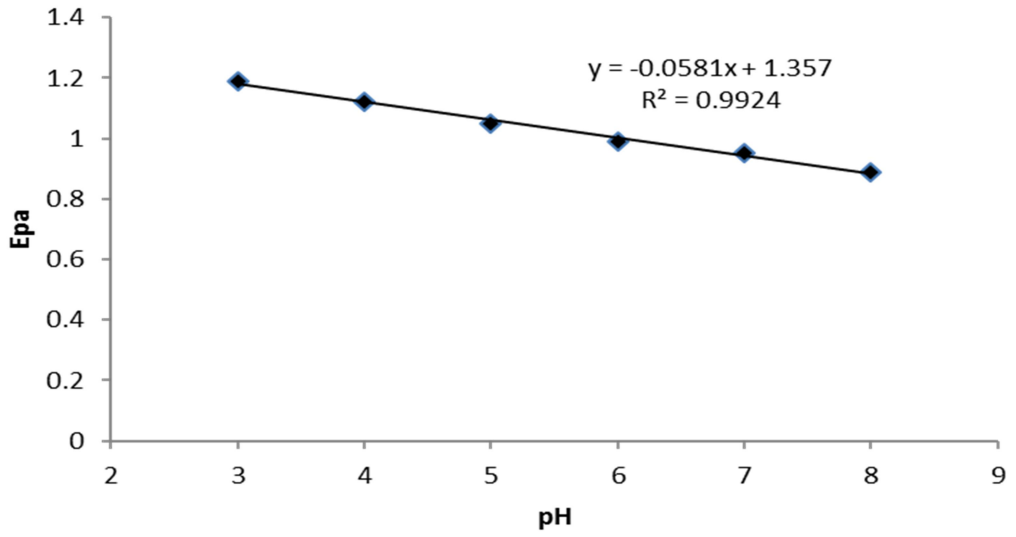


**Fig 4.13: Plot of peak potential against pH for the detection of 1 mM of amitrole on CoTCPc-PANI/$Co_2O_3$NPs-GCE**.

From the plot, it was observed that the peak potential decreased gradually with increasing pHvalues, with a slope of 58mV/pH.The slope is in close agreement with the theoretical value of 59mV/pH at 25 for a one electron transfer process. A two electron transfer oxidation process for amitrole was reported by other workers as well [6].

### 4.14 Order of reaction

The plot shows a linear relationship and from this plot, the order of reaction can also be deduced or rather be estimated. Therefore according to figure 4.14the correlation value was 0.9955 giving evidence that there was linear relationship between log concentration and log of current.

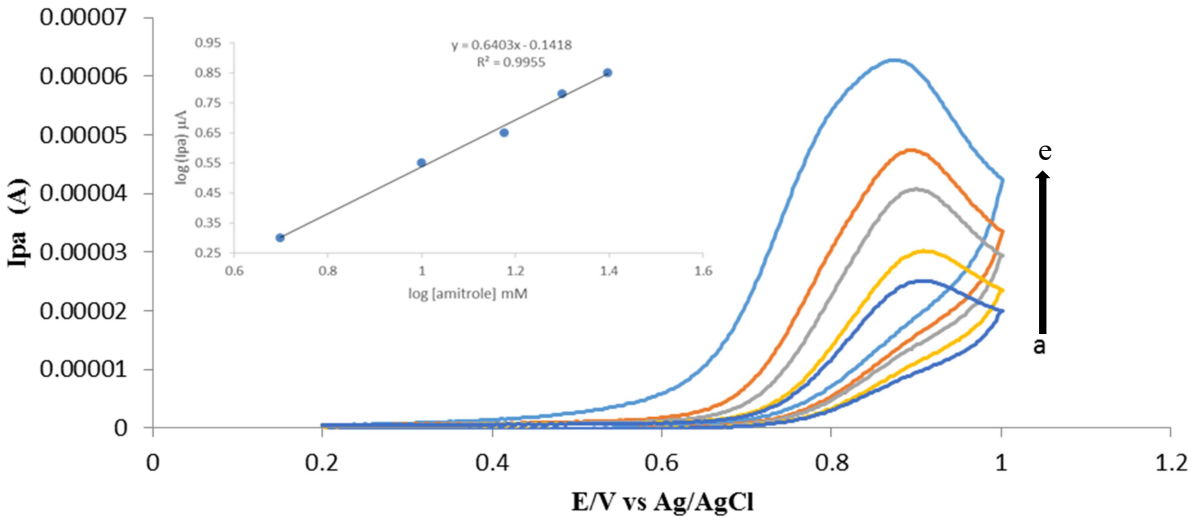


**Fig 4.14Cyclic voltammograms for (a) 2 mM , (b) 10mM, (c) 15mM (d) 20mM and (e) 25mM of amitrole concentrations in pH 4 PBS. *Inset* plot of log $I_{pa}$ vs log [amitrole]**

The electrocatalysis of amitrole was found to be first order from the of plot log Ipa vs log [amitrole] (Fig. 4.14 insert), implying that one analyte molecule interacts with one molecule of CoTCPc-PANI/$Co_2O_3$NPs.

A previous report on the interaction of FePC with amitrole [6] proposed involvement of the $F^{III}Pc^{-2}/Fe^{II}Pc^{-2}$ redox process. $Co^{III}Pc^{-2}/Co^{II}Pc^{-2}$ redox processes may be similarly be involved in the oxidation of amitrole since the $Co^{III}Pc^{-2}/Co^{II}Pc^{-2}$ redox potential is very close to the oxidation

of amitrole. Thus the mechanism through which electrocatalytic oxidation of amitrole operates at the CoTCPc-PANI/$Co_2O_3$NPs-GCE may be represented as shown by Eqs.

$$Co^{II}TCPc^{-2} \longrightarrow Co^{III}TCPc^{-2} + e^{-} \quad (4.5)$$

$$Co^{III}TCPc^{-2} + amitrole^{-} \longrightarrow [Co^{III}TCPc^{-2}(amitrole^{-})] \quad (4.6)$$

$$Co^{III}TCPc^{-2}[(amitrole^{-})] \longrightarrow Co^{II}TCPc^{-2} + amitrole\ (_{oxidized}) \quad (4.7)$$

That is, initial oxidation of the $Co^{II}TCPc^{-2}$ to $Co^{III}TCPc^{-2}$ is followed by the oxidation of the amitrole anion to its products via $Co^{III}TCPc^{-2}$ and subsequent regeneration of the $Co^{II}TCPc^{-2}$complex.

### 4.15 Linear Sweep Studies

Linear sweep voltammetry (LSV) was done to show adsorption behavior of CoTCPc-PANI/$Co_2O_3$NPs-GCE

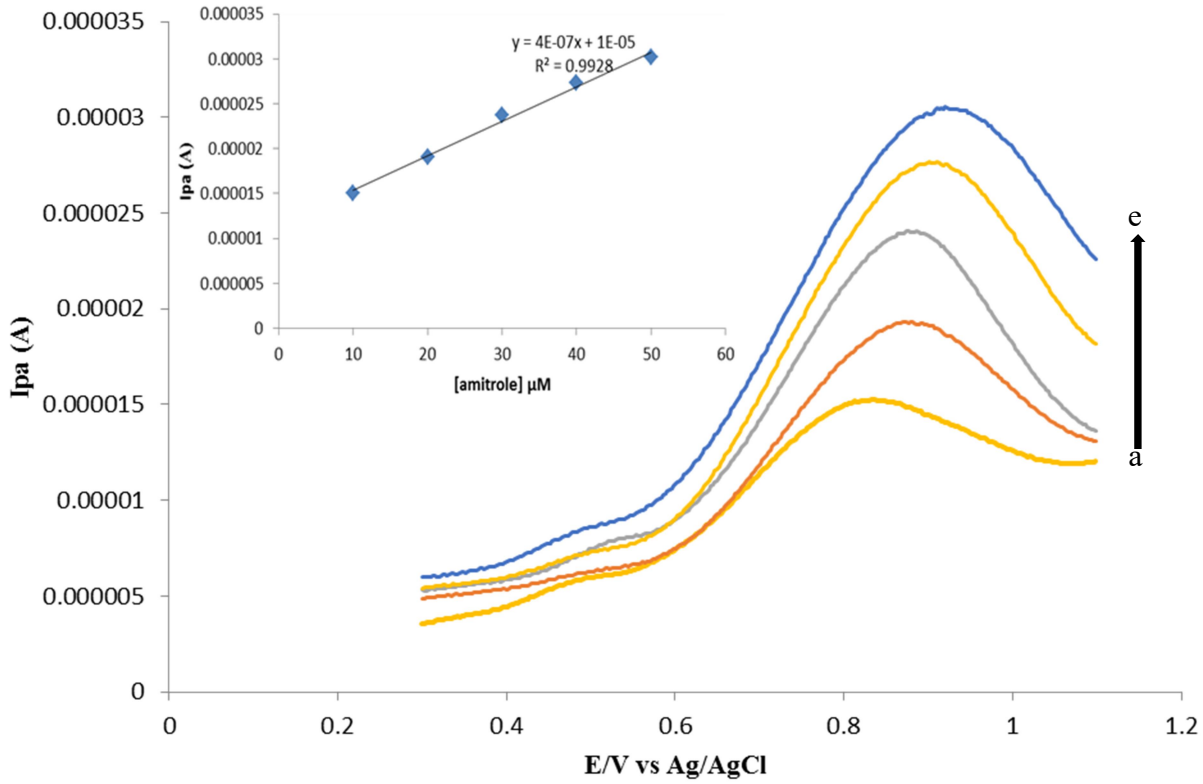


**Fig 4.15 Linear sweep voltammograms(a) 10 µM, (b) 20µM, (c) 30 µM (d) 40 µM and (e) 50 µM of amitrole concentrations in pH 4 PBS. *Inset* plot of $I_{pa}$vs.[amitrole].**

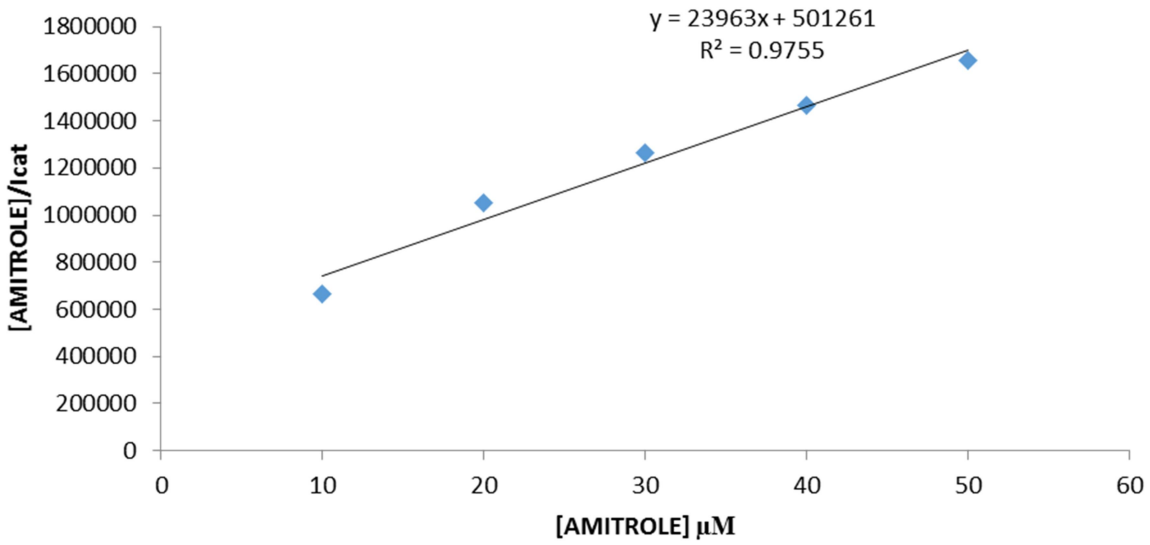


**Fig 4.16 Langmuir adsorption isotherm plot for CoTCPc-PANI/$Co_2O_3$NPs-GCE ina) 10 µM, (b) 20 µM, (c) 30 µM (d) 40 µM and (e) 50 µM of amitrole concentrations in pH 4 PBS. Oxidation currents employed.**

Fig 4.15shows LSV plots obtained after keeping the electrode in a stirred solution for 20 minutes to allow for adsorption. Applying the Langmuir adsorption theory (Eq 4.8) [116] a plot of the ratio of amitrole concentration to catalytic current against concentration of amitrole gave a linear plot which is which can be interpreted as an adsorption controlled electrochemical process.

$$\frac{[Amitrole]}{I_{cat}} = \frac{1}{ßI_{max}} + \frac{[Amitrole\,]}{I_{cat}} \qquad (4.8)$$

where ß is the adsorption equilibrium constant, $I_{max}$ is the maximum current and $I_{cat}$ is the catalytic current. From the slope and the intercept of Fig 4.16the adsorption equilibrium constant ß was established to be 3.8 x$10^3$ $M^{-1}$. Using equation 4.9 which relates Gibbs free energy change

due to adsorption ($\Delta G^{\circ}$) to the adsorption equilibrium constant ß, ($\Delta G^{\circ}$) was found to be -20.42kJ. This value is in comparable to those reported elsewhere for high Tafel slopes [116].

$$\Delta G^{\circ} = -RT\ ln\ ß \qquad (4.9)$$

Where R is the molar gas constant and T is room temperature

### 4.16 Chronoamperometry Studies

Chronoamperometry data was used to determine catalytic rate constant for the oxidation of amitrole. Catalytic rate constants are a measure of how fast redox processes takes place at the electrode /analyte interface.

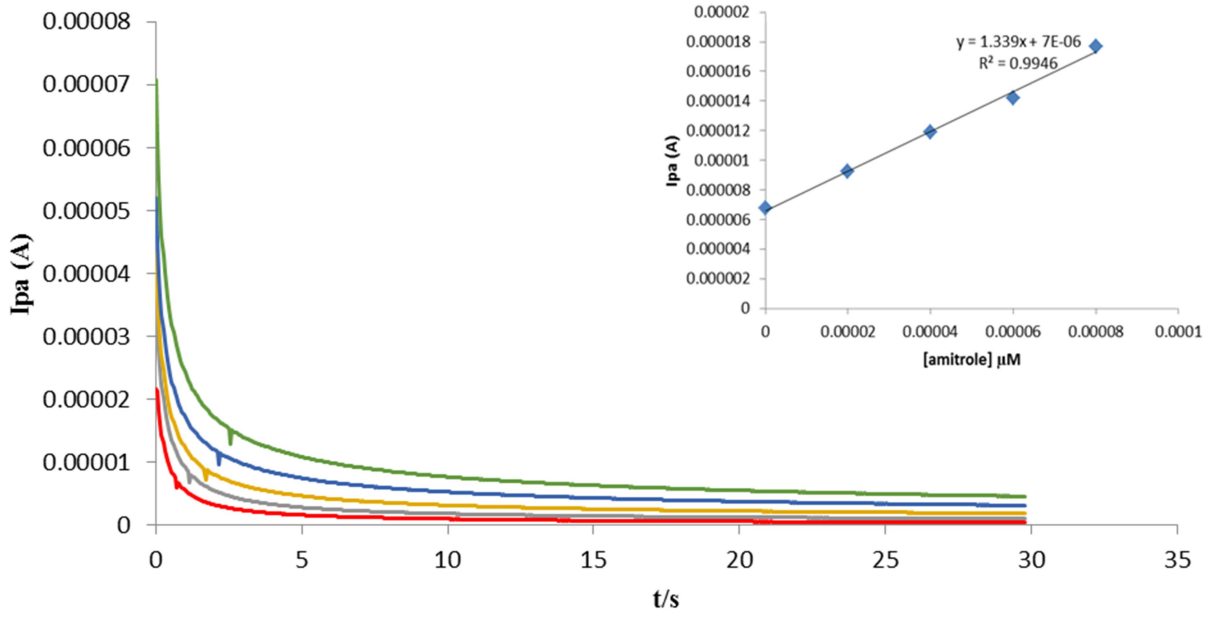


**Fig 4.17 Chronoamperograms for different Amitrole concentrations. In PBS pH 4, 20 µM, 40 µM , 60 µM , 80 µM. *Inset* Ipa vs[amitrole]**

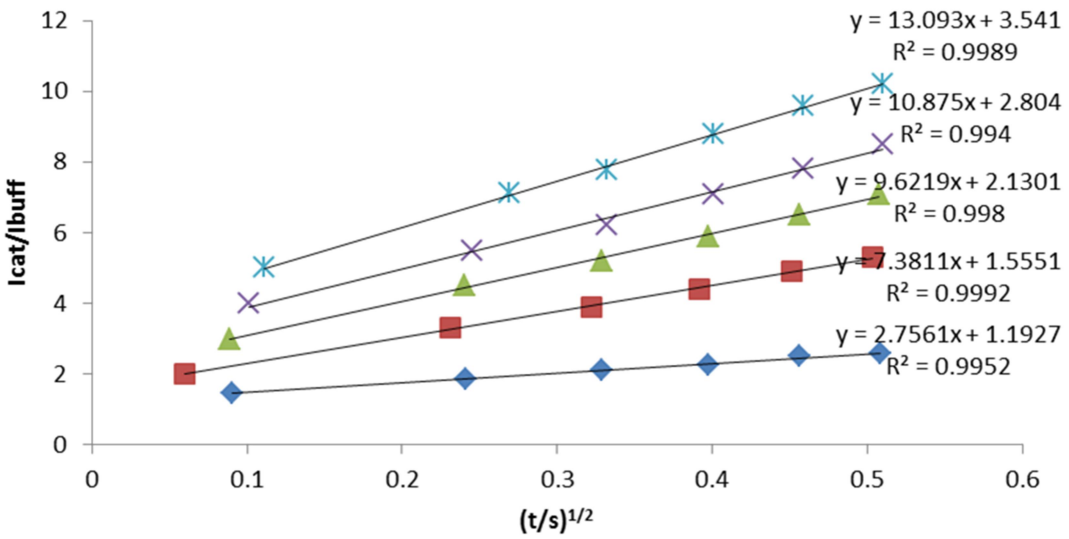


**Fig 4.18 Plots of $I_{cat}/I_{buf}$vs time (s)**

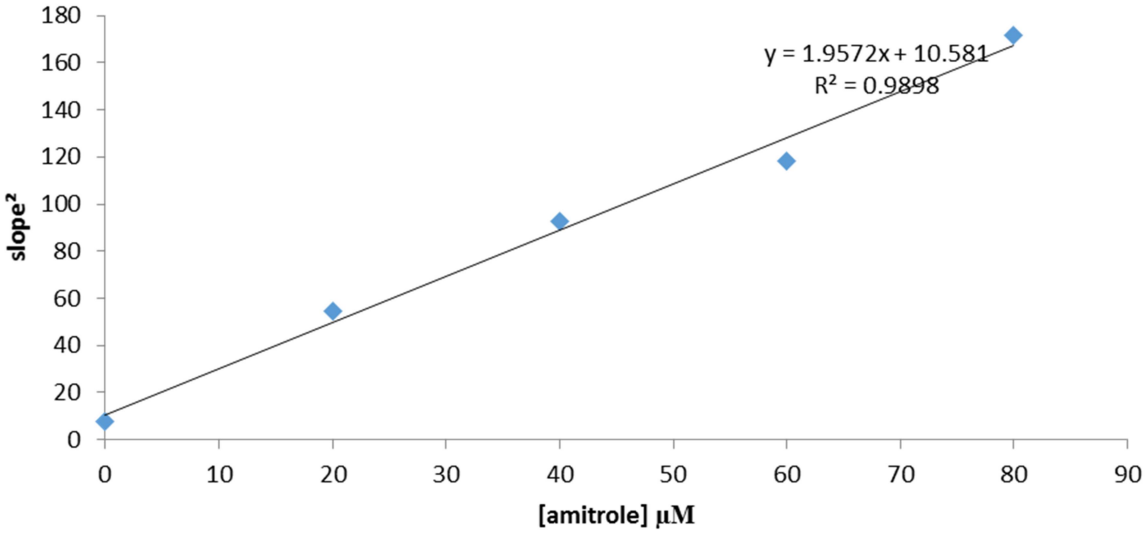


**Fig 4.19 Plot of slopes$^2$ vs.[Amitrole]**

The rate constant for the detection of amitrole was calculated using the equation:

$$\frac{I_{cat}}{I_{buf}} = \pi^{\frac{1}{2}}(kC_O t)^{1/2} \qquad (4.10)$$

Where $I_{cat}$ and $I_{buf}$ are currents in the presence and in the absence of amitrole, k is the catalytic constant ($M^{-1}s^{-1}$) for the amitrole oxidation and t is the time in seconds .Figure 4.17. Shows the linear relationship for Icat and Ibuf vs $t^{1/2}$ plots for different amitrole concentrations obtained from the Chronoamperograms. Fig 4.19 showed the linear relationship for the slope$^2$ vs.[amitrole]. The slope of Figure 4.19 is equal to πk and this gives a k value of 6.26 ×105 M-1s-1. The value of k obtained is large. The larger the k value, the faster the rate of oxidation at the modified electrode. This showed that CoTCPc-PANI/$Co_2O_3$NPs was the best electrode for fast detection of amitrole. Figure 4.18 insert shows the plot of peak current against concentration. A linear relationship was observed from the plot. A linear regression equation was obtained as $i_p = 1.3393x + 7\ \text{x}10^{-5}$ and $R^2 = 0.9946$ where $x$ is the concentration of the analyte. The limit of detection is equivalent to $3\sigma/s$ where $\sigma$is the standard deviation of the intercept and s is the slope of the calibration curve. LOD was found to be 1.12 ×$10^{-5}$M. The LOQ ($10\sigma/s$)was found to be 3.566 × $10^{-5}$ M. This value is slightly lower than what has been observed elsewhere [4].

### 4.17 Differential Pulse Voltammetry

Fig 4.20 shows differential pusle voltammograms of CoTCPc-PANI/$Co_2O_3$NPs-GCE in different concetrations of amitrole .

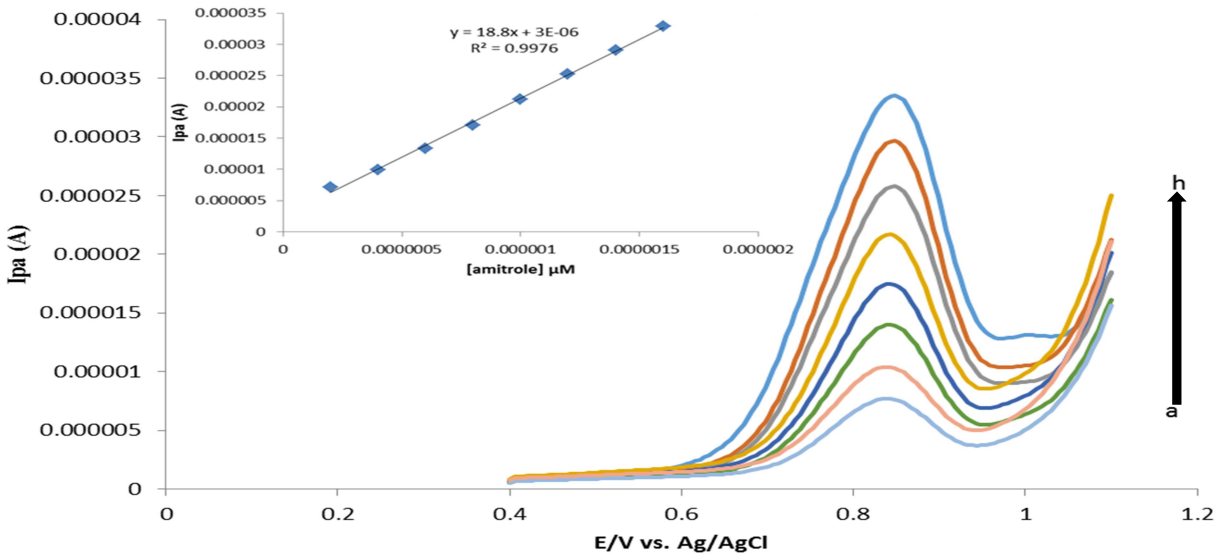


**Figure 4.20DPV for CoTCPc-PANI /$Co_3O_4$NP-GCE in: a) 0.2 µM, b) 0.4 µM, c) 0.6 µM, d) 0.8 µM, e) 1 µM, f) 1.2 µM, g) 1.4 µM, h) 1.6 µM. *Inset*: Plot of $I_{pa}$ vs [amitrole].**

Figure 4.20inset shows the plot of peak current against concentration. A linear relationship was observed from the plot. A linear regression equation was obtained as $i_p = 18.8x + 3\,x10^{-5}$ and $R^2$= 0.9976 where $x$ is the concentration of the analyte. The limit of detection is equivalent to $3\sigma/s$ where $\sigma$is the standard deviation of the intercept and s is the slope of the calibration curve. LoD was found to be 6.612 x $10^{-8}$M. The LoQ ($10\sigma/s$)was found to be 2 x $10^{-7}$ M. In a previous study on the voltammetric determination of amitrole in agricultural waste water [37], the LOD was found to be 0.1 µM, comparing with our obtained results the CoPc-PANI/$Co_3O_4$NPs-GCE is a better electrode in the detection of amitrole .

### 4.18 Electrode Stability

Stability of the modified electrode CoPc-PANI/$Co_3O_4$NPs-GCE was investigated by repeatedly examining the response current to amitrole.

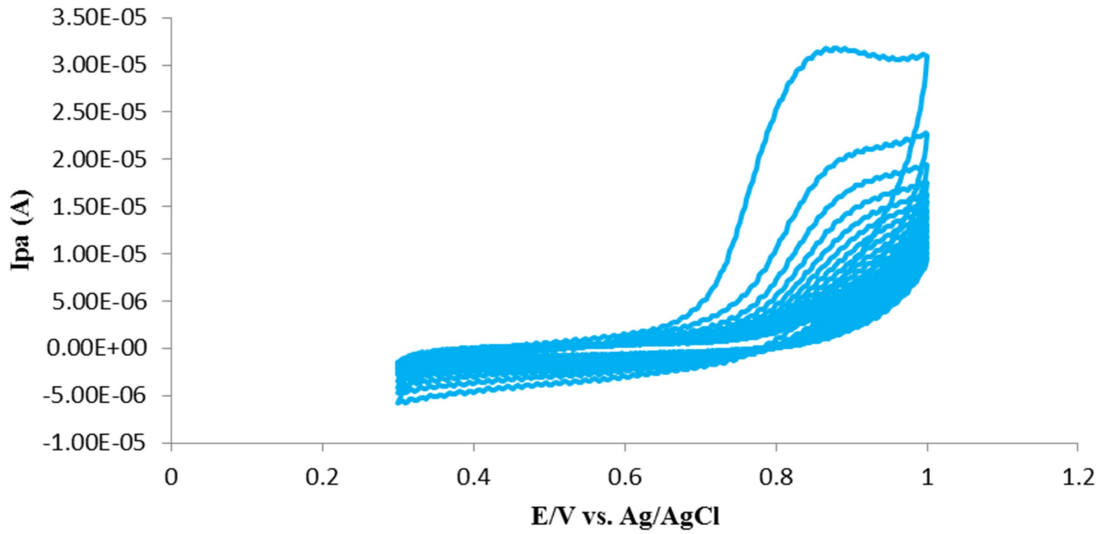


**Figure 4.21:Continuous cyclic voltammetric evolutions for 1 mM Amitrole generated on GCE modified with CoTCPc-PANI /$Co_3O_4$ NP. Scan rate = 100 mV/s. pH 4 PBS**

Figure 4.21 showsa 20cycle continuous scan voltammogram for CoTCPc-PANI /$Co_3O_4$ NP-GCE in 1mM amitrole. The stability of the modified electrode was confirmed by noting the drop in current from scan 1 to scan 2. A percentage decrease of 62.3 % was observed from the first scan to the second scan. Drop in current is a passivation phenomenon and the rate at which the current drops is a measure of resistance to passivation of the electrode towards that analyte [111]. The percentage decrease of 62.3 % from the first scan to the second scan shows that the CoTCPc-PANI/$Co_3O_4$NP was not very stable. Passivation was attributed to amitrole and its interaction with the electrode. Presence of amitrole derivatives which are less electro active could have contributed to the passivation phenomenon.

### 4.19 Reproducibility

The modified surface area provided better reproducibility as indicated by the slight decrease in the peak current after washing the electrode two different times with ethanol with relative standard deviation of 2.58 % and 4.22%, which is below 5 % and this indicated good repeatability of the modified electrode [114].

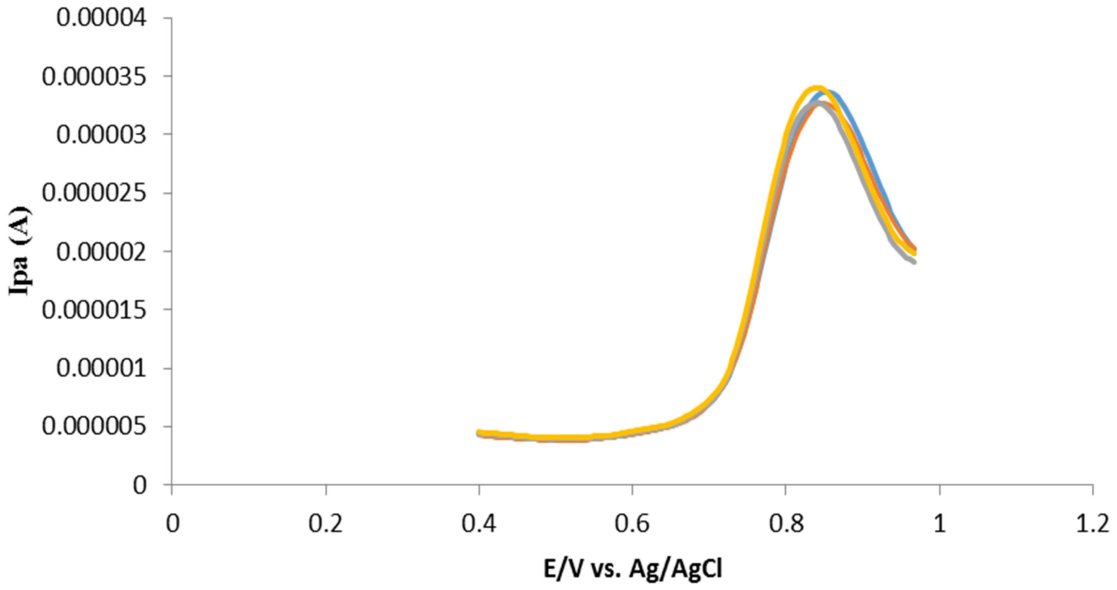


**Fig 4.22: Differential pulse voltammograms for four repetitions in 1mM Amitrole in pH 4 PBS solution at CoTCPc-PANI/$Co_2O_3$NPs-GCE. Scan rate = 100 mV/s at potential 0.4 to 1.0 V**

### 4.20Interference Studies

The interference study was done using DPV onCoTCPc-PANI/$Co_2O_3$NPs-GCEand the concentration of the interfering compounds was carried in a 1:1 ratio of amitrole:nitrates. Peaks were recorded for the amitrole alone and nitrates then finally the two analytes were mixed in a

1:1 ratio and DPV voltammograms were recorded, Figure 4.23. Oxidation of amitrole occurs at a potential 14 mV more positive than that of nitrates.

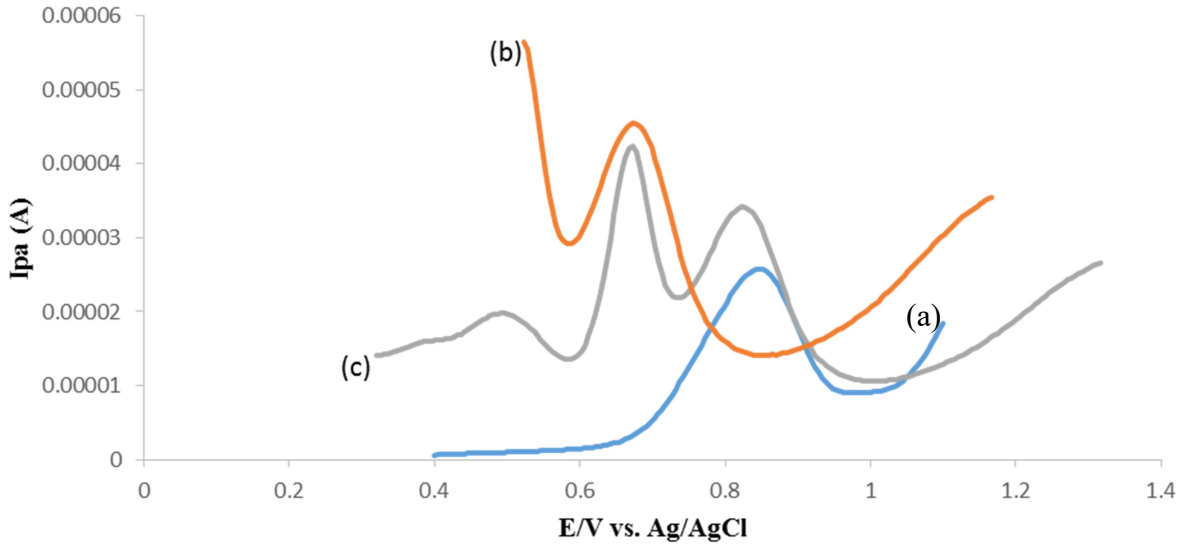


**Fig 4.23 DPV for (a) amitrole, (b) nitrates and (c) amitrole and nitrates mixture in PBS pH 4.**

The effect of these species was determined using DPV and it was observed that there no great significant change in the peak currents and peak potentials of the interfered species. The relative percentage response of the sensor calculated using the formulae:

$$(R\ \%) = [1 - (\frac{I^{analyte} + I^{inter}}{I^{inter}})] \times 100$$

Where $I^{analyte}$ and $I^{inter}$ are the peak currents for the amitrole and for the interfering respectively. The RSD % above 10 % shows that the compound interferes with the analyte [8]. All the interferences showed to have no effect as they had interference effect of less than 10 %.The RSD (%) were 4.2%for amitrole and 6.5% for nitrates.

### 4.21.1 Analysis of amitrole in agricultural waste water

The DPV technique was employed for the standard addition method. In order to ascertain the potential application in practical sample analysis, the developed method was used to detect amitrole in agricultural waste water. The agricultural waste water sample was spiked with aliquots amount of amitrole standard. The average results for four replicate measurements with standard deviation are summarized in table 4.6

**Table 4.6:** Results for determination of amitrole in waste water

| Samples | Added (μM) | Expected (μM) | Found (μM) | Recovery (%) |
|---|---|---|---|---|
| 1 | 0 | - | 1.9 | 109.1± 1.7 |
| | 2.5 | 4.4 | 4.8 | |
| 2 | 0 | - | 3.6 | 95.3± 1.3 |
| | 5 | 8.6 | 8.2 | |
| 3 | 0 | - | 5.2 | 103.2± 1.9 |
| | 7.5 | 12.3 | 12.7 | |

# CHAPTER 5

# CONCLUSION AND RECOMMENDATION

## 5.1 Conclusion

Spectroscopic techniques were used to confirm the formation of chemical linkages between the polyaniline and the MPcs. Use of FTIR was used to monitor the changes in the positions of the C = O vibronic bands as way of confirming chemical linkage between polyaniline and MPcs. Cyclic voltammetry showed the differences in behavior of the modified electrodes in pH 4 buffer solutions. Using peak currents with changes in scan rate the surface coverage of the modifier was found to be 0.40 $cm^2$ almost twice large that of a bare glassy carbon electrode.The modified electrode had a surface coverage of  showing the deposited modifier on the electrode surface. The Gibbs free energy of the electrocatalytic oxidation of amitrole was found to be -22.47kJ which corresponded to high value obtained for the Tafel slope suggesting that the was a strong interaction between the electrode modifiers  and the analyte. The apparent electron transfer rate for CoTcPC-PANI/$Co_2O_3$NPs was found to be 8.84 $\times 10^{-3} cms^{-1}$ indicating that the was fast electron transfer during oxidation. The plot of potential against pH and the graph of order of reaction confirmed that the electrocatalytic oxidation amitrole involved a one electron transfer process.The rate constant k, was $6.26 \times 10^5 M^{-1}s^{-1}$showing fast electron transfer during oxidation. The electrochemical sensing of amitrole was successful with CoTcPC-PANI/$Co_2O_3$NPs-GCE showing high electro catalytic currents as compared to other electrodes. The limit of quantification  was $2 \times 10^{-7}$ Mand limit of detection was $6.612 \times 10^{-8}$M.The electrode showed good reproducibility with lower oxidation potential at 0.8 V and high sensitivity towards amitrole as the rate determining step followed by slow chemical step. It was observed that amitrole c acid interfered with the detection of amitrole.

## 5.2 Recommendations

In our study we, used the dip and dry method for electrode modification. The process involves the modifier solution being dropped onto the electrode surface and then allowed to dry. Immobilization of polyaniline is encouraged by the л-л interactions that occur between them and the GCE. The advantage of this modification process is that it is fast and a relatively stable Pc/PANI layer can be formed on carbon based electrodes where л-л interactions can occur between the MPc and PANI, and the substrate surface. The disadvantages are that the electrode surfaces are not reproducible and unstable over long periods of time. Further work can be done using different electrode modification techniques so as to promote reproducibility.

Metallophthalocyanines (MPcs) exhibit a rich electrochemical behavior due to the accessibility of a range of oxidation states centered on the Pc unit and on the central metal. MPcs are very good electrochemical catalysts and as such they have been used for the detection of many analytes. In our study the modifier comprised of cobalt based metallo phthalocyanine the $Co^{III}/Co^{II}$ was observed to be responsible for the oxidation of amitrole. Further studies can be pursued using other metallo phthalocyanines such as Ni or Fe were both metallo phtalocyanines have been used in previous studies as electrode modifiers. Different morphologies of metallic nanoparticles have been produced by using different solvents. The morphology and particle size of metal nanoparticles may in addition be controlled by reaction temperature the concentration of metal precursors and the type of reducing agent, and in turn these morphologies may have an effect on the electrochemical process. Thus further studies can be undertaken to observe the nanoparticle morphologies so as to observe the different sizes and shapes, and how they affect the electrochemical process. Aspects in the research that can be improved include further conjugation of the overall modifier, it was observed that electrocatalysis improved with the

introduction of polyaniline to the CoTCPc, catalysis was also observed to improve upon introduction of an amide link. Thus further improvement in the electrocatalysis process can be brought about by the introduction of new groups in the conjugated structure.

In the study the results obtained showed that the proposed methods can be recommended for the determination of amitrole in agricultural waste water.

## REFERENCES


[1] Agnolucci L, Dalla F, Roberto V. Amitrole Effects on Chloroplasts of Barley Plants Grown at Different Temperatures. Journal of Plant Physiology 1996;147:493–502. doi:10.1016/j.pp.0176-1617(96)80037-X.

[2] Mugadza T, Nyokong T. Electrocatalytic oxidation of amitrole and diuron on iron ( II ) tetraaminophthalocyanine-single walled carbon nanotube dendrimer.Electrochim Acta 2010;55:2606–13. doi:10.1016/j.electacta.2009.12.051.

[3] Mada D, Idris DN, State A. Effect of Continuous Application of Herbicide on Soil and Enviroment with Crop Protection Machinery in Southern Adamawa State .J Enviromental Science 2013;2:4–9.doi:10.1016/j.environ sc.2013.06.038.

[4] J.M. Zen, A.S. Kumar, M.R. Chang, Electrocatalytic oxidation and trace detection of amitrole using a Nafion/lead–ruthenium oxide pyrochlore chemically modified electrode, Electrochimica Acta 45 (2000) 1691doi:10.3390/j.electacta 110505087.

[5] Simo R. Electroanalytical Detection of the Pesticide Paraquat by Batch Injection AnalysisApplied Surface Science. 2007:1800–10. doi:10.1080/00032710701380806.

[6] Siswana M, Ozoemena KI, Nyokong T. Electrocatalytic behaviour of carbon paste electrode modified with iron ( II ) phthalocyanine ( FePc ) nanoparticles towards the detection of amitrole, Sensors 2014 ; 14 :10432-53. doi: 10.3390/s 140610432.

[7] Soomro MT, Ismail IMI. A Simple Electrochemical Approach for Determination and Direct Monitoring of Drug Degradation in Water.Nano letters 2013;8:375–80.doi:10.1016/nano letters.2012.05.052.

[8] Maringa A, Mugadza T, Antunes E, Nyokong T. Characterization and electrocatalytic behaviour of glassy carbon electrode modified with nickel nanoparticles towards amitrole detection. J Electroanal Chem 2013;700:86–92. doi:10.1016/j.jelechem.2013.04.022.

[9] Maringa A, Mugadza T, Antunes E, Nyokong T. Characterization and electrocatalytic behaviour of glassy carbon electrode modified with nickel nanoparticles towards amitrole detection.J Talanta 2006;69: 1136-42. doi: 10. 1016/j.talanta.2005.12.014

[10] Hoffiotein V. Alveolar Damage due to Inhalation of Amitrole-Containing Herbicide.Plant physiology journal 2010:63-9.doi:10.1007/jpp00604-010-0404-3.

[11] Mani V, Devasenathipathy R, Chen S, Vasantha VS, Ali MA, Huang S, et al. A simple electrochemical platform based on pectin stabilized gold nanoparticles for picomolar detection of biologically toxic amitrole.American Journal of Analytical Chemistry, 2013, doi:10.1039/ajac5an00930h.

[12] Siswana M, Ozoemena KI, Nyokong T. Electrocatalytic behaviour of carbon paste electrode modified with iron ( II ) phthalocyanine ( FePc ) nanoparticles towards the detection of amitrole J Talanta 2006;69:1136–42. doi:10.1016/j.talanta.2005.12.014.

[13] Ben I, Gannouni M, Ben J. Voltammetric Determination of the HerbicideSensors 2013, 13, 4811-4840; doi:10.3390/s130404811

[14] Mugadza T, Arslano Y. Single walled carbon nanotube conjugate platforms and their use in electrocatalysis of amitrole.Electrochimica Acta2012.02.041.doi:10.1016/j.electacta.

[15] Stelzle M, Wagner R, Nisch W, Ja W, Schaldach M. On the chemical modification of

pacemaker electrodes and patterned surface functionalization of planar substrates. American journal of analytical chemistry 2015; 351:927–34. doi: 10.1016/ajac.2015.06.038.

[16] Li JZ, Pang XY, Yu RQ. Substituted cobalt phthalocyanine complexes as carriers for nitrite-sensitive electrodes. Anal Chim Acta 1994;297:437–42. doi:10.1016/anc0003-2670(94)00239-8.

[17] Huang W, Humphrey BD, Macdiarmid AG. Polyaniline , a Novel Conducting Polymer Morphology and Chemistry of its Oxidation and Reduction in Aqueous Electrolytes.Advanced material letters 2014, 5(12), 728-733doi: 10.5185/amlett.2014.amwc550

[18] Transactions CS, Manigandan R, Giribabu K, Suresh R, Vijayalakshmi L, Stephen A, et al. Cobalt Oxide Nanoparticles : Characterization and its Electrocatalytic Activity towards Nitrobenzene.Chemical Science 2013;2:47–50. doi:10.7598/cst2013.10.

[19] Wöhrle D, Schnurpfeil G, Makarov SG, Kazarin A, Suvorova ON. Practical applications of phthalocyanines - from dyes and pigments to materials for optical, electronic and photo-electronic devices. Electrochem Sci 2012;5:191–202. doi:10.6060/es2012.120990w.

[20] Sakamoto K, Ohno-okumura E. Syntheses and Functional Properties of Phthalocyanines.Spectrochimica Acta,Part A 2009:1127–79. doi:10.3390/sap2031127.

[21] Achar BN, Lokesh KS. Studies on phthalocyanine sheet polymers.J Organic chemistry 2004;689:2601–5. doi:10.1016/j.jorganchem.2004.05.017.

[22] Wang Y, Laborda E, Compton RG. Electrochemical oxidation of nitrite : Kinetic, mechanistic and analytical study by square wave voltammetry. J Electroanal Chem 2012;670:56–61. doi:10.1016/j.jelechem.2012.02.016.

[23] Heli H, Pishahang J. Synthesis and application for enhanced electrocatalytic reaction and highly sensitive nonenzymatic detection of hydrogen peroxide. Electrochim Acta 2014;123:518–26. doi:10.1016/j.electacta.2014.01.032.

[24] Siangproh W, Leesutthipornchai W, Dungchai W, Chailapakul O. Electrochemical detection for flow-based system : A Review. J Flow Inject Anal 2009;26:5–25.

[25] Foster CW, Pillay J, Metters JP, Banks CE. Cobalt Phthalocyanine Modified Electrodes Utilised in Electroanalysis: Nano-Structured Modified Electrodes vs. Bulk Modified Screen-Printed Electrodes 2014:21905–22. doi:10.3390/s141121905.

[26] Mphahlele N. Photoeletrochemistry of Metallo- octacarboxyphthalocyanines/Multi-walled carbon nanotubes hybrid for development of Dye Solar Cells. Int J Electrochem 2013:699.doi:10.1007/s00339-008-4922-3.

[27] Z, Zawawi. Study of metallophthalocyanines attached onto pre-modified gold surfaces.Electrochimica Acta 2007;6:7525-31.doi:10.1039/C4AY00837E

[28] Bredow YAOT, Knupfer IMM. The electronic structure of cobalt phthalocyanine 2009:485–9. doi:10.1007/s00339-008-4922-3.

[29] Mugadza T, Nyokong T. Electrochemical , microscopic and spectroscopic characterization of benzene diamine functionalized single walled carbon nanotube-cobalt ( II )

tetracarboxy-phthalocyanine conjugatesElectrochimica Acta. doi:10.1016/j.Elctrochimica acta.2010.10.057.

[30] Mamuru SA. Electrochemical and electrocatalytic properties of iron(II) and cobalt(II) phthalocyanine complexes integrated with multi-walled carbon nanotubes. Res J Chem Sci 2003;145:864–74. doi:10.1149/1.1838359..

[31] Nemykina VN, Lukyanets EA. Synthesis of substituted phthalocyanines. Arkivoc 2010;2010:136–208. doi:10.3998/ark.5550190.0011.104.

[32] Zhou B, Chen W. Preparation and Catalytic Activity of Carbon Nanofibers Anchored Metallophthalocyanine in Decomposing Acid Orange 7. Anal Chim Acta 2014;7:1370–83. doi:10.3390/ma7021370.

[33] Zagal JH. Metallophthalocyanines reactions as catalysts in electrochemical. Electrochem Soc Interface 2013;119:89–136.

[34] Sakamoto K, Ohno-okumura E. Syntheses and Functional Properties of Phthalocyanines. Electrochem Soc Interface 2009:1127–79. doi:10.3390/ma2031127.

[35] Claessens CG, Hahn U, Torres T. Phthalocyanines: From outstanding electronic properties to emerging applications. Chem Rec 2008;8:75–97. doi:10.1002/tcr.20139.

[36] Foster CW, Pillay J, Metters JP, Banks CE. Cobalt Phthalocyanine Modified Electrodes Utilised in Electroanalysis: Nano-Structured Modified Electrodes vs. Bulk Modified Screen-Printed Electro. Electrochem Sci 2014:21905–22. doi:10.3390/s141121905.

[37] Mugadza T, Nyokong T. Covalent linking of ethylene amine functionalized single-walled

carbon nanotubes to cobalt ( II ) tetracarboxyl-phthalocyanines for use in electrocatalysisJ.Synthetic material 2010.07.036.. doi:10.1016/j.synthmet.2010.07.036.

[38] Song E, Choi J. Conducting Polyaniline Nanowire and Its Applications in Chemiresistive Sensing.Nano letters 2013:498–523. doi:10.3390/nano3030498.

[39] Arslan A, Hur E. Electrochemical storage properties of polyaniline-, poly( -methylaniline)-, and poly( -ethylaniline)-coated pencil graphite electrodes .Sensors 2014;68:504–15. doi:10.2478/s11696-013-0475-9.

[40] Yan C, Zou L, Short R. Polyaniline-modi fi ed activated carbon electrodes for capacitive deionisation. DES 2014;333:101–6. doi:10.1016/j.desal.2013.11.032.

[41] Nanocomposites OΓO, Husain J, B CS, Prasad MVNA. Studies on Electrical and Sensing Properties of Polyaniline / Iron.Journal of Materials Chemistry 2014;4:198–202.

[42] Sivaprasad M, Ch S, Dhananjayulu M, Ny S. Analytical & Bioanalytical Graphene and Polyaniline Composite Modified Glassy Carbon Electrode for Electrochemical Determination of Doripenem and Meropenem.Sensors and Actuators B2014;5:5–10. doi:10.4172/2155-9872.1000192.

[43] Çolak Ö, Arslan H, Zengin H, Zengin G. Amperometric Detection of Glucose by Polyaniline-Activated Carbon Composite Carbon Paste Electrode .Electrochemica acta 2012;7:6988–97.

[44] Husain J, B CS, Prasad MVNA. Synthesis, sensing and magnetic properties of p olyaniline / nickel oxide nanocomposites Journal of Advances in Engineering &

Technology 2014;7:620–6doi:10.1039/C4AY00837E.

[45] Etallurgy M, Elgrade UNOFB, Jegoševa N, et al. Electrochemical characteristics of polyaniline | lead -J.Electrochimica 2006;1:435–46.:445–8.

[46] Dhand C, Das M, Sumana G, Srivastava K, Pandey K, Kim CG, et al. Preparation , characterization and application of polyaniline nanospheres to biosensing."Applied Catal B, Environ 2014;148-149:22–8. doi:10.1016/j.apcatb.2013.10.044. 2010:747–54.

[47] Ginic-markovic M, Matisons JG, Cervini R, Simon GP, Fredericks PM. Synthesis of New Polyaniline / Nanotube Composites Using Ultrasonically Initiated Emulsion Polymerization.Chem. Mater. 2006, 18, 6258-6265

[48] Keivani MB, Zare K, Aghaie M, Aghaie H, Monajjemi M, Branch NT. Synthesis of Nano Conducting Polymer Based Polyaniline and it ' s Composite : Mechanical Properties , Conductivity and Thermal Studies.E-Journal of Chemistry 2010;7:105–10.

[49] Talwar V, Singh RC. Different chemical approaches for the synthesis of polyaniline nanofibers and its application in ammonia gas sensing. Key Engineering Material 2014;605:573–6. doi:10.4028/www.scientific.net/KEM.605.573.

[50] Ngai KS, Tan WT, Zainal RM, Zidan M.Conducting polymers have found application in electrochemical biosensors since they are electrically active.Int. J. Electrochem. Sci., 3 (2008) 819 - 853 2013;8:10557–67.

[51] Hayat A, Marty JL. Polyaniline in electrochemical sensing:Tools for enviromental monitoring .Sensor 2014;14:10432-53.doi:10.3390/s140610432.

[52] Lagashetty A, Kalyani S.Polyaniline-SbO2 Composites: Preparation, Characterization and a c conductivity Study.International Journal of Engineering and Science 2012;1:9–13.

[53] Mostafaei A, Zolriasatein A. Progress in Natural Science : Materials International Synthesis and characterization of conducting polyaniline nanocomposites containing ZnO nanorods. Prog Nat Sci Mater Int 2012;22:273–80. doi:10.1016/j.pnsc.2012.07.002.

[54] Gvozdenovi MM, Jugovi BZ, Stevanovi JS, Lj T, Grgur BN. Electrochemical Polymerization of Aniline.Sensors 2014;14:10432–53. doi:10.3390/s140610432.

[55] Bolat G, Kuralay F, Eroglu G, Abaci S. Fabrication of a Polyaniline Ultramicroelectrode via a Self Assembled Monolayer Modified Gold Electrode. Sensors 2013:8079–94. doi:10.3390/s130708079.

[56] Forster PRJ. High sensitivity dna detection using gold nanoparticles J Electroanal Chem 2014;717-718:29–33. doi:10.1016/j.jelechem.2013.12.011.

[57] Fallis A .Preparation , Structural and Electrical Properties of Tin Oxide. J Nanomater Mol Nanotechnol 2015:2–5.

[58] Fu L, Liu Z, Liu Y, Han B, Hu P, Cao L, et al. Beaded Cobalt Oxide Nanoparticles along Carbon Nanotubes: Towards More Highly Integrated Electronic Devices. Adv Mater 2005;17:217–21. doi:10.1002/adma.200400833.

[59] Ali R, Nafady A, Hussain Z, Tufail S, Sherazi H, Willander M, et al. Materials Science in Semiconductor Processing Development of sensitive non-enzymatic glucose sensor using complex nanostructures of cobalt oxide. Mater Sci Semicond Process 2015;34:373–81.

doi:10.1016/j.mssp.2015.02.055.

[60] Athar T, Hakeem A, Topnani N, Hashmi A. Wet Synthesis of Monodisperse Cobalt Oxide Nanoparticles 2012;2012. doi:10.5402/2012/691032.

[61] Bhatte KD, Bhanage BM. Synthesis of cobalt oxide nanowires using a glycerol thermal route. Mater Lett 2013;96:60–2. doi:10.1016/j.matlet.2013.01.019.

[62] Wang H, Si H, Zhao H, Du Z, Li LS. Shape-controlled synthesis of cobalt oxide nanocrystals using cobalt acetylacetonate. Mater Lett 2010;64:408–10. doi:10.1016/j.matlet.2009.11.034.

[63] Singh K, Kate KH, Chilukuri V V, Khanna PK. Glycerol mediated low temperature synthesis of nickel nanoparticles by solution reduction method. Univ Chem Technol Met 2011;11:5131–6. doi:10.1166/jnn.2011.4142.

[64] I. Markova-Deneva. Infrared Spectroscopy Investigation of Metallic Nanoparticles Based on Copper, Cobalt, and Nickel Synthesized Through Borohydride Reduction Method. J Univ Chem Technol Metall 2010;45:351–78.

[65] Tamishaverdree V. The spectral and photophysical characterization of water solubilizing metal phthalocyanines for highly sensitive detection in biological studies. J Univ Chem Technol Met 2007:100–7.

[66] Gómez AR, Sánchez-Hernández CM, Fleitman-Levin I, Arenas-Alatorre J, Alonso-Huitrón JC, Vergara MES. Optical absorption and visible photoluminescence from thin films of silicon phthalocyanine derivatives. Analytical Chimica Acta 2014;6:6585–603.

doi:10.3390

[67] Mamuru SA, Ozoemena I. Heterogeneous Electron Transfer and Oxygen Reduction Reaction at Nanostructured Iron ( II ) Phthalocyanine and Its MWCNTs Nanocomposites Electrochemistry letters 2010:985–94. doi:10.1002/elan.200900438.

[68] Biçer E, Arat C. A Voltammetric Study on the Aqueous Electrochemistry of Acid Red 1 ( Azophloxine ) American Journal of Analytical Chemistry, 2014, 5, 598-603.doi.org/10.4236/ajac.2014.59067

[69] Wang Y, Xu H, Zhang J, Li G. Electrochemical Sensors for Clinic Analysis Biosensors & Bioelectronics 2008:2043–81doi.10.4172/2155-6210.1000154.

[70] Suroviec AH. Introduction to Electrochemistry.Journal of Laboratory Chemical Education 2013, 1(3): 45-48 DOI: 10.5923/j.jlce.20130103.02

[71] Xia C, Ning W. Electrochemistry Communications A novel non-enzymatic electrochemical glucose sensor modi fi ed with FeOOH nanowire. Electrochem Commun 2010;12:1581–4. doi:10.1016/j.elecom.2010.09.002.

[72] Rygar TG, Arken FM, Chröder US, Cholz FS. A Reviewon, spectroscopic , microscopic , and separation techniques.Sensors 2002;67. doi:10.1135/s20020163.

[73] Laborda E, Martı F. Electrocatalysis at Modified Microelectrodes: A Theoretical Approach to Cyclic Voltammetry ´ 2010:14542–51.

[74] Kumar S, Vicente-beckett V. Glassy carbon electrodes modified with multiwalled carbon nanotubes for the determination of ascorbic acid by square-wave voltammetry 2012:388–

96. doi:10.3762/bjnano.3.45.

[75] Lufrano F, Staiti P. Mesoporous carbon materials as electrodes for electrochemical supercapacitors. Int J Electrochem Sci 2010;5:903–16.

[76] Murray BJ, Walter EC, Zach MP, Inazu K, Hemminger JC, Penner RM. Metal nanowire arrays by electrodepositionChemical science journal 2003;6:7529–31. doi:10.1039/CSY00837E

[77] Pillay J, Ozoemena KI. Electrochemical properties of surface-confined films of single-walled carbon nanotubes functionalised with cobalt(II)tetra-aminophthalocyanine: Electrocatalysis of sulfhydryl degradation products of V-type nerve agents. Electrochim Acta 2007;52:3630–40. doi:10.1016/j.electacta.2006.10.022.

[78] Ridge O. Basics of Voltammetry and Polarography. Am J Anal Chem 2005:204–6.

[79] Ozoemena KI, Nkosi D, Pillay J. Influence of solution pH on the electron transport of the self-assembled nanoarrays of single-walled carbon nanotube-cobalt tetra-aminophthalocyanine on gold electrodes : Electrocatalytic detection of epinephrine. Electrochem Commun 2008;53:2844–51. doi:10.1016/j.electroComm.2007.10.076.

[80] Ozoemena KI, Pillay J, Nyokong T. Preferential electrosorption of cobalt (II) tetra-aminophthalocyanine at single-wall carbon nanotubes immobilized on a basal plane pyrolytic graphite electrode. Electrochem Commun 2006;8:1391–6. doi:10.1016/j.elecom.2006.05.031.

[81] Cyclic Voltammetry Analysis of Electrocatalytic Films 2015.

doi:10.1021/acs.jpcc.5b02376.

[82] Kolb HC, Finn MG, Sharpless KB. Click chemistry: Diverse chemical function from a few good reactions. angew chemie - Int Ed 2001;40:2004–21.

[83] Valle M. Introduction to cyclic voltammetry. Anal Chim Acta 2012;2:30–72.

[84] Oliveira UMF De, Lichtig J, Masini JC. Differential Pulse Voltammetry 2004;15:735–41.

[85] Adhikari BR, Govindhan M, Chen A. Sensitive detection of acetaminophen with graphene-based electrochemical sensor. Electrochim Acta 2015;162:198–204. doi:10.1016/j.electacta.2014.10.028.

[86] Search H, Journals C, Contact A, Iopscience M, Address IP. Electrochemical Effect of Different Modified Glassy Carbon Electrodes on the Values of Diffusion Coefficient for Some n.d.;12018. doi:10.1088/1742-6596/431/1/012018.

[87] Lechien A, Valenta P, Ntirnberg HW, Patriarche GJ. Determination of Ascorbic Acid by Differential Pulse Voltammetry 1982:105–8.

[88] Espinosa-calderón A, Contreras-medina LM, Muñoz-huerta RF, Millán-almaraz JR, Gerardo R, González G, et al. Methods for Detection and Quantification of Aflatoxins 2009.

[89] Ikhsan NI, Rameshkumar P, Huang NM. Controlled synthesis of reduced graphene oxide supported silver nanoparticles for selective and sensitive electrochemical detection of 4-nitrophenol. Electrochim Acta 2016;192:392–9. doi:10.1016/j.electacta.2016.02.005.

[90] Mashazi P, Mugadza T, Sosibo N, Mdluli P, Vilakazi S, Nyokong T. The effects of carbon

nanotubes on the electrocatalysis of hydrogen peroxide by metallo-phthalocyanines. Talanta 2011;85:2202–11. doi:10.1016/j.talanta.2011.07.069.

[91] Suni II. Impedance methods for electrochemical sensors using nanomaterials. Int J Electrochem 2008;27:137–40. doi:10.1016/j.trac.2008.03.012.

[92] Guti C. Impedance study of electropolymerized films of polyNi ( II ) -macrocycles 2007;53:792–802. doi:10.1016/j.electacta.2007.07.064.

[93] Mugadza T, Arslano Y, Nyokong T. Electrochimica Acta ( II )— Single walled carbon nanotube conjugate platforms and their use in electrocatalysis of amitrole 2012;68:44–51. doi:10.1016/j.electacta.2012.02.041.

[94] Msimelelo P. Siswana, Kenneth I. Ozoemena and Tebello Nyokong.Electrocatalysis of asulam on cobalt phthalocyanine modified multi-walled carbon nanotubes immobilized on a basal plane pyrolytic graphite electrode.Electrochemical Acta 2010;55:2606-13.doi:10.1016/j.electacta.2009.12.051.

[95] Cordry L, Fosdick E, Larson C. With polymer electrodes there IS a possible kinetic.Sensors 1985;186:87–97doi: 10.1134/S102319350911007X

[96] Vilian ATE, Chen S, Chen Y, Ali MA, Al-hemaid FMA. An electrocatalytic oxidation and voltammetric method using a chemically reduced graphene oxide film for the determination of caffeic acid. J Colloid Interface Sci 2014;423:33–40. doi:10.1016/j.jcis.2014.02.016.

[97] Andrieux CP, Audebert P. Electron Transfer through a Modified Electrode with a Fractal

Structure : Cyclic Voltammetry and Chronoamperometry Responses 2001:444–8.

[98] Bard AJ. Chemical Modification of Electrodes.Sensors 1983;13:302–4.

[99] Ben I, Gannouni M, Ben J.Electrochemical detection of organic and inorganic water pollutants using recompressed exfoliated graphite electrodes Appl Surf Sci 2015;351:927–34. doi:10.1016/j.apsusc.2015.06.038.

[100] Afkhami A, Madrakian T, Ghaedi H, Khanmohammadi H. Impact of double layer modifiers on the signal registered on the renovated solid state electrodes. Electrochim Acta 2012;66:255–64. doi:10.1016/j.electacta.2012.01.089.

[101] Nyoni S, Mugadza T, Nyokong T. Improved l-cysteine electrocatalysis through a sequential drop dry technique using multi-walled carbon nanotubes and cobalt tetraaminophthalocyanine conjugates. Electrochim Acta 2013. doi:10.1016/j.electacta.2013.10.023.

[102] Ortiz B, Park S-M, Doddapaneni N. Electrochemical and spectroelectrochemical studies of cobalt phthalocyanine polymers. J Electrochem Soc 1996;143:1800–5. doi:10.1149/1.1836907.

[103] Li S, Du J, Chen J, Mao N. Electrodeposition of cobalt oxide nanoparticles on reduced graphene oxide : a two-dimensional hybrid for enzyme-free glucose sensing.Sensors 2013. doi:10.1007/s10008-013-2354-2.

[104] Sun F, Li L, Liu P. Nonenzymatic Electrochemical Glucose Sensor Based on Novel Copper Film. Journal Electroanalysis 2011:395–401. doi:10.1002/elan.201000391.

[105] Rodriguez-mendez ML. Materials : Application in the Study of Antioxidants.Sensors2011:1328–44. doi:10.3390/s110201328.

[106] Mugadza T, Nyokong T. Synthesis and electrocatalytic behavior of cobalt (II)-tris(benzyl-mercapto)-monoaminophthalocyanine“single walled carbon nanotube nanorods. Electrochim Acta 2011. doi:10.1016/j.electacta.2010.11.016.

[107] Mugadza T, Nyokong T. Electrochimica Acta Synthesis , characterization and the electrocatalytic behaviour of nickel ( II ) tetraamino-phthalocyanine chemically linked to single walled carbon nanotubes. Electrochim Acta 2010;55:6049–57. doi:10.1016/j.electacta.2010.05.065.

[108] Della C, Rossi M, Maria A, Ponti A, Lo M, Falletta E. One-pot synthesis of polyaniline / $Fe_3$ $O_4$ nanocomposites with magnetic and conductive behaviour . Catalytic effect of $Fe_3$ $O_4$ nanoparticles. Synth Met 2012;162:2250–8. doi:10.1016/j.synthmet.2012.10.023.

[109] Abdolahi A, Hamzah E, Ibrahim Z, Hashim S. Synthesis of Uniform Polyaniline Nanofibers through Interfacial Polymerization.Journal of Materials 2012:1487–94. doi:10.3390/ma5081487.

[110] Mohammad F, Naalweh M. Synthesis of Nano-Sized Cobalt oxide Nano-Particles Stabilized in Surfactant and Polymer Matrix and their Magnetic Properties 2013.

[111] Mugadza T, Nyokong T. Electrochimica Acta Synthesis and characterization of electrocatalytic conjugates of tetraamino cobalt ( II ) phthalocyanine and single wall carbonnanotubes.Electrochimicaacta2009;54:6347–53. doi:10.1016/j.electacta.2009.05.074.

[112] Bachhav SG, Patil DR. Synthesis and Characterization of Polyaniline-Multiwalled Carbon Nanotube Nanocomposites and Its Electrical Percolation Behavior.J.Materials 2015;5:90–5. doi:10.5923/j.materials.20150504.03.

[113] Panwar V, Kumar P, Ray SS, Jain SL. Organic inorganic hybrid cobalt phthalocyanine / polyaniline as efficient catalyst for aerobic oxidation of alcohols in liquid phase. Tetrahedron Lett 2015:1–6. doi:10.1016/j.tetlet.2015.05.003.

[114] Mugadza T, Nyokong T. Synthesis and electrocatalytic behavior of cobalt.Electrochimica Acta2010 doi:10.1016/j.electacta.2010.11.016.

[115] Nasirizadeh N, Shekari Z, Nazari A, Tabatabaee M. Fabrication of a novel electrochemical sensor for determination of hydrogen peroxide in different fruit juice samples. J Food Drug Anal 2016;24:72–82. doi:10.1016/j.jfda.2015.06.006.

[116] Shumba M, Nyokong T. Electrode modification using nanocomposites of boron or nitrogen doped graphene oxide and cobalt (II) tetra aminophenoxy phthalocyanine nanoparticles. Electrochim Acta 2016. doi:10.1016/j.electacta.2016.02.166.

[117] Berros C, Gutirrez C. Impedance study of electropolymerized films of polyNi(II)-macrocycles. Electrochim Acta 2007;53:792–802. doi:10.1016/j.electacta.2007.07.064.

[118] Ozoemena KI, Nyokong T, Nkosi D, Chambrier I, Cook MJ. Insights into the surface and redox properties of single-walled carbon nanotube — cobalt ( II ) tetra-aminophthalocyanine self-assembled on gold electrode.Electrochim Acta 2007;52:4132–43. doi:10.1016/j.electacta.2006.11.039.

# APPENDICES

## APPENDIX A: MATERIALS

### List A: Apparatus used in synthesis and characterisation

Erlenmeyer flask, Buchner funnel, Liebig's condenser, distillation flask, measuring cylinders(25ml,50ml,100ml) ,volumetric flasks(50ml,100ml,250ml,500ml, 1000ml), micropipette, beakers, spatula, pestle ,mortar, wash bottles, conical flasks, petri dishes, burettes, filter papers, vials

**Table A1: Reagents and chemicals**

| Name | Chemical formula | Manufacturer | Concentration/Mass |
|---|---|---|---|
| Trimellitic anhydride | $C_9H_9O_5$ | Skylabs | 4.8g |
| Ammonium chloride | $NH_4CI$ | Skylabs | 0.27g |
| Hydrochloric acid | HCI | Sigma aldrich | 85% |
| Nitric acid | $HNO_3$ | Skylabs | 5M |
| Thionyl chloride | $SOCI_2$ | Glassworld | 5% |
| Ethanol | $CH_3CH_2OH$ | Skylabs | 99% |
| Potassium bromide | KBr | ACE | 0.01g |
| Ammonium molybdate | $(NH4)_2MoO_4$ | ACE | 0.27g |
| Distilled water | $H_2O$ | MSU Lab | - |
| Urea | $CO(NH_2)_2$ | Urea | 15.0g |

| | | | |
|---|---|---|---|
| Ammonium persulphate | $NH_4S_2O_3$ | Skylabs | 0.05M |
| Nitrobenzene | $C_6H_5NO_2$ | Skylabs | 2M |
| Aniline | $C_6H_5NH_2$ | Unichem | 0.2M |
| Cobalt (II) chloride | $CoCI_2$ | Alpha | 4.1g |

**Table A2: Instrumentation**

| **Name** | **Model** | **Manufacturer** | **Use in research** |
|---|---|---|---|
| Analytical balance | GA-110 | OHAUS | Weighing |
| pH meter | Az-8601 | Thermoscientific | pH measurement |
| Sonicator | KQ-250B | China Corp | Ultra-agitation |
| FTIR | Nicolet 6700 | Thermoscientific | Characterisation |
| Potentiostat | PG Stat302N | Autolab | Electroanalysis |

**Cleaning of glassware**

Glassware was cleaned using detergents and was then rinsed using distilled water.Organic stains on glassware were cleaned using aqua-regia .This aided in the minimization of interferences during electroanalysis.

## APPENDIX B:Working electrodes

### B1: Working electrodes used in this study

| Electrode modifier | Method of modification | Electrode designation |
|---|---|---|
| Bare Glassy Carbon Electrode | - | BCGE |
| cobalt(II)tetracarboxyl phthalocyanine | Drop and dry | CoTCPc-GCE |
| Polyaniline | Drop and dry | PANI-GCE |
| Cobalt oxide nanoparticles | Drop and dry | $Co_2O_3$NPs-GCE |
| Polyaniline cobalt(II)phthalocyanito | Drop and dry | PANI-GCE |
| Polyaniline cobalt(II)phthalocyanito/Cobalt oxide | Drop and dry | PANI-CoPc/$Co_2O_3$NPs-GCE |

## APPENDIX C :Calculation

### C1: Effective Surface area

Constant R = 8.314 $Jmol^{-1}$, T = 273 K

Randle-sevick equation

$$m = (2.69 \times 10^5) n^{\frac{3}{2}} A_{eff} D^{\frac{1}{2}} C2$$

D= 7.6 × $10^{-6}$cm$^2$/s$^{-1}$ , C= $1 \times 10^{-6}$ cm$^2$, m= $3.5 \times 10^{-5}$ and $A_{eff} = 0.40cm^2$

**C2: Surface Coverage**

$$ipa = \frac{n^2 \ F^2 \ A\Gamma v}{4RT}$$

$R^2$= 0.9936, m=$2.5 \times 10^{-8}$, $A_{eff} = 0.40cm^2$, $\Gamma = 7.31 \times 10^{-1} \ molcm^{-2}$

**C3: Limit of Detection and Limit of Quantification**

Excel Linest function

| | |
|---|---|
| Slope | Intercept |
| Standard error of the slope | Standard error of the intercept |
| $R^2$ | Standard error in y |

LOD= $6.612 \times 10^{-8}$M

LOQ=$2 \times 10^{-7} M$

**C4: Real sample analysis**

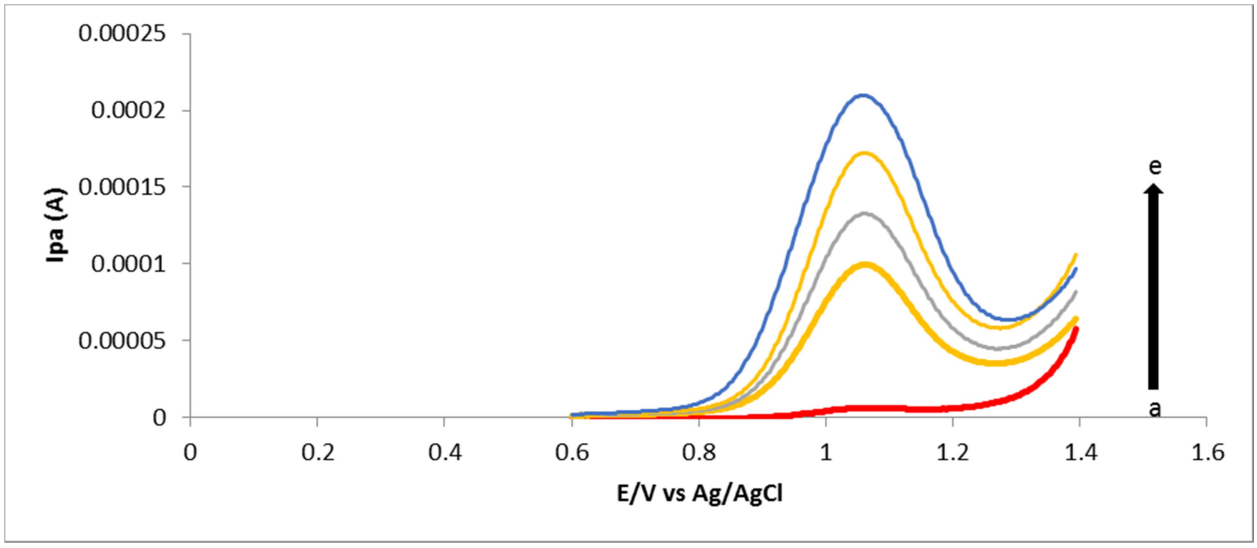


DPV voltammograms for real sample analysis for amitrole (a) waste water + PBS pH 4 (b) waste water spiked (c) 2.5 µM (d) 5 µM and (e) 7.5 µM standard solutions for amitrole

.